
UNIVERSITY OF BIRMINGHAM

# MAINTENANCE AND RETIREMENT OF AGEING POWER SYSTEM ASSETS AND REINFORCEMENT OF TRANSMISSION SYSTEMS WITH SEISMIC RISK

by

WILSON ANDRES VASQUEZ GUERRERO

A thesis submitted to the University of Birmingham for the degree of

DOCTOR OF PHILOSOPHY

Department of Electronic, Electrical and Systems Engineering

The University of Birmingham

January 2022

UNIVERSITY OF BIRMINGHAM

**University of Birmingham Research Archive**
**e-theses repository**

This unpublished thesis/dissertation is under a Creative Commons Attribution 4.0 International (CC BY 4.0) licence.

**You are free to:**

**Share** — copy and redistribute the material in any medium or format

**Adapt** — remix, transform, and build upon the material for any purpose, even commercially.

The licensor cannot revoke these freedoms as long as you follow the license terms.

**Under the following terms:**

**Attribution** — You must give appropriate credit, provide a link to the license, and indicate if changes were made. You may do so in any reasonable manner, but not in any way that suggests the licensor endorses you or your use.

**No additional restrictions** — You may not apply legal terms or technological measures that legally restrict others from doing anything the license permits.

**Notices:**

You do not have to comply with the license for elements of the material in the public domain or where your use is permitted by an applicable exception or limitation.

No warranties are given. The license may not give you all of the permissions necessary for your intended use. For example, other rights such as publicity, privacy, or moral rights may limit how you use the material.

Unless otherwise stated, any material in this thesis/dissertation that is cited to a third-party source is not included in the terms of this licence. Please refer to the original source(s) for licencing conditions of any quotes, images or other material cited to a third party.

*To my parents and my sister, for encouraging me to keep working beyond my comfort zone.*

# ACKNOWLEDGEMENTS

Many people have helped me in developing my research project and writing this thesis. I would like to first thank my project supervisor, Dr Dilan Jayaweera, for all the help provided throughout my PhD studies. I am very grateful to Dr Franklin Quilumba and Daniel Donaldson for proofreading the chapters of this thesis. I would like to thank my fellow researchers—Dr Zafar Khan, Dr Hasan Gunduz, Dr Manuel Alvarez, Dr Abdullah Altamini, Waleed Al Abri, Bader Alharbi, Dr Peju Oyewole, and Daniel Donaldson—for their continuous and valuable help. I am also very grateful to the power engineering professionals who I had the pleasure to meet at conferences and workshops and via the Internet for sharing their knowledge with me.

Finally, special thanks to the School of Engineering of the University of Birmingham for the scholarship received to fund my PhD studies.

# ABSTRACT

Power system components age over time, due to thermal, electrical, mechanical, and chemical stresses. Ageing components tend to fail more frequently, increasing the risk of power supply interruptions during normal system operation and under extreme events such as earthquakes. Maintenance and retirement activities should be targeted at critical components that pose the highest risks of interruptions. However, developing failure models of ageing medium voltage underground cables and old power transformers, used for quantitative risk assessment, is a challenging task for utilities due to the lack of failure data. Using non-traditional failure models, i.e., models that incorporate components' condition data and loading levels, is an interesting alternative that would allow utilities to enhance their risk-based maintenance and retirement approaches. This thesis addresses the modelling challenges for cable maintenance prioritisation, power transformer retirement, and transmission system reinforcement considering earthquakes.

This thesis presents an approach to prioritise the maintenance of ageing medium voltage underground cables. The approach combines, for the first time, the index known as maintenance potential index with a new aged-related repairable failure model to identify cables whose maintenance would yield the greatest benefits to the reliability of a power distribution system. The case study in this thesis suggested that cable maintenance prioritisation significantly depends on the impacts of age-related repairable failures on the expected system interruption cost, which emphasises the importance of considering the effects of cable ageing. The proposed model for aged-related repairable failures was compared with the IEC-Arrhenius-Weibull model through computer simulations, which consist of failure rate and cable ranking calculations as well as sensitivity analysis. The results revealed that using Arrhenius relationship may negatively affect the calculation of the failure rate of ageing cables, reducing its value and making it very dependent on the shape parameter of the Weibull distribution. This thesis also presents a risk-based approach for planning the retirement of power transformers. To overcome the problem of limited end-of-life failure data, the approach calculates the apparent age of power transformers using health index data, and estimates the scale parameter of the Weibull distribution using the Arrhenius relationship, the IEC thermal model, and an equivalent load model. The case study results suggested that the improved ageing failure model

yields better predictions of the unavailability due to ageing failure, increasing its value as power transformers get older and thus enhancing retirement decisions.

Finally, a two-stage adaptive robust optimisation problem to determine reinforcement decisions of transmission systems with seismic risk and aged equipment is presented. The availability of generating units, lines, and transformers is modelled by classifying these components into several groups (based on seismic hazard zone, ageing status, and risk of being damaged by a tsunami), and by using a polyhedral uncertainty set for each group. Unlike traditional optimisation problems, the proposed problem calculates the expected capacity of all aged components by using models of repairable and ageing failures, helping system planners to obtain more accurate reinforcement decisions. The assessment proposed in the thesis suggested that transmission systems with aged components require more reinforcements (i.e., more transmission lines and power transformers) to mitigate the impacts of earthquakes.

## Thesis-Based Publications

1. **W. A. Vasquez** and D. Jayaweera, "Prioritization of Aging Underground Power Distribution Cables for Maintenance Activities", presented at International Conference on Probabilistic Methods Applied to Power Systems (PMAPS), Liege, Belgium, 2020, oral presentation. The first part of Chapter 4 is based on this publication.

2. **W. A. Vasquez** and D. Jayaweera, "A Study of Repairable Failure Models of Aging Underground Power Distribution Cables", presented at IEEE PES Innovative Smart Grid Technologies Conference (Europe), Espoo, Finland, 2021, oral presentation. The second part of Chapter 4 is based on this publication.

3. **W. A. Vasquez** and D. Jayaweera, "Risk-based approach for power transformer replacement considering temperature, apparent age, and expected capacity", IET Generation, Transmission & Distribution, vol. 14, no. 21, pp. 4898-4907, July 2020. Chapter 5 is based on this publication.

4. [1]**W. A. Vasquez** and D. Jayaweera, "Power Transmission System Reinforcement Considering Seismic Events and Equipment Ageing". Chapter 6 is based on this work, which will be submitted for publication.

[1]This work was presented at IEEE PES Student Presentation Competition held at the University of Birmingham on 30 November 2021 (winning 1st place).

# Contents

# List of Figures

# List of Tables

# Nomenclature

**Indices**

| | |
|---|---|
| $c$ | Components (transmission lines or power transformers) |
| $d$ | Demands |
| $g$ | Generating units |
| $n$ | Nodes |
| $v$ | Iterations |

**Sets**

| | |
|---|---|
| $r(c)$ | Receiving-end node of component $c$ |
| $s(c)$ | Sending-end node of component $c$ |
| $\Omega_n^E$ | Generating units located at node $n$ |
| $\Omega_n^D$ | Demands located at node $n$ |
| $\Omega_g^{HH}$ | Generating units in high seismic hazard zone |
| $\Omega_g^{HHT}$ | Generating units in high seismic hazard zone and with risk of damage due to tsunami |
| $\Omega_g^{MH}$ | Generating units in moderate seismic hazard zone |
| $\Omega_g^{LH}$ | Generating units in low seismic hazard zone |
| $\Omega_c^{HH}$ | Components in high seismic hazard zone |
| $\Omega_c^{HHA}$ | Aged components in high seismic hazard zone |
| $\Omega_c^{MH}$ | Components in moderate seismic hazard zone |
| $\Omega_c^{MHA}$ | Aged components in moderate seismic hazard zone |
| $\Omega_c^{LH}$ | Components in low seismic hazard zone |

| | |
|---|---|
| $\Omega_c^{LHA}$ | Aged components in low seismic hazard zone |
| $\Omega_n^{C+}$ | Prospective components |

**Parameters**

| | |
|---|---|
| $B_c$ | Susceptance of component $c$ [S] |
| $C_d^{LS}$ | Load-shedding cost of demand $d$ [$/MWh] |
| $C_g^E$ | Production cost of generating unit $g$ [$/MWh] |
| $F_c^{max}$ | Power transfer capacity of component $c$ [MW] |
| $\overline{F}_c^{max}$ | Upper bound of component $c$'s capacity [MW] |
| $I_c^C$ | Annualised investment cost of component $c$ [$] |
| $I^{C,max}$ | Maximum annualised investment budget [$] |
| $P_d^{Dmax}$ | Load of demand $d$ [MW] |
| $\underline{P}_d^{Dmax}$ | Lower bound of load demand $d$ [MW] |
| $\overline{P}_d^{Dmax}$ | Upper bound of load demand $d$ [MW] |
| $P_g^{Emax}$ | Production capacity of generating unit $g$ [MW] |
| $\overline{P}_g^{Emax}$ | Upper bound of production capacity of generating unit $g$ [MW] |
| $\Gamma_c$ | Uncertainty budget for power transfer capacity |
| $\Gamma_d$ | Uncertainty budget for maximum load demand |
| $\Gamma_g$ | Uncertainty budget for power generation capacity |

**Binary Variable**

| | |
|---|---|
| $x_c^C$ | This variable is 1 if prospective component $c$ is built and 0 otherwise. |

**Continuous Variables**

| | |
|---|---|
| $p_c^C$ | Power flow through component $c$ [MW] |
| $p_g^E$ | Power produced by generating unit $g$ [MW] |
| $p_d^{LS}$ | Amount of curtailed load [MW] |
| $\eta$ | Auxiliary variable used to gradually reconstruct the objective function of the problem [$] |
| $\theta_n$ | Voltage angle at node $n$ |

# Chapter 1

# Introduction

## 1.1 Background and Research Motivation

Electrical power systems have a great number of components (generators, transformers, overhead lines, underground cables, etc.) that constantly produce and carry electricity to supply the demand of residential, commercial, and industrial customers. To achieve this function, utilities perform several activities that are commonly grouped into the following main processes: system development, asset management, and system operation [1]. System development involves planning the expansion or reinforcement of generation, transmission, and distribution systems, i.e., planning the construction of power plants, substations, and transmission and distribution lines. Asset management comprises several activities, such as acquisition, installation, operation, maintenance, and retirement of power equipment [2]. These activities allow asset managers to optimally handle power system assets over their entire life cycle [3]. This thesis focuses on maintenance and retirement of ageing components as well as transmission system reinforcement.

To plan the maintenance and retirement of ageing components, it is necessary to create mathematical models of both repairable failures and non-repairable (end-of-life) failures, so that the potential impacts of failures on power system reliability indices can be quantified [4], [5]. The research work presented in this thesis was motivated by the technical difficulties to create accurate age-related repairable and non-repairable failure models. These models require large failure data sets for each type of component, which may not be available. In the United Kingdom, few non-repairable failures of power transformers have been recorded [6]; they have occurred mainly due to random events (e.g., external short-circuits, lightnings, switching transients, etc.). Since these failures have not been influenced by the ageing process, it is very difficult to formulate statistical models to plan power transformer retirement. Furthermore, traditional models do not take into account the influence of loading and weather conditions on failure rates or failure probabilities.

The research work was also motivated by the significant amount of ageing assets in some power systems. Ageing assets increase the probability of power service interruptions, as their ability to withstand mechanical, electrical, thermal, and chemical stresses decreases over the time. A 2015 report published by the United States Department of Energy indicated that 70% of power transformers and 70% of transmission lines were 25 years or older, and 60% of circuit breakers were 30 years or older [7]. The problem of ageing components has been also identified in the United Kingdom, where transmission and distribution systems have ageing assets that are unable to adapt to changing power generation and needs [8]. A 2014 report published by UK Power Networks indicated that the average service age of 132-kV power transformers that are part of London Power Networks was 33 years, and that the average service age of the oldest 10% of those transformers was 56 years [9]. To enhance the reliability of power distribution systems, major electric utilities in the United States doubled their capital investments from 1997 to 2017

to replace old equipment (poles, conductors, and substation transformers) [10]. Equipment maintenance expenditures of those utilities were also increased in the same period [10].

There is another important factor that motivated this research work. Maintenance strategies used in power systems have changed over time. Preventive maintenance is the strategy in which inspections and tests are performed at regular time intervals (e.g., every six months, or once a year). To reduce maintenance costs and the number of spare equipment, some electric utilities employ a more advanced strategy called condition-based maintenance, in which maintenance actions are carried out when the condition of a component needs it [11]. This approach is used particularly for critical ageing assets whose replacements require high capital investments [11]. This is the case of power transformers, whose replacement may cost several millions of U.S. dollars, and manufacturing their replacement may take up to two years [7]. There are several techniques used to monitor the condition of power transformers, including in-service partial discharge testing, insulting oil monitoring, tap changer monitoring, internal temperature measurement, etc. [11]. These techniques provide a lot of data that can be used to determine the actual condition of power transformers, which is usually done by calculating health indices [12]. Considering that some electric utilities are continuously collecting transformer condition monitoring data, there is an exciting opportunity to incorporate this information into non-repairable failure models, and to use these advanced models for planning the retirement of power transformers.

Power transmission systems in some parts of the world are subject to extreme events, such as earthquakes, hurricanes, and wildfires, and they should be considered when making transmission system reinforcement plans. Although earthquakes have low probability of occurrence, their impacts on power systems, especially those located in the Ring of Fire,

can be very significant [13]. The 2011 Japan earthquake, with a magnitude of 9.0 (Mw), caused severe damages to power plants, transmission lines, and substations, which led to long, widespread blackouts [14]. Considering that electric utilities are not replacing aged transmission system equipment at an appropriate rate (mainly due to limited budgets) [15], and that aged equipment has higher failure probability, the impacts of earthquakes could be much worse. Thus, it is also vital to investigate how aged components can affect reinforcement plans of transmission systems with seismic risk.

## 1.2 Scope of the Research

This thesis focuses on two research areas. The first is maintenance prioritisation of ageing underground power distribution system cables and retirement planning of aged power transformers. Medium voltage underground power cables and power transformers used in transmission, subtransmission, and distribution substations will be considered in the research. The mathematical modelling of both repairable failures of ageing cables and non-repairable failures of aged power transformers will be a part of this thesis. The data needed to develop failure models have been taken from the power system literature and/or created using probability distributions. Computer programs have been developed using the software MATLAB to analyse the performance of failure models and their effects on cable maintenance prioritisation and transformer retirement plans.

The second research area is reinforcement planning of power transmission systems with seismic risk and aged equipment. Mathematical optimisation tools have been employed to solve this problem, especially tools that can cope with uncertainties. The 24-bus IEEE Reliability Test System [16] has been used to validate the formulation of the optimisation problem, which has been solved using the software GAMS.

## 1.3 Research Aim and Objectives

As mentioned in Section 1.1, maintenance and retirement planning of ageing components is a difficult task due to the lack of data needed to develop appropriate age-related failure models (particularly, failure models for underground cables and power transformers). Furthermore, power transmission systems with seismic risk might experience greater infrastructure damages due to the higher failure probabilities of ageing components. Considering these problems, the aim of this thesis is to investigate the maintenance prioritisation of ageing underground cables, the retirement planning of power transformers, and the reinforcement planning of transmission systems that are subject to seismic events and have aged equipment. The objectives to achieve the overall aim are:

1. To perform a critical review of conventional mathematical models of age-related repairable and non-repairable failures, as well as of the methods to incorporate those models into power system reliability assessment. (Chapters 2 and 3 present this review.)

2. To develop an age-related repairable failure model for underground cables incorporating the effects of loading conditions. (Chapter 4 details the model development.)

3. To develop an approach to prioritise the maintenance of underground cables considering age-related repairable failures, and implement it on MATLAB. (The approach is presented in Chapter 4.)

4. To improve the conventional non-repairable failure model, considering the current condition and future winding temperature of power transformers. (Chapter 5 explains the proposed improvements.)

5. To develop an approach to plan the retirement of power transformers considering non-repairable failures, and implement it on MATLAB. (The approach is presented in Chapter 5.)

6. To formulate an optimisation problem to determine reinforcement plans for transmission systems with seismic risk and aged equipment, and solve it using the software GAMS. (Chapter 6 presents the proposed optimisation problem.)

## 1.4 Research Contributions

Below are the research contributions that will be presented in Chapters 4-6.

- **Approach for prioritising the maintenance of ageing underground power distribution system cables.** Unlike traditional approaches for cable maintenance prioritisation, the approach presented in the first part of Chapter 4 combines, for the first time, the index known as maintenance potential index with a new age-related repairable failure model to identify critical cables whose maintenance would produce the greatest benefits to the reliability of a power distribution system. To incorporate the effects of loading conditions, the proposed failure model employs a model that converts the time-varying loading conditions of cables into a single equivalent load, capturing hidden patterns that further improve the maintenance prioritisation process.

- **Critical analysis and comparison of the proposed age-related repairable failure model and the IEC-Arrhenius-Weibull model.** The IEC-Arrhenius-Weibull model is the first attempt to model age-related repairable failures of underground cables considering their loading conditions. In the second part of Chapter

4, a comprehensive study was performed to critically analyse and compare the main aspects of the IEC-Arrhenius-Weibull model and the failure model developed in this thesis. The study provides several novel and important insights that can help researchers and asset managers successfully implement both models as well as develop new models.

- **Improved method for calculating the unavailability due to ageing failure of power transformers.** The conventional model to calculate the unavailability due to ageing failure requires enough end-of-life failure data. Two major improvements were made to the conventional ageing failure model (which are presented in Chapter 5), so that it can be used when limited end-of-life failure data is available. First, the apparent (condition-based) age of power transformers is calculated using health index data. Second, the scale parameter of the Weibull distribution is estimated by combining, in a novel way, the Arrhenius relationship, the IEC thermal model, and an equivalent load model. Incorporating the apparent age and the winding hottest-spot temperature of each power transformer improves significantly the accuracy of the calculation of the unavailability due to ageing failure, a key aspect of the transformer retirement planning process.

- **New approach for planning the retirement of power transformers.** The proposed approach, described in Chapter 5, has two parts: identification of the best retirement candidates and calculation of the retirement year. An advanced version of the credible improvement potential index is used to rank aged power transformers considering their expected capacity. To enhance the ranking process and the calculation of the retirement year, the approach uses the improved method to calculate the unavailability due to ageing failure, which incorporates information on the current condition and future winding hottest-spot temperature of each power transformer. Furthermore, considering that special events, such as partial discharges, thermal

faults, and winding deformations, may reduce the operating capacity of aged power transformers, the proposed approach includes this aspect in the calculation of the expected capacity to further enhance retirement decisions.

- **Two-stage adaptive robust optimisation problem for reinforcing power transmission systems with seismic risk and aged equipment.** The two-stage adaptive robust optimisation problem, described in Chapter 6, models the availability of components differently, by creating groups of components based on their location with respect to the epicentre, ageing status, and risk of damage by a tsunami, and by using a polyhedral uncertainty set for each group. The advantage of this modelling approach is that fragility curves of components are not needed. Moreover, the effects of equipment ageing, commonly neglected in reinforcement planning studies, are incorporated into the optimisation problem constraints to produce more accurate reinforcement plans.

## 1.5 Thesis Structure

This section outlines the content of Chapters 2-7.

***Chapter 2: Literature Review***

Chapter 2 presents a summary and a critical analysis of previous works about component failure models, risk-based approaches for retiring power transformers, methods for prioritising the maintenance and retirement of power system components, and approaches for reinforcing power transmission systems with seismic risk. Furthermore, the chapter presents the research gaps that will be addressed in Chapters 4-6.

***Chapter 3: Concepts, Models, and Techniques Used in Power System Risk Assessment***

Chapter 3 explains the most important concepts, mathematical models, and techniques used in power system risk assessment, which will be mainly employed for developing the approaches for cable maintenance prioritisation (Chapter 4) and power transformer retirement (Chapter 5). The conventional models of repairable and non-repairable failures are reviewed in detail. Then, the use of Monte Carlo simulation techniques to sample component states is explained. Furthermore, the chapter briefly describes the procedures for evaluating the impacts of component failures on power systems and the models for calculating adequacy indices of composite (generation and transmission) and distribution systems.

***Chapter 4: Maintenance Prioritisation of Power Distribution Cables Considering Age-Related Repairable Failures***

An age-related repairable failure model for underground cables and the procedure for estimating its parameters are presented in Chapter 4. The failure model takes into account the effects of cable loading conditions. The chapter also presents several indices used to rank power system components and the changes made to these indices for prioritising the maintenance of ageing cables. The performance of the age-related repairable failure model and the cable maintenance prioritisation approach are carefully examined using a test system and computer simulations. Chapter 4 also includes a critical analysis and a computer simulation-based comparison of the IEC-Arrhenius-Weibull model and the proposed cable failure model.

***Chapter 5: Estimating the Retirement of Power Transformers***

Chapter 5 describes a risk-based approach for planning the retirement of power transformers. The approach includes several methods for calculating and incorporating the apparent age and winding hottest-spot temperature of power transformers into the conventional ageing failure model. The chapter also details the procedures to calculate the expected capacity of power transformers, to identify the best retirement candidates (using a modified version of a component ranking index presented in Chapter 4), and to calculate their year of retirement. The application of the approach is demonstrated through a case study, which considers several aged power transformers of subtransmission and distribution substations.

***Chapter 6: Transmission System Reinforcement Considering Earthquakes and Aged Equipment***

A two-stage adaptive robust optimisation problem to determine reinforcement plans of power transmission systems with seismic risk is presented in Chapter 6. The problem formulation includes a method to model the availability of generating units, lines, and transformers using polyhedral uncertainty sets. Furthermore, the chapter also describes the procedure to incorporate the effects of equipment ageing into the optimisation problem (using the expected capacity calculation method described in Chapter 5). The case study and changes made to the 24-bus IEEE Reliability Test System are explained in detail.

***Chapter 7: Conclusions and Future Work***

The last chapter of this thesis, Chapter 7, contains the main conclusions of the research work and some suggestions for future research.

# Chapter 2

# Literature Review

## 2.1 Introduction

This chapter presents a literature review on maintenance prioritisation and retirement of ageing power system components, and on transmission system reinforcement planning (which are the areas that will be investigated in this thesis, as mentioned in Chapter 1, Subsection 1.2). The literature review starts with a brief description of the main tasks of power system risk assessment. Then, the main features of component failure models used in power system risk assessment are described and critically analysed[1]. The literature review continues with indices for prioritising maintenance and retirement activities of power equipment. Risk-based equipment retirement strategies and mathematical models for transmission system reinforcement planning are also analysed. The chapter ends with a summary, which includes problems and aspects that need further study.

[1]The theoretical details of relevant component failure models, techniques used in power system risk assessment, such as Monte Carlo simulation and contingency analysis, and mathematical models of some system risk indices will be presented in Chapter 3.

## 2.2 Risk Assessment of Power Systems

Power system risk assessment allows us to analyse both system adequacy and system security. Adequacy relates to the existence of sufficient assets in a power system to meet its load demand and operational constraints, whereas security relates to the ability of a power system to respond to dynamic and transient perturbations [17]. Power system risk assessment can be used for several applications. This chapter focuses on applications for system adequacy studies, particularly reliability-centred maintenance and equipment retirement planning.

Power system risk assessment comprises four main tasks [17]: to determine component outage models, to sample system states and calculate their probability of occurrence, to determine the consequences of system states (this task is also known as contingency analysis), and to calculate system risk indices. Outages of power system components are classified into independent and dependent outages. This thesis focuses on independent repairable and non-repairable failures. The main features of repairable and non-repairable failure models of power system components will be analysed in detail in the next section of this chapter, as these models are needed to develop maintenance and retirement plans presented in Chapters 4 and 5.

The second task, sampling system states and calculating their probability of occurrence, is performed as follows. System states can be generated using two methods, state enumeration and Monte Carlo simulation. Their use depends on the characteristics of power system components and the system itself (e.g., size and operating conditions) [18]. The state enumeration method is used when a system has simple operating conditions and components have low failure probabilities. On the other hand, Monte Carlo simulation is employed when a system has complex operating conditions and components have high failure probabilities, since the number of system states can be very high. To generate

system states with the Monte Carlo method, sequential or non-sequential techniques can be applied. The approach to calculate the probability of occurrence of system states depends on the method used to select them. For instance, for the non-sequential Monte Carlo technique, this probability is calculated by dividing the occurrence number of the system state $s$ by the total number of samples [17].

The third and fourth tasks, determining the consequences of system states and calculating system risk indices, depend on the type of system under study. Risk assessment studies are usually carried out for generation-demand systems, composite generation and transmission systems, and radial distribution systems. For composite generation and transmission systems, the procedure to determine the consequences of system states (known as contingency analysis) includes power flows and optimal power flows [18]. For radial distribution systems, the consequences of system states are determined by identifying load points that are affected by component failures and restoration actions [19].

System risk indices reflect the system performance considering equipment failures and ratings, load demand, variable power generation, etc. Most system risk indices are calculated as the expected value of a random variable. The Expected Energy Not Supplied (EENS) index is commonly used in composite system studies, whereas the System Average Interruption Frequency Index (SAIFI) and the System Average Interruption Duration Index (SAIDI) are usually used in distribution system studies [18].

## 2.3 Component Failure Models

As mentioned before, power system components undergo repairable and non-repairable (end-of-life) failures throughout their operation. Failures change the status of components

[20]. When a repairable failure occurs, the status of a component changes from an operating state to a failure state. After being repaired, the component returns to operation. On the other hand, when a component experiences its end-of-life failure, the component cannot longer be repaired, and should be replaced or upgraded depending on the system requirements. Repairable and end-of-life failures can be analysed using the bathtub curve.

The bathtub curve is usually employed to describe the relationship between the failure rate of power system components and their age [21]. As shown in Figure 2.1, the bathtub curve has three regions: the infant stage, the normal operating stage, and the wear-out stage. In the infant stage, the failure rate starts with a high value and then rapidly decreases, stabilising at time $t_1$. Failures in this region occur due to several reasons, including design and manufacturing errors, transportation and installation problems, etc. In the normal operating stage, the failure rate is approximately constant, indicating that failures occur randomly. The normal operating stage ends at time $t_2$. After this, the wear-out stage begins, and the failure rate increases due to ageing. Repairable and end-of-life failures of power system components can occur at any of these three regions. External short-circuits can cause end-of-life failures of power transformers during their normal operating stage, and repairable failures of power generators can occur during their wear-out stage. This thesis focuses on repairable and end-of-life failures that occur in the last region, i.e., age-related repairable failures and age-related end-of-life failures.

### 2.3.1 Age-Related Repairable Failure Models

Repairable failures of power system components can be modelled as an up-down-up cycle [18], as depicted in Figure 2.2. This cycle can also be described as a sequence of up times and down times. An up time is also known as time to failure (TTF), and a down time is also known as time to repair (TTR). When components show no signs of ageing, up times

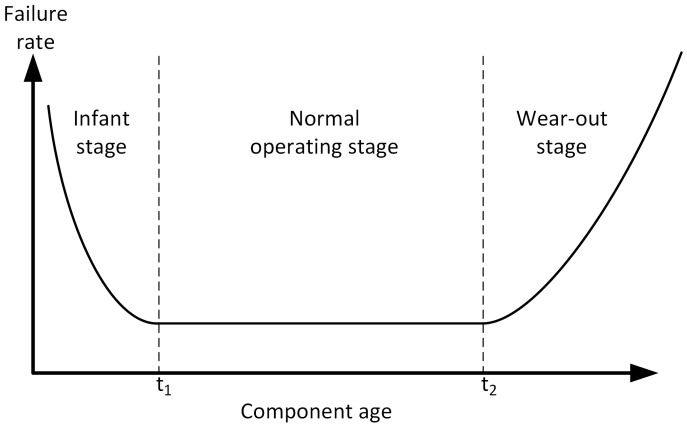


FIGURE 2.1: Idealised bathtub curve [22]

are modelled using a homogeneous Poisson process, in which the times between successive failures are independent and identically distributed [23]. A homogeneous Poisson process has constant failure rate, and has been commonly used in power system risk assessment studies.

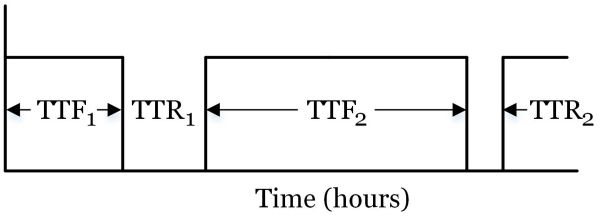


FIGURE 2.2: Up-down-up cycle of a two-state component [18]

When component ageing is taken into account, up times can be modelled using a nonhomogeneous Poisson process. In this case, the times between successive failures are not independent and identically distributed [23]. The failure rate of a nonhomogeneous Poisson process increases over time, and can be modelled using the failure rate function of the two-parameter Weibull distribution [24]. This case is known as Weibull process, in which only the time to the first failure is Weibull distributed [25]. More details on the Weibull process are given in Chapter 3, Subsection 3.3.2.

To calculate the parameters of the failure rate function, consecutive inter-failure times of identical components that have shown ageing signs are required [23]. However, collecting this information is a difficult task, due to the following reasons: power system components have long lifespans (e.g., the average lifetimes of underground cables and overhead conductors that operate at $\geq$110 kV are 51 and 54 years, respectively [15]), and power system components may operate under different loading and weather conditions, factors that can affect both their ageing process and their failure times. Despite the problem of failure time data availability, several works ([26], [27]) have employed the failure rate function of the Weibull process to model repairable failures of ageing underground power distribution cables.

The authors of [26] utilised another type of data to calculate the scale and shape parameters of the Weibull distribution. They employed annual cable failure data, without identifying whether failures are due to random events or ageing. Then, the parameters are calculated by using the maximum likelihood method.

In [27], repairable failures of ageing cables are modelled by combining the failure rate function of the Weibull process with the Arrhenius relationship. To this end, the authors of the study assumed that cable sections of a distribution feeder are identical components. The Arrhenius relationship, which models the lifetime of cable insulation as a function of its temperature, is used to calculate the scale parameter ($\alpha$) of the Weibull distribution. Cable temperatures are calculated using the standard IEC (International Electrotechnical Commission) 60287-1-1 and loading data. A methodology is proposed to determine the Arrhenius relationship parameters. The parameter $\beta$ of the Weibull distribution was not calculated in the study, and took values between 1.0 and 1.8 to describe different degrees of ageing. The proposed model is called IEC-Arrhenius-Weibull model.

Two observations can be made regarding the IEC-Arrhenius-Weibull model. First, its authors did not explain the following: why are repairable failures of ageing cables influenced by the lifetime of their insulation? Second, it is assumed that loading conditions of cables influence the occurrence of their repairable failures. The latter idea has also been investigated in [28] and mentioned in [29].

The influence of loading conditions on failure times of power cables is explored in [28]. A mathematical model was developed to calculate failure times considering short-term and long-term emergency loading conditions. The model also depends on two coefficients that incorporate information of power cables (e.g., information on installation, condition, and degradation risks).

As mentioned in [29], the influence of loading conditions on cables' repairable failures may be investigated using the model proposed in [30]. The model combines the failure rate function of the two-parameter Weibull distribution with an exponential function. The exponential function is utilised to integrate the effect of loading conditions. However, no previous study has applied this modelling approach for ageing power distribution cables.

### 2.3.2 Age-Related End-of-Life Failure Models

The incorporation of age-related end-of-life failures (also known as ageing failures) into power system risk assessment studies was first investigated in [31]. The author of the study developed a method, whose theoretical details are presented in Chapter 3, Section 3.3.3, to calculate the unavailability due to ageing failure, which is the parameter needed for risk assessment studies. The unavailability due to ageing failure of a component is determined by calculating the probability of transitioning to ageing failure within a time period (usually one year), given the service age of the component. This probability is

calculated using normal or Weibull distributions, whose parameters are determined using end-of-life failure data (which consist of two parts: the year in which components were installed, and the year in which components were retired). Then, the unavailability due to ageing failure and the non-sequential Monte Carlo technique are used to sample system states. A 230-kV transmission system was used to analyse the impact of ageing failures of cables on the system EENS index. The results showed that both the unavailability due to ageing failure and the system EENS index increase significantly as cables get older.

A different method to calculate the unavailability due to ageing failure is proposed in [32]. The method can be applied only when the normal distribution is utilised to calculate the probability of transitioning to ageing failure. The results are very similar to the ones obtained with the previous method [31].

Building ageing failure models of power system components is a difficult task, because electric utilities have limited end-of-life failure data of their equipment. Electric utilities have retired only a small amount of their components because of their long lifetimes and limited budgets [15]. Furthermore, random events, such as maintenance errors, lightnings, natural disasters, may cause end-of-life failures of power system components [33]. In this case, end-of-life failure data cannot be used to build ageing failure models.

The availability of end-of-life failure data of power transformers has been investigated. In [6], failures of power transformers installed in the United Kingdom were analysed. The statistical analysis determined that failures of power transformers are random in nature, i.e., transformer failures are not age related. Furthermore, the authors of [34] argue that some electric utilities own small fleets of power transformers; and therefore, enough end-of-life failure data are not available for the calculation of the ageing failure model parameters.

Several works have addressed the problem of lack of data for ageing failure modelling. In [35], a method that uses both end-of-life failure data of retired components and survival data (i.e., service age data) of existing components was developed to calculate the parameters of normal or Weibull distributions. The influence of survival data on ageing failure models of power transformers is investigated in [36], [37]. The results indicate that utilising survival data can make ageing failure models more accurate. The authors of [38] and [39] analyse the uncertainty in ageing failure models of power transformers and transmission lines, and quantify its effect on the system EENS index. Other ways to address the problem of limited data for power transformer ageing failure modelling will be discussed in the next section.

## 2.4 Retirement of Power Equipment

Ageing failure models of power system components are crucial for planning their retirement. These models have been incorporated into advanced retirement approaches. In [4], an approach to determine the year in which a piece of equipment should be retired was developed. The year of retirement is determined by comparing two variables: the expected system damage cost and the saved capital due to delaying the retirement of the equipment. This comparison is performed annually and over a future planning period. The expected system damage cost is the potential cost that ageing failures of power equipment would produce, and is calculated by multiplying the system EENS index by the service interruption cost. As explained in Section 2.3.2, the system EENS index captures the effects of equipment ageing failures. The saved capital due to delaying the retirement of a piece of equipment is calculated by multiplying the investment cost by an interest rate. The retirement year is found when the cumulative expected system damage cost is greater than the cumulative savings of the investment interests. This approach has been

used in other research works to further analyse the retirement of power equipment and its components.

The approach mentioned above was applied in [40] to decide which components of an HVDC system should be replaced. The HVDC system is part of a power transmission system, and the authors of the study considered that the HVDC system can operate at derated capacities if any of its components fail. The derated capacity operation of the HVDC system was included in the risk assessment of the transmission system.

The authors of [41] modified the approach given in [4] to allow the retirement of two or more aged power system components. Firstly, an index is utilised to identify the most important components for the reliability of a transmission system. Retirement scenarios with the biggest beneficial impacts on system reliability indices are then determined through Pareto analysis. Finally, the economic comparison, previously described, is performed for each scenario. A test system with aged power transformers was used to evaluate the improved retirement strategy. End-of-life failure data and survival data of UK power transformers were used to calculate the parameters of the ageing failure model.

The retirement strategies developed in [4], [40], [41] do not include two important aspects of power transformers: condition and loading level. In some cases, old power transformers can be in good or acceptable condition; and therefore, they should not be retired. The condition of power transformers has been included in other studies [42], [43]. Power transformer retirement decisions should also consider loading levels, because transformers with higher loading levels can deteriorate faster than transformers with lower loading levels [22]. These factors, condition and loading levels of power transformers, have been recently analysed.

The conventional ageing failure model is modified in [44], [45] to consider the influence of loading levels of power transformers. Instead of the traditional annual load curve, six

loading levels are utilised to calculate the temperature of power transformers. Then, the Arrhenius relationship uses these temperatures to estimate the lifetime of their insulating paper, and this value is used for the scale parameter of the Weibull distribution. The studies also include a method for the calculation of the Arrhenius relationship parameters.

The studies mentioned above (i.e., [44], [45]) have some drawbacks. First, the unavailability due to ageing failure of power transformers cannot be calculated annually, because the authors used the time intervals of their multi-step load model; and hence, the unavailability values cannot be used in the retirement strategy proposed in [4]. Second, the method for the calculation of the Arrhenius relationship parameters does not take into account that transformers accumulate moisture over time, and this reduces the lifetime of their insulating paper.

The authors of [46] also modified the retirement strategy given in [4] by incorporating condition monitoring information of power transformers. Data of carbon monoxide, carbon dioxide, and furanic compounds are used to calculate a condition-based age of the insulating paper of several power transformers. The service age of power transformers used in their ageing failure model is substituted for the condition-based age of their insulating paper.

The previous study,[46], has some drawbacks. The content of carbon monoxide and carbon dioxide can indicate ageing of the insulating paper, but it can also indicate ageing of the insulating oil [47]. Therefore, using data of carbon monoxide and carbon dioxide to calculate the age of the insulating paper potentially yields to inaccurate results. Moreover, the condition of other important components of power transformers, such as bushings, windings, tap changer, is excluded in the study. A better approach is needed to incorporate condition monitoring information of power transformers into their ageing failure model and

retirement decisions. The approach should consider the overall condition of transformers, and this could be achieved by using their health index.

A health index that evaluates the overall condition of circuit breakers was calculated and incorporated into the failure model proposed in [48]. The index uses data of different parameters, including moisture, gas pressure, and closing action times. Studies [46] and [48] show that researchers are interested in developing methods to incorporate condition monitoring data of power system components into conventional failure models.

Strategies that do not use ageing failure models for planning the retirement of power equipment are described in [27], [49], [50]. These studies employ unconventional models of age-related repairable failures and the sequential Monte Carlo technique to plan the retirement of power distribution equipment (underground cables and overhead conductors). Ageing failures are not considered in the risk assessment because they, as explained in Section 2.3, allow only one state transition, and this is not compatible with the sequential Monte Carlo technique [17]. In other words, ageing failures can be incorporated into power system risk assessment only if the non-sequential Monte Carlo technique is employed. The studies also employ component level reliability indices to prioritise the retirement of power distribution equipment. Component level reliability indices will be analysed in the next section of this chapter.

## 2.5 Ranking Indices of Power System Components

Systems used in engineering applications, such as transmission and distribution systems, have multiple components that are connected and operate together. Some components are more important (critical) than others for the reliability of a system. The importance of a component depends on both its location in the system and its reliability performance

measure [51]. The failure probability or the failure rate of a component can be used to measure its reliability performance (i.e., its ability to operate correctly). Identifying the most important components of a power system enables us to prioritise maintenance or retirement activities. To this end, several component level reliability indices (also known as measures of component importance) can be used, depending on the aim of the study (e.g., maintenance or retirement).

Several component level reliability indices have been proposed to rank power system components. The authors of [52] employ three indices to identify the most important components of a transmission system. The indices utilise constant failure rates and evaluate the impact of random failures on the system security margin, the load supply, and the generating units. An index that calculates the total system energy cost is proposed in [53]. To calculate the total system energy cost, random failures of power generators, transmission lines, and power transformers as well as equipment ratings given by manufacturers, load profiles, and power generation bids are considered.

In [54], critical components of composite generation and transmission systems are identified through an index that calculates both the probability of outages caused by cut sets (events in which several components fail at the same time) and the amount of load shedding caused by outages of components that belong to cut sets. Another index is proposed in [55]. The index calculates the impact that small changes in the failure rates of components have on the expected system interruption cost. Furthermore, the authors of [41] propose an index to prioritise the retirement of power transformers. The index uses the ageing failure model of power transformers and non-sequential Monte Carlo simulation to calculate the impact of ageing failures on the transmission system reliability.

All indices mentioned above evaluate the impact of components' random repairable failures and ageing failures on system reliability (security and adequacy). However, these

indices do not take into account other important factors, such as age-related repairable failures, operating conditions, and capacity reduction due to ageing. Further studies could improve the ranking of power system components.

## 2.6 Transmission System Reinforcement

Reinforcement of transmission systems is another topic explored in this chapter. Mathematical models for determining transmission system reinforcements can be classified into three groups [56]: heuristic models, optimisation models, and meta-heuristic models (which have heuristic and optimisation features). Optimisation models usually have an objective function and several constraints. The objective function can be minimised or maximised. The objective function and the constraints describe technical and economic aspects of transmission systems, e.g., the maximum power flow through components, generation and load-shedding costs, the maximum investment budget, etc. [57].

Optimisation models consider several reinforcement options and allow us to find the optimal reinforcement plan. Classical optimisation models used for transmission system reinforcement include linear and non-linear programming [58], [59], [60], dynamic programming [61], and mixed integer programming [62], [63]. Some parameters used in the reinforcement planning problem, such as future load demand, future generation costs, and equipment availability, are uncertain. If these uncertain parameters follow a specific probability distribution, stochastic optimisation is employed [64], [65]. On the contrary, if the uncertain parameters do not follow a specific probability distribution, robust optimisation is employed to solve the transmission system reinforcement planning problem [66].

In recent years, reinforcement of generation and transmission systems that are exposed to seismic events has been investigated. The authors of [67] formulated a two-stage

stochastic optimisation model to determine the optimal investment strategy for a composite generation and transmission system, i.e., the set of new power generators and transmission lines that should be built to mitigate potential damages due to earthquakes. Earthquakes with different magnitudes are simulated, and then the probability of damage for each power system component is calculated using fragility curves. Fragility curves use the magnitude of an earthquake as input and give the probability of damage for each component, considering that several damage levels can occur (e.g., moderate, extensive, or complete damage). Probabilities of damage are used to determine the availability of components, information that is needed before solving the stochastic optimisation model.

A different optimisation model was developed in [68]. It employs optimisation via simulation to identify transmission network investments. The behaviour of a transmission system during and after a seismic event is simulated. The simulation considers both the proposed network reinforcements and the process of disconnecting and restoring the loads of the transmission system. The simulation of events (equipment failures and load restoration) is performed using the sequential Monte Carlo technique. The proposed model calculates, through multiple simulations, the conditional expectation of the energy not supplied (ENS). The conditional expectation of ENS is the model's objective function. Fragility curves for generating units, transmission towers, and substations are used in the study.

Two remarks are made about the previous work. First, modelling and simulating the response and restoration of a power system when earthquakes occur, particularly modelling repair and replacement times of damaged equipment, are complex tasks. For instance, in the 2016 earthquake in Ecuador, personnel from different electric utilities travelled to the affected zones to help restore the electricity supply [69]. In this case, the

restoration process took several weeks. Second, earthquakes can cause end-of-life failures in some components. This is not addressed in the simulation performed in [68].

A different approach for reinforcing transmission systems is presented in [70]. Four indices are used to prioritise the replacement of substation equipment (e.g., porcelain insulators, bushings of power transformers). The indices take into account several factors: equipment seismic withstand capability, seismic performance of the transmission system, and replacement costs. Fragility curves are also used in the study to calculate the probability of damage of substation equipment.

As mentioned above, fragility curves facilitate the calculation of the probability of damage, due to an earthquake, of each power system component. However, there are some important drawbacks that make the application of fragility curves in transmission system planning studies difficult. First, building fragility curves requires large data sets for each type of component. Data sets can be obtained from actual earthquake damages, laboratory tests, or analytical approaches. The studies [67], [68], and [70] used fragility curves created by U.S. government institutions and research centres [71], [72]. Applying those fragility curves in studies of power systems located in other countries may not be correct, because there are several parameters that influence the seismic vulnerability (failure probability) of power equipment. Examples of these parameters include equipment type, voltage level, equipment manufacturer, seismic design criteria, installation and anchorage, foundations and soil conditions, and connection to other equipment [73]. The lack of data for building fragility curves is also mentioned in [74]. To solve this problem, structural models of transmission lines are employed in [74] to calculate the damage caused by windstorms.

Second, building fragility curves is a difficult task that may require expertise in other areas, such as structural engineering [72] and data analytics [75]. For example, the authors of [75] created fragility curves for overhead lines by ascribing 12,000 electrical failures to

a windstorm model, and considered the effects of the spatial resolution of the electrical failures on the fragility curves. And third, uncertainty is inherent in fragility curves, and it may affect system reinforcement decisions. Therefore, new approaches are needed to deal with the transmission system reinforcement problem.

Previous studies did not consider the impact of equipment ageing on transmission system reinforcement decisions. The influence of equipment ageing on reinforcement plans has been investigated only in a recent study [76]. Its authors proposed a two-stage stochastic optimisation model in which old power generators can be either retired or refurbished. Ageing models of power generators were not part of the solution, which assumed that their capacity reduces 3% each year.

Equipment ageing models have been used only for asset management purposes, e.g., maintenance and retirement. Transmission system reinforcement studies consider long planning periods, e.g., 20-30 years [66], in which the performance of some power system components can deteriorate significantly. Including equipment ageing in reinforcement studies could help system planners obtain more accurate investment decisions.

## 2.7 Summary

This chapter presents a critical review of the most relevant and recent models and methods used for planning the maintenance and retirement of ageing power equipment and for planning transmission system reinforcements. Several limitations of existing works were identified in this chapter. First, traditional models of age-related repairable and non-repairable failures can be further improved by developing new methodologies to incorporate the effects of loading conditions of underground power distribution system cables and power transformers, and by developing more advanced approaches to calculate the

condition-based age of power transformers and the Arrhenius relationship parameters. Second, component ranking indices can be enhanced by incorporating the effects of loading conditions, age-related failures, and capacity reduction. Third, optimisation models for reinforcing transmission systems that are subject to earthquakes can also be improved by including equipment ageing models and by developing new approaches to determine equipment availability.

These problems (or limitations) will be addressed comprehensively in the next chapters, beginning with Chapter 4 which presents a new approach for the maintenance prioritisation of ageing cables. Chapter 4 covers the second and third objectives of this thesis.

# Chapter 3

# Concepts, Models, and Techniques Used in Power System Risk Assessment

## 3.1 Introduction

As mentioned in the previous chapter, power system risk assessment comprises four main tasks: determining component failure models, sampling system states and calculating their probabilities of occurrence, determining the impacts of component failures, and calculating system risk indices. This chapter explains in detail how to perform each of these tasks, considering composite (generation and transmission) systems as well as distribution systems. This chapter also provides the necessary background information for most of the research that will be presented in the next chapters, particularly information on traditional mathematical models of age-related repairable and non-repairable failures. These mathematical models will be used in the subsequent chapters.

The chapter content is organised as follows. Probability distributions used for component failure modelling are first discussed. Then, traditional mathematical models of repairable and ageing failures are presented. The chapter continues by explaining the mains aspects of Monte Carlo simulation. Then, the procedure for determining the impacts of component failures on system operation, known as contingency analysis, is presented. Finally, this chapter provides several mathematical models used for calculating traditional system risk indices.

## 3.2 Probability Distributions in Risk Assessment

The behaviour of power system components is considered as stochastic, i.e., components of a certain type can fail at different times. This is because components are exposed to different factors, such as loading and weather conditions as well as different maintenance procedures, that may influence the ability of components to stay in operation [3], [77]. Repairable and ageing (end-of-life) failures can be modelled through random variables. When repairable failures are being analysed, two variables that are commonly used are the failure time and the repair time [78]. It is assumed that failure and repair times follow specific probability distributions (e.g., exponential, normal, Weibull). Probability distributions and other time-dependent functions are used for component failure modelling, as explained below.

Let us start with the cumulative probability distribution function. Based on probability theory, any cumulative probability distribution function increases from zero to one. The probability of ageing failure of power system components behaves in a similar way. Components with few service years have low failure probabilities. However, if they remain in service for long periods of time, their failure probabilities can eventually reach values

close to 1.0. Because of this similarity, the cumulative probability distribution function is known in power system risk assessment as the cumulative failure distribution function, $Q(t)$. The cumulative failure distribution has a complementary function known as the survivor function, $R(t)$. The relationship between the survivor function and the cumulative failure distribution is given by [18]:

$$R(t) = 1 - Q(t). \tag{3.1}$$

Another function that is commonly used in failure modelling is the probability density function, whose name also changes slightly. If the derivative of the cumulative failure distribution, $Q(t)$, is calculated, the outcome is known as the failure density function, $f(t)$, which is given by [18]:

$$f(t) = \frac{\mathrm{d}Q(t)}{\mathrm{d}t} = -\frac{\mathrm{d}R(t)}{\mathrm{d}t}. \tag{3.2}$$

Based on (3.2), $Q(t)$ and $R(t)$ can be expressed as follows [18]:

$$Q(t) = \int_0^t f(t)\,\mathrm{d}t \tag{3.3}$$

$$R(t) = 1 - \int_0^t f(t)\,\mathrm{d}t. \tag{3.4}$$

The relationships among the previously mentioned functions (cumulative failure distribution, survivor function, and failure density function) are illustrated in Figure 3.1. In this figure, time, $t$, represents the service age of a certain type of components.

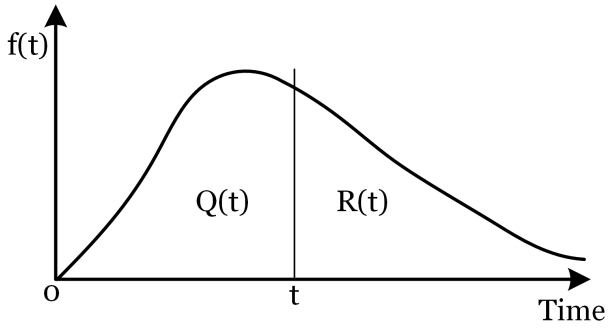


FIGURE 3.1: Hypothetical failure density function [78]

Another important function is the transition rate. The transition rate in power system risk assessment can be referred as the hazard rate (function), failure rate (function), repair rate (function), etc. When component failures are analysed, the hazard rate, $\lambda(t)$, indicates the rate at which failures occur in a specific time period. The hazard rate can be calculated by dividing the number of failures per unit time by the number of components exposed to failure, as shown in (3.5), or by dividing the failure density function by the survivor function, as shown in (3.6) [78].

$$\lambda(t) = \frac{\text{number of failures per unit time}}{\text{number of components exposed to failure}} \tag{3.5}$$

$$\lambda(t) = \frac{f(t)}{R(t)} \tag{3.6}$$

The concepts presented in this section, particularly the concepts of failure density function and failure rate, are essential for understanding the conventional mathematical models of repairable and ageing failures, which will be discussed in the next section.

## 3.3 Component Failure Models

When a power system component undergoes a repairable or ageing failure, the outcome is completely different. If a repairable failure occurs, the component is removed from service, repaired, and put back into operation. On the other hand, if an ageing failure occurs, the component must be retired from the system, and in some cases replaced by a new component. Thus, repairable and ageing failures require different modelling approaches. Stochastic processes are typically used to model random and age-related repairable failures. Two types of stochastic processes will be analysed in this chapter: Markov processes and arrival-type processes. To model ageing failures, traditional probability distributions can be employed only if enough end-of-life failure data are available.

### 3.3.1 Modelling Approach for Random Repairable Failures

Random repairable failures are usually modelled through a two-state stationary Markov process [78]. Figure 3.2 shows a two-state space diagram of a repairable component, which indicates that the component remains in one of its states (up or down) until a transition occurs. In this two-state stationary Markov process, transition rates are modelled using a constant failure rate, $\lambda$, and a constant repair rate, $\mu$. These parameters are constant because they are characterised by exponential probability distributions. The time-dependant probabilities of being found in the up and down states are given by [18]:

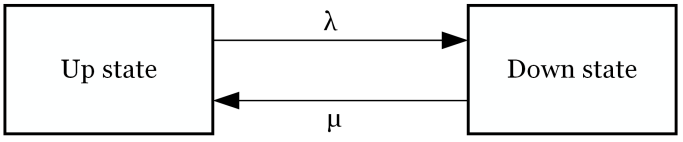


FIGURE 3.2: Two-state space diagram of a repairable component [17]

$$P_0(t) = \frac{\mu}{\lambda + \mu} - \frac{\lambda e^{-(\lambda+\mu)t}}{\lambda + \mu} \tag{3.7}$$

$$P_1(t) = \frac{\lambda}{\lambda + \mu} - \frac{\lambda e^{-(\lambda+\mu)t}}{\lambda + \mu} \tag{3.8}$$

where $P_0(t)$ and $P_1(t)$ are the probabilities of being in the up and down states, respectively.

The unavailability due to repairable failure, a steady-state failure probability required in power system risk assessment studies that employ non-sequential Monte Carlo simulation, is calculated by letting $t \to \infty$ in (3.8), as shown below [18]:

$$U = \frac{\lambda}{\lambda + \mu} \tag{3.9}$$

where $U$ is the unavailability due to repairable failure, $\lambda$ is the failure rate (in failures/year), and $\mu$ is the repair rate (in repairs/year). The derivation of (3.9) is explained in detail in [18].

If power system risk assessment studies employ sequential Monte Carlo simulation, random repairable failures are modelled differently. Instead of calculating the unavailability due to repairable failure, an artificial sequence of up and down states is generated over a time period using failure and repair rates [19]. This topic will be further discussed in Section 3.4.2.

### 3.3.2 Modelling Approach for Age-Related Repairable Failures

As mentioned above, the two-state Markov process models random repairable failures of power system components as transitions between their up and down states. However, random repairable failures are not the only ones that occur in actual power systems. Some power systems have ageing components whose performance (reliability) reduces over time.

In these cases, it is necessary to model repairable failures that are influenced by the service age of components, i.e., by their ageing process.

Age-related repairable failures can be modelled by utilising another type of stochastic process—the arrival-type process. Figure 3.3 provides an example of an arrival-type process, in which a sequence of events with magnitudes $X_1$, $X_2$, $X_3$, etc. occurs. In the context of age-related repairable failures, these events and their magnitudes represent repairable failure events and their failure times, respectively. An important characteristic of arrival-type processes is that each failure time (i.e., $X_1$, $X_2$, $X_3$,...) is modelled using different random variables. When all failure times follow an exponential distribution, the arrival-type process is known as a homogeneous Poisson process. On the other hand, when failure times do not follow an exponential distribution, the arrival-type process is known as a non-homogeneous Poisson process.

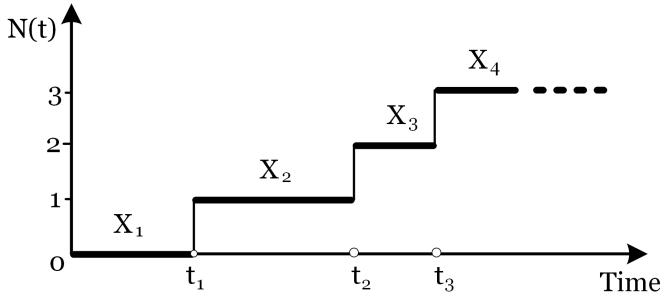


FIGURE 3.3: An example of an arrival-type process [79]

The non-homogeneous Poisson process has two important characteristics [23]. First, it allows us to incorporate the influence of service age into the failure times of ageing components. And second, when a non-homogeneous Poisson process is applied to describe the occurrence of repairable failures, the times between successive failures are not independent and identically distributed. These characteristics make the non-homogeneous Poisson process a valuable modelling tool for power systems with ageing components, and it is usually applied considering a Weibull distribution.

The Weibull process is a special case of the non-homogeneous Poisson process. In a Weibull process, only the time to the first failure follows a Weibull distribution [25]. The failure rate function of a Weibull process is given by [24]:

$$\lambda_0(t) = \lambda\beta t^{(\beta-1)} \tag{3.10}$$

where $t$ represents the component age, $\lambda$ is equal to $1/\alpha^{\beta}$, and $\alpha$ and $\beta$ are the scale and shape parameters of the Weibull distribution, respectively. The values of $\alpha$ and $\beta$ can be calculated using historical inter-failure time data of identical components.

When repairable failures are influenced by ageing, the parameter $\beta$ is greater than one, and the failure rate function shown in (3.10) increases as the age of components, $t$, increases. (However, some components can enhance their performance over time, experiencing fewer failures. In this case, their failure rate function should decrease as the age of components increases ($\beta$ is less than one) [24].) The failure rate function, $\lambda_0(t)$, is used to generate consecutive failure times of ageing components when power system risk assessment studies employ time sequential Monte Carlo simulation. Failure time sampling will be further discussed in Section 3.4.2.

Besides repairable failures, ageing components can undergo non-repairable (end-of-life) failures. This topic is analysed in the next section.

### 3.3.3 Ageing Failure Model

Ageing (end-of-life) failures of power system components are modelled differently. A key aspect of ageing failure modelling is the concept of probability of transition to ageing failure. To explain this concept, two factors must be first considered: component age, $T$, and a subsequent period, $t$; they are shown in Figure 3.4. The probability of transition

to ageing failure is defined as the probability that a component will fail within $t$ given that the component has operated for $T$ years [18]. The probability of transition to ageing failure, $P_f$, is a conditional probability (because the component age must be specified), and can be calculated as follows [31]:

$$P_f = \frac{\int_T^{T+t} f(t)dt}{\int_T^{\infty} f(t)dt} \tag{3.11}$$

where $f(t)$ is, as explained in Section 3.2, the failure density function. To model ageing failures, the probability density function of the normal (Gaussian) and Weibull distributions can be utilised. These continuous probability distributions have been extensively used in reliability engineering because they can model different types of lifetime behaviours [22].

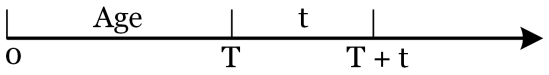


FIGURE 3.4: Diagram used to explain the concept of probability of transition to ageing failure [17]

Ageing failures cannot be incorporated into power system risk assessment studies using (3.11); it is necessary to calculate the unavailability due to ageing failure. This parameter allows us to determine, during the non-sequential Monte Carlo simulation, whether a component is in the up or down state. The unavailability due to ageing failure is considered as the average probability that a component will fail within $t$ given that it has survived for $T$ years [31]. To calculate this parameter, the subsequent period $t$ is divided into $N$ intervals with length $\Delta x$, as shown in Figure 3.5. The probability of transition to ageing failure in the sub-periods $t_0$ and $t_1$, $t_0$ and $t_2$, ..., $t_0$ and $t_n$ is calculated as follows [31]:

$$P_f = \frac{\int_T^{T+t_i} f(t)dt}{\int_T^{\infty} f(t)dt} \qquad (i = 1, 2, ..., N). \tag{3.12}$$

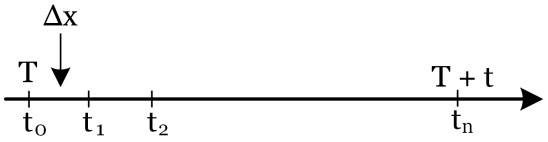


FIGURE 3.5: Intervals in time period $t$ [17]

The probability of failure in the $i$th interval, $P_i$, can be calculated through the difference between two consecutive $P_f$ [31], as shown in (3.13).

$$P_i = \frac{\int_T^{T+i\Delta x} f(t)dt - \int_T^{T+(i-1)\Delta x} f(t)dt}{\int_T^{\infty} f(t)dt} \qquad (i = 1, 2, ..., N) \tag{3.13}$$

Calculating $P_i$ is a computationally intensive task due to the integrals. However, its calculation can be approximated; this will be discussed later in this section.

Therefore, the unavailability due to ageing failure for the subsequent period $t$ (typically one year) is calculated as follows [31]:

$$U_a = \sum_{i=1}^{N} P_i \frac{UD_i}{t} \tag{3.14}$$

where $UD_i$ is the average unavailable duration for the $i$th interval, and is given by [31]:

$$UD_i = t - (2i - 1)\frac{\Delta x}{2} \qquad (i = 1, 2, ..., N). \tag{3.15}$$

Equation (3.13) is substituted for an approximation (this allows us to easily calculate the unavailability due to ageing failure, $U_a$). When the normal distribution is utilised, $P_i$ can be calculated as follows [31]:

$$P_i = \frac{Q\left(\frac{T+(i-1)\Delta x-\mu}{\sigma}\right) - Q\left(\frac{T+i\Delta x-\mu}{\sigma}\right)}{Q\left(\frac{T-\mu}{\sigma}\right)} \qquad (i = 1, 2, ..., N) \tag{3.16}$$

where

$$Q(y) = \begin{cases} w(y) & \text{if } y \geq 0 \\ 1 - w(-y) & \text{if } y < 0 \end{cases} \tag{3.17}$$

$$w(y) = z(y)(b_1 s + b_2 s^2 + b_3 s^3 + b_4 s^4 + b_5 s^5) \tag{3.18}$$

$$z(y) = \frac{1}{\sqrt{2\pi}} \exp\left(-\frac{y^2}{2}\right) \tag{3.19}$$

$$s = \frac{1}{1 + ry} \tag{3.20}$$

and $r = 0.2316419$, $b_1 = 0.31938153$, $b_2 = –0.356563782$, $b_3 = 1.781477937$, $b_4 = –1.821255978$ and $b_5 = 1.330274429$. On the other hand, if the Weibull distribution is employed, $P_i$ is given by [31]:

$$P_i = \frac{\exp\left[-\frac{T+(i-1)\Delta x}{\alpha}\right]^{\beta} - \exp\left[-\frac{T+i\Delta x}{\alpha}\right]^{\beta}}{\exp\left[-\frac{T}{\alpha}\right]^{\beta}} \qquad (i = 1, 2, ..., N). \tag{3.21}$$

The parameters of the normal and Weibull distributions, ($\mu$, $\sigma$) and ($\alpha$, $\beta$) respectively, in (3.16) and (3.21) are calculated using historical end-of-life failure data. It is also important to mention that if the unavailability due to ageing failure is calculated for several years, the component age, $T$, must be updated after each year.

Determining failure and repair rates as well as the unavailability due to repairable and ageing failures is just the first step for power system risk assessment. The next section explains how these values are utilised to randomly generate system states.

## 3.4 Monte Carlo Simulation

Non-sequential and sequential Monte Carlo simulations are essential simulation techniques in power system risk assessment. They enable us to generate system states, taking into account failure rates, repair rates, and failure probability (unavailability) of power system components. In this section, the basic principles of these simulation techniques are described.

### 3.4.1 Non-Sequential Monte Carlo Simulation

The non-sequential Monte Carlo simulation is also known as the state sampling approach, because it randomly determines the states of all system components. The state of a component is obtained by comparing a random number that follows a uniform distribution between $[0, 1]$ with the component's failure probability. The comparison determines if either the component is in the success (up) state or the component is in the failure (down) state. The comparison is explained below [78]:

$$s_i = \begin{cases} 0 & \text{(success state)} \quad \text{if } R_i \geq Q_i \\ 1 & \text{(failure state)} \quad \text{if } 0 \leq R_i < Q_i \end{cases} \tag{3.22}$$

where $s_i$ is the state of the $i$th component, $R_i$ is a random number, and $Q_i$ is the failure probability (unavailability) of the $i$th component.

When a power system has aged components, their states must be determined considering both their unavailability due to repairable failure ($U$) and their unavailability due to ageing failure ($U_a$). In this case, two separate random numbers must be employed for each component.

Power systems have multiple states, which can be determined after knowing the states of all components. The state of a system with $m$ components can be expressed using the following vector $s$ [78]:

$$s = (s_1, ..., s_i, ..., s_m). \tag{3.23}$$

Each system state has a probability of occurrence. The probability of the system state $s$ can be calculated using (3.24) if the number of samples used in power system risk assessment studies is sufficiently large [17], [78].

$$P(s) = \frac{m(s)}{M_s} \tag{3.24}$$

where $M_s$ is the number of samples, and $m(s)$ is the number of times the system state $s$ appears during the sampling.

### 3.4.2 Sequential Monte Carlo Simulation

The sequential Monte Carlo simulation is also known as the state duration sampling approach, and can be applied only for repairable failures. This simulation technique generates an artificial sequence of up and down states over a period of time for each system component. Then, these sequences are combined to determine the system state. The steps for the simulation process are described below [17], [78].

- Specify the initial state of each component. It is usually assumed that all components start with the success (up) state.
- Sample the duration of each component staying in its current state, using state duration distribution functions. When these functions follow an exponential distribution,

the duration of the $i$th component state ($D_i$) can be calculated by:

$$D_i = -\frac{1}{\lambda_i} \ln(R_i) \tag{3.25}$$

where $R_i$ is a uniformly distributed random number between $[0, 1]$ for the $i$th component, $\lambda_i$ is the failure rate if the $i$th component is in the up state, and $\lambda_i$ is the repair rate if the $i$th component is in the down state.

It is important to mention that when aged-related repairable failures are incorporated into power system risk assessment, up times of components cannot be determined using (3.25). Other sampling techniques are required, and will be described in the next chapter.

- Repeat the previous step throughout the simulation period, and save the sampled values (the duration of up and down states). This simulation process yields chronological state transitions for each component, such as the one illustrated in Figure 2.2.

- Determine the state sequence of the system by combining the up-down-up cycles of all its components.

- Analyse all system states and calculate the system risk indices. The calculation of system risk indices when the sequential Monte Carlo simulation is used will be discussed in Section 3.6.

## 3.5 Risk Assessment of Composite Systems

The main aspects of contingency analysis and the calculation of system risk (adequacy) indices are presented in this section. Understanding how to perform these tasks is vital

for assessing the risk of a composite (generation and transmission) system.

### 3.5.1 Contingency Analysis

Failures of generating units, transmission lines, and power transformers can cause several problems to a composite system, including violations of thermal and voltage limits as well as load shedding. These problems can be identified in power system risk assessment studies. When several generating units are located at the same bus, contingencies can be identified as follows [78]. When a generating unit fails, the other units may not be operating at their full capacity, so they can be used to supply the load demand of the failed unit. If the available generating capacity cannot supply the local load demand, then it is necessary to reschedule the power generation in the system through an optimal power flow (OPF) model. An OPF model determines whether power generation changes avoid load curtailments. Two models can be applied: the AC power-flow-based OPF model (which is a non-linear programming problem) and the DC power-flow-based OPF model (which is a linear programming problem) [17].

Identifying contingencies due to failures of lines or power transformers is more difficult. If lines and/or power transformers fail, problems, such as overloading, voltage violations, and isolating buses, can be identified by performing load flow calculations. Load flow calculations shall consider the annual load curve of each load point (a load modelling approach will be described in detail later in the chapter). If problems exist, then remedial actions, generation rescheduling and load shedding, shall be carried out using any of the OPF models previously mentioned and considering failures of generating units.

As mentioned above, load modelling is an important aspect in a contingency analysis, particularly in load flow studies. Traditional annual load curves contain load levels that are chronologically ordered. To incorporate annual load curves in composite system risk assessment, three approaches can be used [78]: sampling of load states, multi-step load models, and sampling load levels using multi-step models. The second approach is typically used due to its computational merits, and consists of two main steps [78]. First, the annual load curve is converted into a load duration curve whose load levels are arranged in a descending order. Second, the load duration curve is approximated by a multi-step load model, which is created using the k-means algorithm as explained below.

The k-means algorithm is a clustering technique that groups the load duration curve's 8760 elements into several load levels (also known as clusters). Each cluster contains multiple load points whose mean value is the cluster's load level. The iterative process to create a multi-step load model is the following [78]:

- Choose initial cluster means, $M_i$, where $i$ represents cluster $i$ ($i = 1, ..., NL$).
- Calculate the distance between hourly load points $L_k$ ($k = 1, ..., 8760$) and their cluster mean. This distance is denoted as $D_{ki}$ in (3.26).

$$D_{ki} =\mid M_i - L_k \mid \tag{3.26}$$

- Assign load points to their nearest cluster, and then calculate new cluster means as follows:

$$M_i = \frac{\sum_{k \in IC} L_k}{NI_i} \tag{3.27}$$

  where $NI_i$ is the number of load points of cluster $i$, and $IC$ is a set that contains the load points of cluster $i$.

- Repeat the last two steps until the cluster means do not change between iterations. The final values of $M_i$ and $NI_i$ represent the load level in MW and the time length in hours of the $i$th step, respectively.

Derated states of generating units and the effects of regional weather on transmission line availability can also be included in the contingency analysis of composite systems. Further information on these topics can be found in [78].

### 3.5.2 Adequacy Indices for Composite Systems

Risk (adequacy) indices allow us to measure the adequacy of composite power systems taking into account component failures and ratings, loading patterns, and system configuration. To include all these factors, risk indices are calculated, during Monte Carlo simulations, as the expected values of random variables. Several risk indices can be used for assessing the risk of composite systems. Two commonly used indices are shown below [17]:

1. Probability of load curtailment (PLC):

$$\text{PLC} = \sum_{i=1}^{NL} \left( \sum_{s \in F_i} P(s) \right) \frac{T_i}{T_{tp}} \tag{3.28}$$

   where $P(s)$ is the probability of system state $s$, $F_i$ is the set of all failure system states at the $ith$ load level, $T_i$ is the time length of the $ith$ load level, and $T_{tp}$ is the total period (in hours) of the annual load curve.

2. Expected energy not supplied (EENS, MWh/period):

$$\text{EENS} = \sum_{i=1}^{NL} \left( \sum_{s \in F_i} P(s) C(s) \right) T_i \tag{3.29}$$

where $C(s)$ is the curtailed load (in MW) in the state $s$.

The indices PLC and EENS can be calculated for single buses or for the entire system. If they are calculated for single buses, $F_i$ contains only system states that cause load curtailments at each bus.

Figure 3.6 shows the basic steps for composite system risk assessment that were described in Sections 3.4 and 3.5.

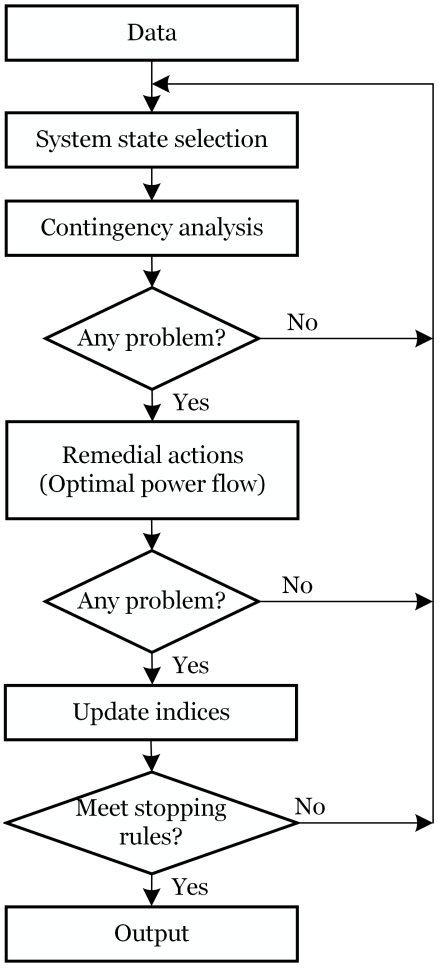


FIGURE 3.6: Basic steps for composite system risk assessment [17]

## 3.6 Risk Assessment of Power Distribution Systems

Power distribution systems mainly consist of distribution substations, primary (main) and lateral feeders, distribution transformers, secondary circuits, and consumers' connections [19]. Electric power is distributed through main feeders and lateral distributors. Main feeders originate from distribution substations and can be built using different configurations, e.g., single, parallel, or meshed circuits. Distribution systems that use single-circuit main feeders are known as radial distribution systems. If a distribution system has meshed feeders, they can be converted into radial feeders by opening their switches. Distribution transformers are connected to lateral feeders, and are responsible for supplying the consumers' load demand. However, a continuous electric power supply is not always possible.

Failures of distribution system components can affect the connection between supply points and load points, causing service interruptions [78]. When component failures occur, service interruptions depend on the switching logic of breakers and section switches as well as on backup supply sources. All these factors that influence the electric power supply must be considered in distribution system risk assessment studies.

In risk assessment of power distribution systems, non-sequential and sequential Monte Carlo simulation can be used. Most studies employ the state duration sampling approach (sequential Monte Carlo simulation), because frequency and duration risk indices can be calculated at each load point [19]. These indices give customers an estimate of the interruptions' frequency and duration. Another advantage of using the state duration sampling technique is that probability distributions of risk indices can be calculated.

To evaluate the performance of power distribution systems using the state duration sampling approach, the following procedure must be considered [17], [19]:

1. Generate artificial up-down-up operating cycles for all distribution system components (feeder sections, distribution transformers). To do this, utilise their failure and repair rates and (3.25), for random repairable failures.

2. Create up-down-up operating histories for all load points, considering component failures, system configuration, and switching logic of breakers and section switches. Load points' operating histories are similar to components' operating cycles, which are illustrated in Figure 2.2.

3. Calculate the basic load point indices (average outage rate, average outage duration, and average annual outage time) as follows:

$$\lambda_i = \frac{M_i}{\sum T_{ui}} \tag{3.30}$$

$$r_i = \frac{\sum T_{di}}{M_i} \tag{3.31}$$

$$U_i = \frac{\sum T_{di}}{\sum T_{ui} + \sum T_{di}} \tag{3.32}$$

   where $\lambda_i$, $r_i$, and $U_i$ are the average outage rate, outage duration, and annual outage time of the $i$th load point, respectively. $M_i$ is the number of outages of the $i$th load point. $\sum T_{ui}$ and $\sum T_{di}$ are the total up and down times of the $i$th load point.

4. Calculate the system indices and their average values for each year. (Typical system indices are described later.)

5. Repeat this procedure until completing the total simulation years.

### 3.6.1 Adequacy Indices for Distribution Systems

Two risk indices commonly used for power distribution systems are the following: the System Average Interruption Frequency Index (SAIFI) and the System Average Interruption Duration Index (SAIDI). They are calculated using the basic load point indices $\lambda_i$ and $U_i$ as follows [18]:

$$\text{SAIFI} = \frac{\sum_{i \in R} \lambda_i N_i}{\sum_{i \in R} N_i} \qquad \text{(interruptions/system customer/year)} \tag{3.33}$$

$$\text{SAIDI} = \frac{\sum_{i \in R} U_i N_i}{\sum_{i \in R} N_i} \qquad \text{(hours/system customer/year)} \tag{3.34}$$

where $\lambda_i$ and $N_i$ are the average outage rate and the number of customers of the $i$th load point, respectively. $R$ is the set of load points, and $U_i$ is the average annual outage time of the $i$th load point.

## 3.7 Summary

This chapter presents basic concepts, mathematical models, and techniques used in power system risk assessment. An essential concept is the use of time-dependent probability functions to model the behaviour of power system components. Components' random repairable failures are usually modelled using a two-state stationary Markov process, whereas components' age-related repairable failures can be modelled using a non-homogeneous Poisson process. A special case of the non-homogeneous Poisson process, known as the Weibull process, will be utilised in the next chapter (Chapter 4) for modelling age-related repairable failures of underground power distribution system cables and for prioritising their maintenance. Ageing failures are modelled using a different approach, in which both the probability of transition to ageing failure and the unavailability due to

ageing failure must be calculated. This modelling approach will be employed in Chapter 5. The chapter includes a description of the non-sequential and sequential Monte Carlo simulation techniques, which allow us to sample system sates. Finally, the main aspects of contingency analysis and the calculation of some important system risk indices (EENS, SAIFI, and SAIDI) are described.

# Chapter 4

# Maintenance Prioritisation of Power Distribution System Cables Considering Age-Related Repairable Failures[1]

## 4.1 Introduction

Cables used in power distribution systems age over time. Their ageing is a complex process influenced by several factors, including loading and soil conditions, mechanical stress, manufacturing imperfections, and maintenance. Ageing cables tend to have higher failure probabilities, which increase the risk of service interruptions [82]. Therefore, it is essential to identify which cables in a power distribution system pose the highest risks, so

[1]This chapter is based on publications [80] and [81].

that their maintenance can be prioritised. In other words, maintenance activities should be targeted at ageing cables whose failures might cause the highest economic losses.

As explained in Chapter 2, previous studies [52]-[55] have proposed several indices to create rankings of power system components, including underground cables. However, those indices take into account only random repairable failures, neglecting other important factors, such as ageing and loading conditions. The influence of ageing and loading conditions on repairable failures of cables has been studied in [26]-[28], but those studies have not integrated these factors (ageing and loading conditions) into cables' rankings and maintenance prioritisation. Hence, further research is needed in this area.

This chapter presents an approach to incorporate the effects of both ageing and loading conditions into an index used to rank power distribution system cables. The approach includes an age-related repairable failure model, which combines the failure rate function given in [30] with a method that converts the time-varying load of cables into a constant equivalent load, and a methodology to calculate the model parameters. Age-related repairable failures of cables are then included in the calculation of the maintenance potential index, which was slightly modified to capture the impacts of random and age-related repairable failures. *The proposed approach is the first contribution of this thesis, and was published in [80].*

The proposed approach has two benefits. It identifies the most important cables of a power distribution system taking into account their age-related repairable failures and their respective loading conditions. Asset managers can leverage advanced cable rankings to target maintenance activities at critical ageing cables to make sure power distribution systems operate reliably. Moreover, the approach provides an age-related repairable failure model for underground cables that can be used not only for maintenance planning studies but also for power distribution system reliability studies.

This chapter also presents a detailed comparison between the age-related repairable failure model mentioned above and the age-related repairable failure model proposed in [27]. Their modelling assumptions, methods for incorporating cables' loading conditions, and parameter estimation approaches are critically analysed. Furthermore, the performance of both models is carefully evaluated, by plotting cable failure rates and creating cable rankings. *This comprehensive analysis of two age-related repairable failure models of underground cables is the second contribution of this thesis, and was published in [81].*

## 4.2 Age-Related Repairable Failure Model for Underground Power Distribution Cables

Age-related repairable failures of medium voltage underground cables can be modelled using a non-homogeneous Poisson process if two important assumptions are made: all cable sections are identical components, and the occurrence of cable failures is influenced by loading conditions. The failure rate function given in [30] is used to model the occurrence of age-related repairable failures of cables, and is given by:

$$\lambda_x(t) = \lambda_0(t) g(\boldsymbol{x}; \boldsymbol{\delta}) \tag{4.1}$$

where $\lambda_0(t)$ is a baseline failure rate function, $t$ represents the service age of cables, $g(\boldsymbol{x}; \boldsymbol{\delta})$ is a positive-valued function used to incorporate the loading conditions of cables, $\boldsymbol{x}$ is a $k \times 1$ covariate vector (which can contain information on the loading patterns of cables or other stress factors), and $\boldsymbol{\delta}$ is a vector of parameters.

The failure rate function of the Weibull process, which is a special non-homogeneous Poisson process, is used for $\lambda_0(t)$ as follows:

$$\lambda_0(t) = \lambda\beta t^{(\beta-1)} \tag{4.2}$$

where $\lambda$ is equal to $1/\alpha^{\beta}$, and $\alpha$ and $\beta$ are the scale and shape parameters of the Weibull distribution.

Furthermore, an exponential function with one covariate is employed to incorporate the effects of cables' loading conditions into (4.1), as suggested in [30]. Therefore, the failure rate model given in (4.1) can be written as follows [80]:

$$\lambda_x(t) = \lambda\beta t^{(\beta-1)} \exp(\delta_1 x_1) \tag{4.3}$$

where $x_1$ is the equivalent load (in per unit) of a cable section, and $\delta_1$ is a parameter of the exponential function. The subscript 1 indicates that one covariate, $x_1$, is used for the failure rate model; and hence, the covariate vector $\boldsymbol{x}$ in (4.1) has a single element.

### 4.2.1 Calculation of Cables' Equivalent Load

The equivalent load of cable sections, $x_1$, is calculated by using the method given in [83]. This method was originally designed for mineral-oil-immersed transformers, and it is assumed that it can also be applied for underground cables [80]. The method converts a time-varying load into a constant equivalent load that produces the same total losses from a temperature standpoint. The equivalent load of a cable section for a one-year period is

calculated as follows [83]:

$$x_1 = \left[ \frac{L_1^2 t_1 + L_2^2 t_2 + ... + L_{M_{ls}}^2 t_{M_{ls}}}{t_1 + t_2 + ... + t_{M_{ls}}} \right] \quad \text{(p.u.)} \tag{4.4}$$

where $L_1,\ L_2,\ ...,\ L_{M_{ls}}$ are the loading conditions (in p.u.) of a cable section (which are calculated using backward/forward sweep power flow methods and hourly peak load demand data), $t_1,\ t_2,\ ...,\ t_M$ are the duration of the load steps, and $M_{ls}$ is the total number of load steps. Since $x_1$ is calculated using hourly load demand data and a one-year period, the values of $t_i$ and $M_{ls}$ are 1 and 8,760 hours, respectively.

### 4.2.2 Parameter Estimation

The failure rate model given by (4.3) has three parameters—$\alpha$, $\beta$, and $\delta_1$—that must be calculated using consecutive failure times of a group of cable sections. To understand the meaning of consecutive failure times, see Figure 3.3, which shows a sequence of events with magnitudes $X_1, X_2, ..., X_n$. This sequence of events may represent the occurrence of age-related repairable failures of a cable section, and in that case, the magnitudes $X_1, X_2, ..., X_n$ represent consecutive failure times $TTF_1,\ TTF_2,\ ..., TTF_n$. Consecutive failure times of a group of cables must reflect that the number of failures increases as cables get old. In other words, consecutive failure times must indicate that an ageing trend exists.

However, collecting consecutive failure times of ageing cables is a challenging task for asset managers due to the following reasons: cables have long lifetimes (typically between 40 and 70 years [84]), the type of failure (random or age-related) may not be properly identified, and some electric utilities own a great number of cables. On other hand, if cable failure times are available, they may indicate that an ageing trend does not exist, as

investigated in [85]. The study revealed that XLPE cables that operated in Denmark for at least 30 years did not show signs of ageing. That is, their failures occurred randomly.

Consecutive failure time data of cable sections are not available in the power system literature, so an iterative approach for generating artificial consecutive failure times of ageing cables and for estimating the parameters of the failure rate model is proposed.

The approach comprises six steps, which are described below [80]:

- Step 1: Choose a power distribution system, and collect its technical data (hourly load demand data as well as the resistance, reactance, lengths, ratings, and constant failure rates of cables). Artificial failure times of the power distribution system's cable sections are created using the Thinning method (Step 4), considering that they are subject to different loading conditions, and assuming that cable sections have operated for several decades. In other words, the system is used to generate failure times of its ageing cables; information that is not available for actual power distribution systems.

- Step 2: Calculate the equivalent load of each cable section of the power distribution system selected in the previous step, using (4.4) and the year with the highest load demand. The year with the highest load demand is utilised because it is the scenario in which cable sections are more stressed, and this may influence the occurrence of age-related repairable failures.

- Step 3: Classify cable sections into two groups: the first group contains cables with high equivalent loads, whereas the second group contains cables with low equivalent loads. This step is performed to consider, in the generation of failure times (Step 4), that cable sections with higher loading levels may experience more repairable failures than cable sections with lower loading levels.

- Step 4: Generate artificial consecutive failure times for each cable section using the Thinning method. The Thinning method randomly generates a sequence of failure times $(S_0, S_1, ..., S_n)$ over the interval $[0,\ T]$ as follows [86]:

$$S_i = S_{i-1} - \frac{1}{K}\log(U_i) \qquad (i = 0, 1, ..., n) \tag{4.5}$$

where $S_0 = 0$, $U_i$ is a uniformly distributed random number between $[0,\ 1]$, and $K$ is given by:

$$K = \max_{\{0 \le t \le T\}} \lambda_s(t) < \infty \tag{4.6}$$

where $\lambda_s(t) = \lambda_s \beta_s t^{(\beta_s - 1)}$. $\lambda_s(t)$ is a failure rate function used specifically for generating failure times of cable sections. The calculation of its parameters ($\lambda_s$ and $\beta_s$,) will be explained later.

Failure times are generated until $S_n > T$, and they are accepted only if [86]:

$$V_i \le \frac{\lambda_s(S_i)}{K} \tag{4.7}$$

where $V_i$ is a uniformly distributed random number between $[0,\ 1]$. (Equation (4.7) is known as the thinning step, because it reduces the number of failure times.)

As seen in (4.6), the values of $\lambda_s$ and $\beta_s$ must be calculated to generate failure times of cable sections using the Thinning method. $\lambda_s$ is calculated by neglecting the effects of cable ageing. That is, $\lambda_s$ is equal to the product between the constant failure rate of cables (in failures/(year×miles)) and the average length of the cable sections in the system (in miles).

$\beta_s$, which is used in (4.6), also influences the generation of failure times. Its value must be greater than one to increase the number of repairable failures as cables get old. The value of $\beta_s$ is sampled, at each iteration, from two uniform probability

density functions, using the Markov chain Monte Carlo (MCMC) method (more details on the MCMC method can be found in [87]). Sampling $\beta_s$ at each iteration allows us to generate different sequences of failure times for each cable section. The intervals of the uniform probability density functions are [1.25, 1.40] (for cable sections with high equivalent load) and [1.05, 1.20] (for cable sections with low equivalent load). These intervals were chosen based on [27], and can be modified using failure statistics or condition monitoring data of cables.

- Step 5: Once failure times are generated, calculate $\alpha$, $\beta$, and $\delta_1$ using the maximum likelihood method developed in [30]. Below are only the equations needed for the failure rate model under study.

  Equation (4.3) can be rearranged as follows:

$$\lambda_x(t) = \beta t^{(\beta-1)} \exp(\boldsymbol{x}'\boldsymbol{\delta}) \tag{4.8}$$

  where $\boldsymbol{x}'\boldsymbol{\delta} = \delta_0 x_0 + \delta_1 x_1$, and $x_0 = 1$.

  The log-likelihood function and its derivatives are given below:

$$l(\beta, \boldsymbol{\delta}) = n \log \beta + (\beta - 1) \sum_{i=1}^{m} \sum_{j=1}^{n_i} \log t_{ij} + \sum_{i=1}^{m} n_i \boldsymbol{x_i'}\boldsymbol{\delta} - \sum_{i=1}^{m} T_i^{\beta} \exp(\boldsymbol{x_i'}\boldsymbol{\delta}) \tag{4.9}$$

$$\frac{\partial l}{\partial \beta} = \frac{n}{\beta} + \sum_{i=1}^{m} \sum_{j=1}^{n_i} \log t_{ij} - \sum_{i=1}^{m} T_i^{\beta} (\log T_i) \exp(\boldsymbol{x_i'}\boldsymbol{\delta}) \tag{4.10}$$

$$\frac{\partial l}{\partial \delta_r} = \sum_{i=1}^{m} n_i x_{ir} - \sum_{i=1}^{m} T_i^{\beta} x_{ir} \exp(\boldsymbol{x_i'}\boldsymbol{\delta}), \quad r = 0, 1. \tag{4.11}$$

  where $m$ is the number of cable sections, $[0,\ T_i]$ is the interval in which cable section $i$ experiences $n_i$ failures (at times $t_{i1} < \cdots < t_{in_i}$), and $n = \sum_{i=1}^{m} n_i$.

The maximum likelihood estimates $\hat{\alpha}$, $\hat{\beta}$, and $\hat{\delta_1}$ are found by solving (4.10) and (4.11), using the software MATLAB; the solution procedure is described in [30].

- Step 6: Repeat Step 4 (except the part related with $\lambda_s$) and Step 5 until the averages of $\hat{\alpha}$, $\hat{\beta}$, and $\hat{\delta_1}$ do not change significantly.

Figure 4.1 summarises the steps of the approach previously described.

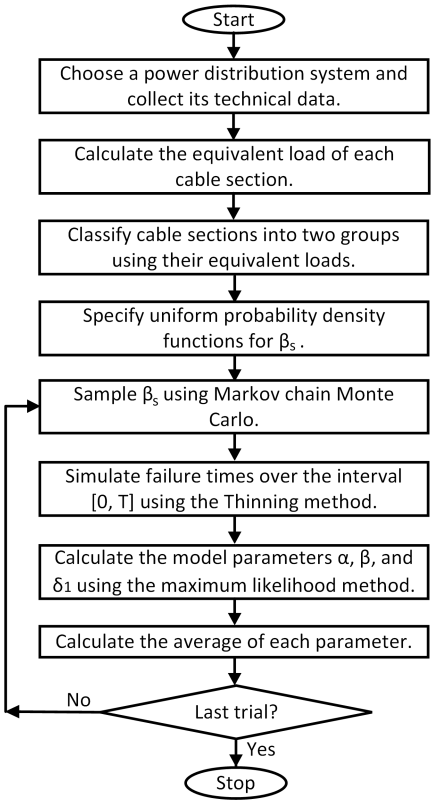


FIGURE 4.1: Flowchart of the approach for generating consecutive failure times of cables sections and estimating the model parameters (this flowchart is a slightly modified version of the one published in [80]).

## 4.3 Indices for Creating Cable Rankings

Cables can be ranked using several indices that quantify the impact of repairable failures on the reliability of a power distribution system [5], [55]. Those indices, however, were not initially developed for power distribution systems, but for any engineering (technical) system. The original indices (in particular, the index known as Birnbaum's measure and the improvement potential index [51]) as well as their adaptations for power distribution systems will be briefly explained below.

### 4.3.1 Birnbaum's Measure

To understand how the Birnbaum's measure can be used to rank multiple components of a system, it is necessary to first explain some important concepts and mathematical notation, which can be applied for any system with $n$ independent components.

The reliability of component $i$, i.e., the probability of being in the up state, at time $t$ is denoted as $p_i(t)$, whereas the unreliability of component $i$, i.e., the probability of being in the down state, at time $t$ is denoted as $q_i(t)$. The relationship between $p_i(t)$ and $q_i(t)$ is given by [51]:

$$q_i(t) = 1 - p_i(t). \tag{4.12}$$

Likewise, $p_s(t)$ and $Q_0(t)$ represent the reliability and unreliability of any system under study, respectively. In other words, $p_s(t)$ is the probability that the system is functioning at time $t$, and $Q_0(t)$ is the probability that the system is not functioning at time $t$. The relationship between $p_s(t)$ and $Q_0(t)$ is as follows [51]:

$$Q_0(t) = 1 - p_s(t). \tag{4.13}$$

Considering a system with $n$ independent components, its reliability, $p_s(t)$, can be expressed as a function, $h$, that depends on the reliability of all its components, as shown below [51]:

$$p_s(t) = h(p_1(t),\ p_2(t),\ ...,\ p_n(t)) = h(\boldsymbol{p}(t)). \tag{4.14}$$

The reliability of a system $h(\boldsymbol{p}(t))$ can be determined by analysing how its components are arranged. Components can be connected in series, parallel, series and parallel combinations, etc., as shown in Figure 4.2. For example, when all components are connected in series (as in Figure 4.2(a)), the reliability of the system is calculated by multiplying the reliability of each component, as shown in (4.15).

$$h(\boldsymbol{p}(t)) = \prod_{i=1}^{n} p_i(t) \tag{4.15}$$

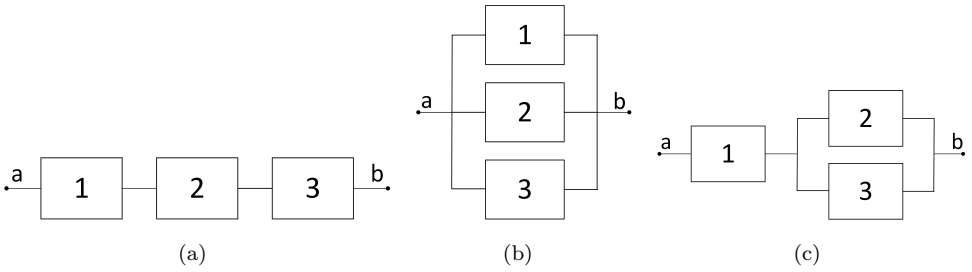


FIGURE 4.2: Basic representation of a system with 3 components: (a) series structure, (b) parallel structure, and (c) series and parallel structure [51]. The system is functioning when the end points $a$ and $b$ are connected.

Considering the definitions given above, the Birnbaum's measure (which is the first index for ranking components) determines how small changes in the reliability of component $i$ may affect the reliability of a system. This index is given by [88]:

$$I_i^B(t) = \frac{\partial h(\boldsymbol{p}(t))}{\partial p_i(t)} \quad \text{for } i = 1, 2, ..., n \tag{4.16}$$

where $I_i^B(t)$ is the Birnbaum's measure for component $i$, and can also be calculated using the definitions of system and component unreliability:

$$I_i^B(t) = \frac{\partial Q_0(t)}{\partial q_i(t)} \quad \text{for } i = 1, 2, ..., n. \tag{4.17}$$

It is important to mention that the calculation of the Birnbaum's measure is typically considered as a sensitivity analysis. The most important components in a system are the ones whose reliability (or unreliability) variations produce the greatest effects in the reliability of a system.

### 4.3.2 Improvement Potential Index

The improvement potential index measures how much the reliability of a system improves if component $i$ is replaced by a new component. That is, the index quantifies the potential benefits for the reliability of a system if an existing component is replaced by a new one. The improvement potential index, $I_i^{IP}(t)$, with respect to component $i$ is given by [51]:

$$I_i^{IP}(t) = h(1_i,\ \boldsymbol{p}(t)) - h(\boldsymbol{p}(t)) \quad \text{for } i = 1, 2, ..., n \tag{4.18}$$

where $h(1_i,\ \boldsymbol{p}(t))$ denotes the reliability of the system when component $i$ is replaced by a new one, whose reliability, $p_i(t)$, is 1.0 (or $1_i$ as used in (4.18)).

### 4.3.3 Indices for Power Distribution System Components

The authors of [5] modified the Birnbaum's measure, (4.16), and the improvement potential index, (4.18), by including variables used in power distribution system reliability

assessment. The first variable is the failure rate of power distribution system components, and the second variable is the total interruption cost. Thus, the new version of the Birnbaum's measure for power distribution systems, which calculates the change of the total interruption cost due to a small variation in the failure rate of component $i$, is given by [5]:

$$I_i^H = \frac{\partial C_s}{\partial \lambda_i} \quad (\$/\text{failure}) \tag{4.19}$$

where $\lambda_i$ is the failure rate of component $i$ (in failures/year), and $C_s$ is the total (system) interruption cost (in \$/year), which is calculated using the method given in [55].

Likewise, if the failure rate and the total interruption cost are included in the improvement potential index, its new version for power distribution systems is given by [5]:

$$I_i^{MP} = C_s(\boldsymbol{\lambda}) - C_s(0_i,\ \boldsymbol{\lambda}) \quad (\$/\text{year}) \tag{4.20}$$

where $\boldsymbol{\lambda}$ is a vector that represents the failure rates of all components. $I_i^{MP}$ is known as the maintenance potential index, because it quantifies how much the total interruption cost reduces if the failure rate of component $i$ reduces to zero ($0_i$) through maintenance.

## 4.4 Rankings of Ageing Cables

As mentioned in Subsection 4.3.3, cables of a power distribution system can be ranked using the maintenance potential index, $I_i^{MP}$. The calculation of this index was modified to incorporate the age-related repairable failure model presented in Section 4.2. The first modification is to utilise the expected value of the system interruption cost. Considering this change, equation (4.20) is written as follows [80]:

$$I_i^{MP} = EIC_s(\boldsymbol{\lambda}) - EIC_s(0_i,\ \boldsymbol{\lambda}) \quad (\$/\text{year}) \tag{4.21}$$

where $EIC_s$ is the expected system interruption cost.

The expected system interruption cost is calculated by adding the interruption costs of all load points, as shown below [78]:

$$EIC_s = \sum_{k=1}^{n_{lp}} EIC_k \tag{4.22}$$

where $n_{lp}$ is the total number of load points, and $EIC_k$ is the expected interruption cost of load point $k$. $EIC_k$ is given by [78]:

$$EIC_k = \frac{\sum_{i=1}^{N_k} W_k(D_i) \times P_{ik}}{M_{ni}} \tag{4.23}$$

where $W_k(D_i)$ is the customer damage function (in \$/kW) at load point $k$, $D_i$ is the duration of interruption $i$, $P_{ik}$ is the demand at load point $k$, and $N_k$ is the number of interruptions over the time period $M_{ni}$.

The second modification involves generating two up-down-up cycles for each cable section (these cycles are used in power distribution system reliability assessments with sequential Monte Carlo simulations) [80]. By doing this, random and age-related repairable failures are incorporated into the calculation of the maintenance potential index. The failure (up) times of the first cycle are sampled using a constant failure rate and the sampling method given by (3.25), whereas the failure times of the second cycle are sampled using the proposed failure rate model and the Thinning method, which was described in Section 4.2.2. Repair (down) times of the up-down-up cycles are sampled using the repair rate of cables and (3.25).

## 4.5 Case Study

The performance of the age-related repairable failure model and rankings of cable sections of the power distribution system given in [19] are presented in this section.

### 4.5.1 Test System

The test system has four main feeders (F1-F4) and three subfeeders (F5-F7), as shown in Figure 4.3. It is assumed that the system has single core copper conductors installed in underground electrical ducts. The system's maximum load demand was used to calculate the conductors' cross-sectional areas and ratings, which are given below:

- The main sections of feeders F1-F3 have a cross-sectional area of 240 $mm^2$. The resistance and reactance of these cables are 0.098 and 0.103 ($\Omega$/km), respectively, and their rating is 530 (A).
- The main sections of feeder F4 have a cross-sectional area of 300 $mm^2$. The resistance and reactance of these cables are 0.079 and 0.114 ($\Omega$/km), respectively, and their rating is 570 (A).
- The main sections of subfeeders F5-F7 and all lateral sections have a cross-sectional area of 70 $mm^2$. The resistance and reactance of these cables are 0.342 and 0.144 ($\Omega$/km), respectively, and their rating is 270 (A).

The test system has 40 load points (LP1-LP40), whose hourly load profile was taken from [16], and their customer types are shown in Table 4.1. Maximum and average load demands, number of customers, and customer damage functions (needed to calculate the expected system interruption cost) were taken from [78], [89]. Failures of substation and

distribution transformers, breakers, and switches were not considered in the case study as it analyses only cable failures. More information on the test system is given in the appendix, Section A.1.

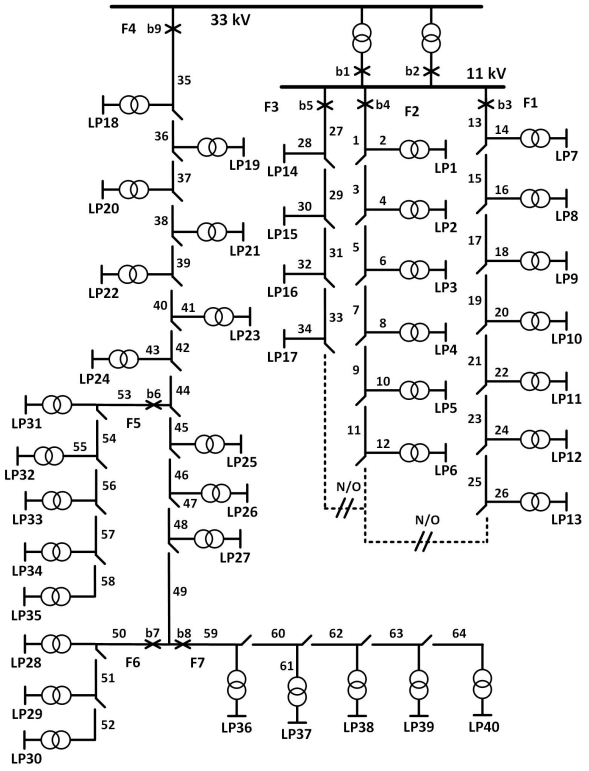


FIGURE 4.3: The test system is a modified version of the system given in [19].

TABLE 4.1: Customer types of the test system's load points [80]

| Customer type | F1 | F2 | F3 | F4 |
|---|---|---|---|---|
| Residential 1 | 7-10 | 1-3 | | 18-21, 28-34, 39-40 |
| Residential 2 | 11 | 4-5 | 16 | 22-23, 26-27, 35-36 |
| Commercial | 12-13 | 6 | | 24-25, 37-38 |
| Small user 1 | | | 14, 17 | |
| Small user 2 | | | 15 | |

### 4.5.2 Failure Rate of Ageing Cables

The test system was utilised to calculate the parameters of the failure rate model, $\lambda_x(t)$, following the procedure described in Section 4.2.2. The equivalent loads of cable sections were calculated using MATPOWER [90] and hourly load demand data. Then, cable sections were classified into two groups. The group of cables with high equivalent load contains cable sections that are located at the beginning of feeders F1-F4 (cables 1, 3, 13, 15, 27, 29, 35-38). For this group, $\beta_s$ can take any value between 1.25 and 1.40, whereas for the second group, $\beta_s$ can take any value between 1.05 and 1.20. Based on the cable ageing analysis carried out in [26], it was assumed that all (11 and 33 kV) cable sections start to experience age-related repairable failures after 18 years of operation. Cable failures were generated over a 20-year period using the Thinning method. Therefore, (artificial) age-related repairable failures are simulated when the service age of cables varies between 18 and 38 years. Equations (4.10) and (4.11) are solved using the failure times of all cable sections, and the resulting parameters are $\hat{\alpha} = 10.59$, $\hat{\beta} = 1.16$, and $\hat{\delta_1} = 0.31$.

Figure 4.4 shows the failure rates (in failures/year) calculated using the proposed model and two equivalent loads (0.15 and 0.40 p.u.). It can be seen that both failure rates increase as the service age of cables increases. Failure rates are also influenced by the equivalent loads; this means that a cable section with an equivalent load of 0.40 p.u. has a higher failure rate than a cable section with an equivalent load of 0.15 p.u. It is important to mention that the equivalent loads used for Figure 4.4 remain constant over the 20-year period. Constant equivalent loads were utilised only to illustrate the results the proposed failure rate model. The equivalent loads of cables should be calculated annually to capture the effects of load demand variation.

The failure rate that is commonly used to describe random repairable failures of cables is also depicted in Figure 4.4. This failure rate is constant and is for a 0.8-km cable

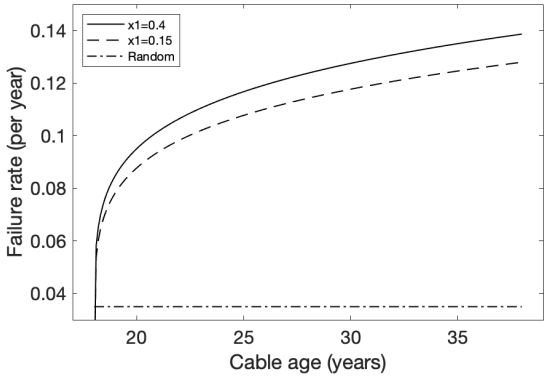


FIGURE 4.4: Failure rates of the test system's cable sections [80]. The failure rates were calculated using artificial consecutive failure times and two equivalent loads (0.15 and 0.40 p.u.). The figure also shows the conventional failure rate of a 0.8-km cable section, which indicates the occurrence of random repairable failures.

section. It can be clearly seen that the conventional failure rate has a much lower value; only 16% of the maximum value of the failure rate used to describe age-related repairable failures with an equivalent load of 0.40 p.u.

### 4.5.3 Rankings of the Test System's Cables

The most important part of this study is to rank cable sections based on their importance for the test system reliability, so that maintenance activities can be prioritised. The maintenance potential index, $I_i^{MP}$, is calculated for all cable sections taking into account both random and age-related repairable failures. To calculate the conventional failure rate of cables, the cable length data given in [89] are utilised. For age-related repairable failures, the failure rate is calculated using (4.3), the estimated parameters, and the equivalent load of each cable section. The maintenance potential index is calculated over a year (the cable age increases from 18 to 19 years). A computational program was developed using MATLAB to perform sequential Monte Carlo simulations and to calculate the expected system interruption costs.

Figure 4.5a shows the maintenance potential index (in k$/year) of cable sections located in the 11-kV network. The most important component is cable section 29, whose index is 22.5 k$/year. This means that performing maintenance to cable section 29 would result in the greatest reduction of the expected system interruption cost. It can also be seen that the first six places in the ranking are occupied by cable sections of feeder F3 (27-30, 33-34). This is because small users located at load points 14, 15, and 17 (see Table 4.1) have higher interruption costs than residential and commercial users, and when any of these six cables fails, the expected system interruption costs are higher. The next six places in the ranking are occupied by cables 23-26 and 11-12, which supply electricity to commercial customers. The remaining cables supply the demand of residential customers.

Figure 4.5b shows the ranking for the cable sections located in the 33-kV network. The first twelve positions are occupied by cables located in feeder F4 (35-40, 42, 44-46, 48-49). It can also be seen that the indices of the 33-kV cables are greater than the indices of the 11-kV cables. For example, the index of cable section 35 is 82.9 (k$/year), whereas and the index of cable section 29 is 22.5 (k$/year). These results occur due to the radial configuration of feeder F4 and the lack of normally open switches in this part of the test system.

Figures 4.5a and 4.5b also show that the impact of age-related repairable failures on the index of each cable section is greater than the impact of random repairable failures. This can be clearly seen in the index of cable section 35 (Figure 4.5b), where the effects of age-related and random repairable failures represent 63% and 37% of the index, respectively. This happens because, as seen in Figure 4.4, the failure rate that describes the occurrence of age-related repairable failures is greater than the failure rate that describes the occurrence of random repairable failures, and this behaviour is captured by the expected system interruption cost, parameter used for the calculation of cable indices.

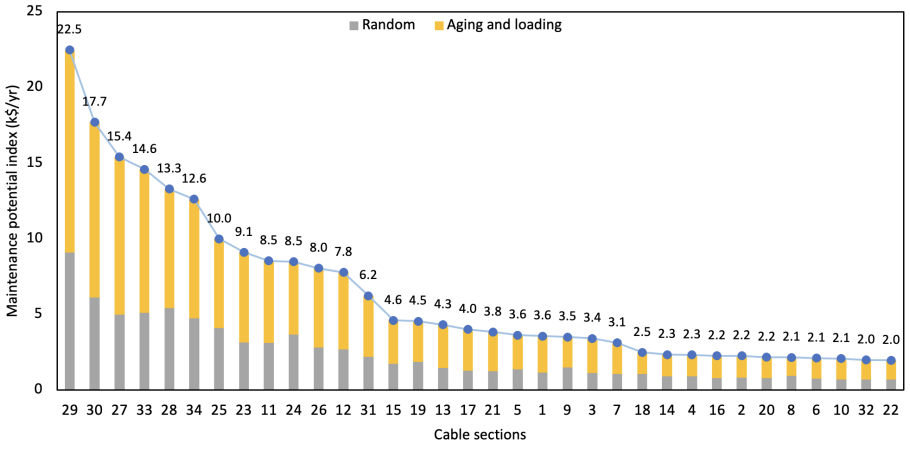


(a)

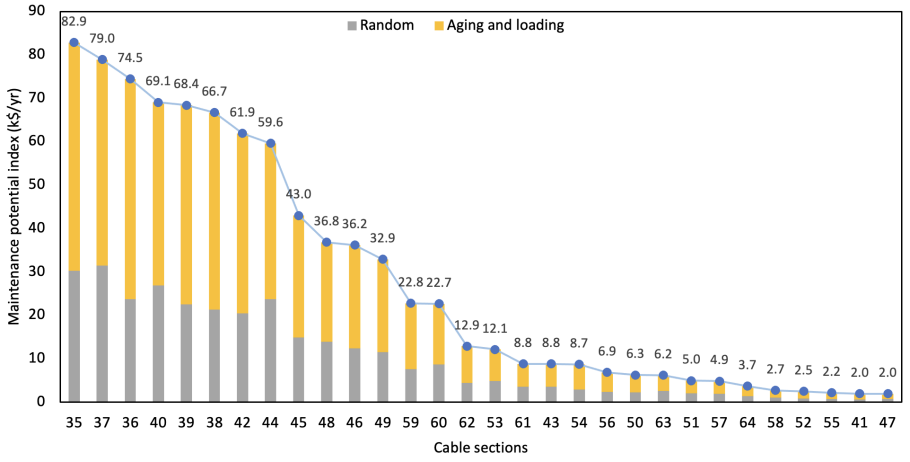


(b)

FIGURE 4.5: Maintenance potential index-based rankings for the (a) 11-kV and (b) 33-kV cable sections of the test system depicted in Figure 4.3 [80]. The maintenance potential indices are calculated considering both random and age-related repairable failures.

It is important to mention that the cable rankings shown in Figure 4.5 can change significantly if only random repairable failures are taken into account (i.e., if cable ageing is neglected), or if different loading conditions are used. In the first case, cable rankings can change because the maintenance potential index would only capture the effects of random repairable failures on the expected system interruption cost. In this case, only one up-down-up cycle for each cable section should be generated. For instance, if only

the effects of random repairable failures are quantified, cable section 37 would occupy the first place in Figure 4.5b; the index of this cable section would be around 32 k$/year.

In the second case, considering different hourly load profiles or different annual load growths (due to solar PV generation [91] and/or transportation electrification [92]) might change the loading conditions of the test system's cable sections, affecting both future age-related repairable failures as well as cable rankings. Figure 4.6 shows the rankings of the ageing cables considering a service age of 22 years and annual load growths of 0.6%, 0.4%, 0.5%, 0.3%, and 0.8% for customers classified as Residential 1, Residential 2, Commercial, Small user 1, and Small user 2, respectively. The results indicate that the maintenance prioritisation changes. For example, cable section 40 dropped in the ranking from the fourth to the fifth place, whereas cable section 24 rose from 10 to 9 in the ranking (see also Figure 4.5).

In recent years, extreme weather events—storms, hurricanes, and floods—as well as wildfires have occurred more frequently in some countries like Japan, Philippines, Germany, United States, and Australia [93], causing long power supply interruptions [94]. To reduce the impact of these events, some electric utilities (like Florida Power & Light Company and Pacific Gas and Electric Company) have replaced overhead power distribution lines with underground cables [95]. As the number of underground cables increases in power distribution systems, asset managers need advanced methods to identify critical cables and prioritise their maintenance. This maintenance prioritisation process can be done by using the approach presented in this chapter.

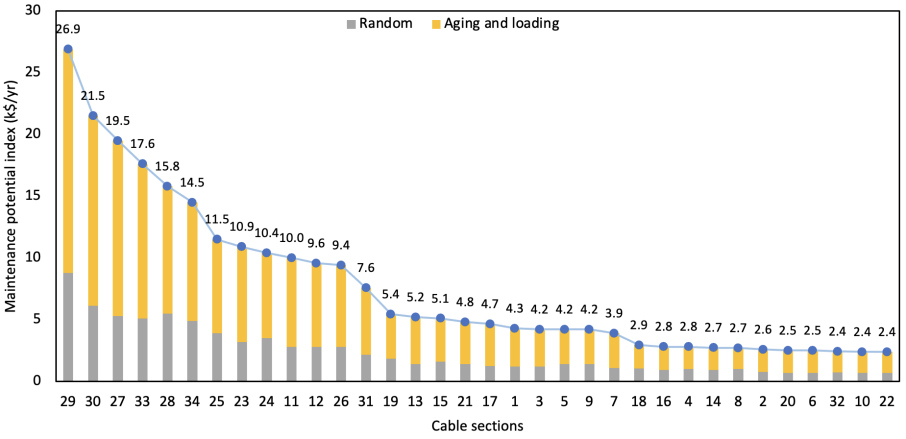


(a)

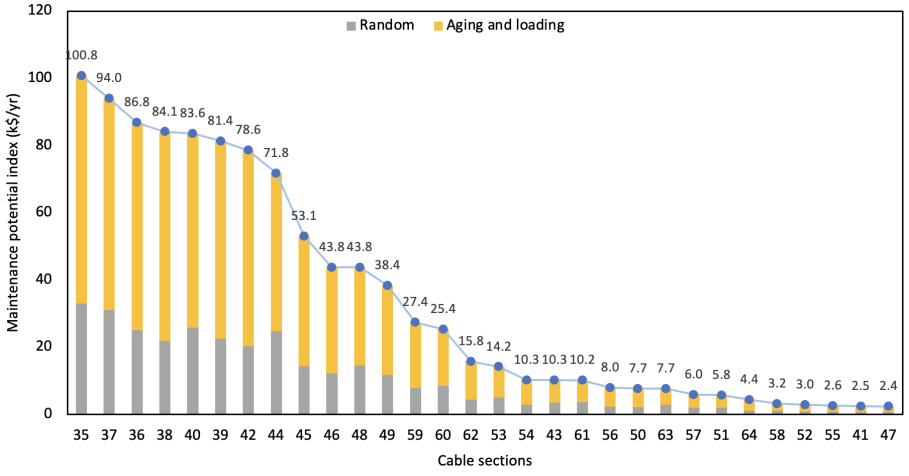


(b)

FIGURE 4.6: Maintenance potential index-based rankings for the (a) 11-kV and (b) 33-kV cable sections of the test system depicted in Figure 4.3 considering load increments.

## 4.6 IEC-Arrhenius-Weibull Model

Another age-related repairable failure model for underground power distribution cables is proposed in [27]. The model, which is called IEC-Arrhenius-Weibull, also incorporates the loading conditions of cables into their failure rate, but this is done using a different approach. The approach combines the failure rate function for the two-parameter Weibull distribution, shown in (4.2), with the Arrhenius relationship and the industrial standard IEC 60287-1-1.

The Arrhenius relationship is used in [83] to calculate the life of the paper insulation of mineral oil-immersed transformers if a constant winding hottest-spot temperature is provided. Studies that investigate ageing (end-of-life) failures of power transformers have assumed that since the paper insulation is a critical component, the parameter $\alpha$ of the Weibull distribution that models the lifetime of power transformers can be approximated by the life measure of the Arrhenius relationship [44]. That is, $\alpha$ is equal to the life measure of the paper insulation. The authors of [27] made the same approximation (as underground cables also have paper insulation), but in their study the approximation is used for modelling age-related repairable failures of cables.

The Arrhenius relationship is given by [27]:

$$L(\theta_c) = A \exp\left(\frac{B}{\theta_c}\right) \tag{4.24}$$

where $L(\theta_c)$ is a life measure of cables (in years), $\theta_c$ is the cable temperature (in $^\circ K$), and $A$ and $B$ are constants whose values are calculated using historical cable loading data. The standard IEC 60287-1-1 [96] is used to calculate the cable temperature.

When $\alpha$ equals $L(\theta_c)$, the failure rate of the IEC-Arrhenius-Weibull model, can be written as follows [27]:

$$\lambda(t) = \frac{1}{\left[A \exp\left(\frac{B}{\theta_c}\right)\right]^{\beta}} \beta t^{(\beta-1).} \tag{4.25}$$

## 4.7 Analysis of Age-Related Repairable Failure Models

So far two approaches for modelling age-related repairable failures of cables have been presented. Model 1 consists of a compound failure rate, (4.3), whereas Model 2 modifies the failure rate of the Weibull distribution by including the Arrhenius relationship, (4.25). Their modelling assumptions, methods for incorporating cables' loading conditions, and parameter estimation approaches are deeply analysed and compared in this section.

### 4.7.1 Modelling Assumptions

Models 1 and 2 are based on the principle of a non-homogeneous Poisson process, which means that consecutive failure times are not independent and identically distributed. A requirement for modelling age-related repairable failures using a non-homogeneous Poisson process is that components must be identical. In Models 1 and 2, it is assumed that cable sections are identical components. Some actual power distribution systems have cables with the same manufacturing, installation, and maintenance characteristics, but cable sections usually have different lengths and undergo different loading conditions. There is no evidence in the power system literature that the occurrence of age-related repairable failures depends on cable length. In other words, there is no evidence that a 1-mile cable section undergoes more age-related repairable failures than a 0.5-mile cable section, assuming both cables have the same service age. However, cable length is taken into account when random repairable failures are modelled, by multiplying the failure rate of a particular class of cables (in failures/(year×mile)) by the length of a cable (in miles).

The other assumption made in Models 1 and 2 is that loading conditions influence the occurrence of age-related repairable failures; therefore, ageing cables with higher loading levels fail more frequently than cables with lower loading levels, as discussed in Section 4.5.2. This assumption is reasonable because loading conditions directly affect the temperature of any piece of equipment, and temperature plays an important role in the electrical, mechanical, chemical, and physical deterioration of materials [22]. In the case of cables, high operating temperatures may gradually deteriorate the insulation, metallic sheath, terminals, or other components until eventually a failure occurs.

### 4.7.2 Incorporation of Cables' Loading Conditions

As mentioned above, cable sections in a power distribution system usually have different loading conditions, and their influence on age-related repairable failures is considered in Models 1 and 2. To incorporate the influence of loading conditions, Model 1 employs a straightforward method: an exponential function that modifies the failure rate $\lambda_0(t)$ depending on the equivalent load of each cable section. Calculating the equivalent load of cables only requires to collect hourly load demand data, perform load flows, and use (4.4). Because of the simplicity of the method, it can be applied to power distribution systems with a great number of cable sections.

Model 2 uses the Arrhenius relationship to incorporate cables' loading conditions. This method is more complicated because it requires to calculate the temperature of each cable section, using the method given in the standard IEC 60287-1-1. The method was originally developed to calculate a constant electrical current that yields the maximum cable temperature [96]. However, the authors of Model 2 use the method in a different way: they calculate cable temperatures using known loading conditions. Calculating the temperature of cables requires more data, such as dielectric losses, thermal resistances,

and alternating current resistances. Furthermore, it is not clear in [27] whether the temperature is calculated using the average or maximum loading level of each cable. Utilising the Arrhenius relationship also requires to calculate its parameters, $A$ and $B$. This task can be very challenging because there is not enough information in the power system literature.

### 4.7.3 Estimation of Model Parameters

Due to the lack of cable failure data, an iterative approach, described in Section 4.2.2, was developed to estimate the parameters of Model 1. The approach generates, over a time period $[0,\ T]$, consecutive failure times of cable sections of a power distribution system and then uses the maximum likelihood method. Two important observations are made about the approach. First, although artificial failure times are generated over the interval $[0,\ T]$, this does not mean that cable sections start experiencing age-related repairable failures just after their installation (i.e., cable ageing does not begin at time 0). If failure times for an 18-year-old cable are generated over 20 years, its service age would increase from 18 to 38 years, but the proposed approach uses the interval $[0,\ 20]$. In other words, artificial failure times are generated considering the simulation period.

Second, condition monitoring information of cables and/or knowledge of asset managers can be used to enhance artificial failure time generation. For example, if condition monitoring information indicates that some cables in a power distribution system are ageing faster than others, the interval $[1.25,\ 1.40]$ used to generate failure times should be adequately modified.

Model 2 has two parameters ($\alpha$ and $\beta$) whose values were not calculated using actual or artificial consecutive failure time data. As mentioned before, $\alpha$ is approximated through

the Arrhenius relationship. However, a great disadvantage of the Arrhenius relationship is that it does not provide information on consecutive failure times of cables. It provides an estimation of cable lifetimes, information that might be irrelevant for age-related repairable failure modelling. The parameter $\beta$ takes values between 1.0 and 1.8 to consider different ageing levels; however, those limits were not based on failure statistics of power distribution system cables.

## 4.8 Model Comparison

Models 1 and 2 have been used in [80] and [27] to perform studies that quantify the impact of age-related repairable failures of cables on the reliability of power distribution systems. Those studies involve time sequential Monte Carlo simulations, contingency analysis, and system reliability index calculations. Considering all this, a four-step process is proposed to carefully evaluate the performance of Models 1 and 2. The process is described below [81]:

1. Select appropriate values for the parameters of Models 1 and 2 (including the Arrhenius relationship parameters). The parameter values must allow the comparison of the performance of Models 1 and 2.

2. Calculate and plot the failure rate (function) of ageing cables using both models.

3. Perform a sensitivity analysis of the Arrhenius relationship parameters ($A$ and $B$). This analysis will help us understand how small changes of the Arrhenius relationship parameters influence the failure rate of cables.

4. Create cable rankings by calculating the maintenance potential index, $I_i^{MP}$, and by considering only age-related repairable failures when sampling the states of cable sections.

### 4.8.1 Failure Rates

Based on the procedure described above, the parameters of Models 1 and 2 are selected as follows. The test system depicted in Figure 4.3 will be used to create cable rankings, so the parameters that were calculated in Section 4.5.2 ($\alpha = 10.59$, $\beta = 1.16$, and $\delta_1 = 0.31$) are utilised for Model 1. (Remember that those parameters were calculated by generating artificial consecutive failure times of cable sections and by using the maximum likelihood method.) For Model 2, the parameter $\beta$ takes the same value, i.e., $\beta = 1.16$, and the parameter $\alpha$ is calculated through the Arrhenius relationship. The Arrhenius relationship parameters for XLPE cables calculated in [27] ($A = 2.414$ and $B = 1020$) are utilised for the model comparison.

The next step is to calculate the failure rates using the parameters previously determined. Figure 4.7 shows the failure rates calculated using Model 1, with an equivalent load of 0.30 p.u., and Model 2, with a temperature of 90°C. Power distribution cables usually operate at temperatures below 90°C; however, this value was chosen because it represents the worst case. When the cable age is 18 years, both failure rates have an initial value of 0.035 (failures/year), which represents the rate of random repairable failures of a 0.8-km cable section. Then, both failure rates increase as the age of cables increases. However, it can be seen that Model 1 yields higher failure rates than Model 2. This result is mainly because Models 1 and 2 employ very different values for $\alpha$ (10.59 and 40.05, respectively). Furthermore, it can be seen that the failure rate of Model 2 increases very slowly over the 20-year period, although the cable temperate is 90°C.

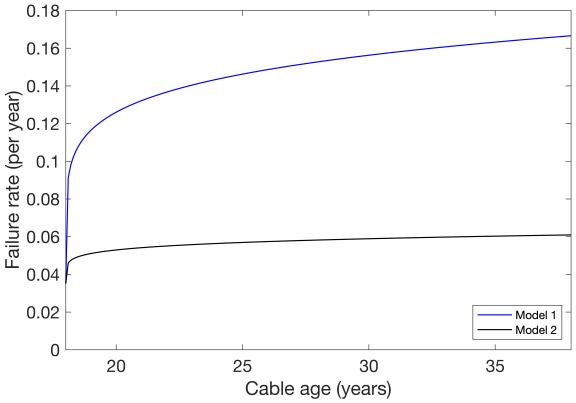


FIGURE 4.7: Failure rates calculated using Models 1 and 2, an equivalent load of 0.30 p.u., and a temperature of 90°C [81]

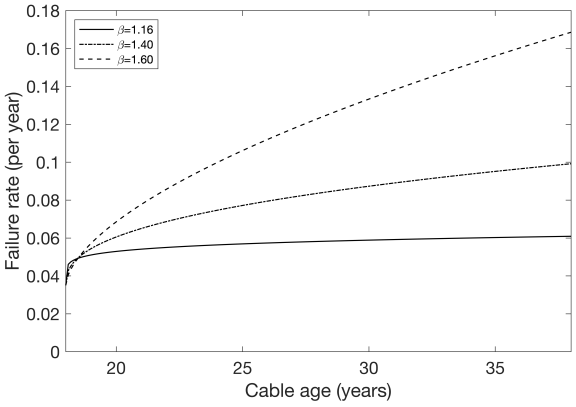


FIGURE 4.8: Failure rate calculated using Model 2, a temperature of 90°C, and three values of $\beta$ [81]

The failure rate of Model 2 is further investigated by using three values for the parameter $\beta$ (1.16, 1.40, and 1.60), as shown in Figure 4.8. The results indicate that unlike Model 1, Model 2 significantly depends on $\beta$ to describe different levels of cable ageing. This dependence can be clearly seen in (4.25), and is the result of using the Arrhenius relationship. To reach almost the maximum failure rate of Model 1 shown in Figure 4.7 (0.17 failures/year when the cable age is 38 years), $\beta$ must increase from 1.16 to 1.60.

### 4.8.2 Sensitivity Analysis

Calculating the Arrhenius relationship parameters used in Model 2 is a difficult task that involves making assumptions about the ageing of different types of power distribution cables, as discussed in [27]. For that reason, performing a sensitivity analysis, the third step of the proposed procedure, is important to investigate how small changes of the Arrhenius relationship parameters (±5%) influence the failure rate of cables. The same cable temperature (90°C) is used for the sensitivity analysis. If this temperature and the original Arrhenius relationship parameters for XLPE cables ($A = 2.414$ and $B = 1020$) are utilised, the resulting life measure is 1.0 p.u. (or 40 years as explained in [27]). When the Arrhenius relationship parameters suffer minor changes (±5%), the resulting life measures are 0.83 p.u. (or 33.1 years) and 1.21 p.u. (or 48.4 years).

Figure 4.9 depicts the failure rate calculated using Model 2 and considering the new life measures, 33.1 and 48.4 years, and $\beta = 1.16$. The failure rate increases when the life measure reduces to 33.1 years. It can also be seen that the failure rate reduces when the life measure increases to 48.4 years. These changes are not significant, but it is unclear if the use of cables' life measures is suitable for modelling age-related repairable failures (as discussed in Section 4.7.3). Life measures only provide an estimate of the lifetime of cables given a constant temperature. Therefore, if life measures are used as the scale parameter of the Weibull distribution in Model 2, information on age-related repairable failures of cables is not incorporated into the model. In other words, life measures provide estimates of cable lifetimes, but those estimates do not provide information on the occurrence of age-related repairable failures.

### 4.8.3 Cable Rankings

The last step to evaluate the performance of Models 1 and 2 is to create cable rankings. To this end, the maintenance potential index of the test system's 11-kV cable sections was calculated using Models 1 and 2, for a one-year period. The equivalent load of each cable section, used in Model 1, was calculated through power flow simulations, with one hour granularity, and using (4.4). The temperature of all cable sections, used in Model 2, was assumed to be 90°C. This assumption was made because as seen in Figure 4.8, the failure rate of cables mainly depends on the value of the parameter $\beta$; and therefore, calculating the temperature of each cable section would not cause significant changes in the failure rate.

The rankings of the 11-kV cable sections calculated using Models 1 and 2 are depicted in Figure 4.10(a) and Figure 4.10(b), respectively. Both rankings have similar trend lines, but the positions of some cable sections differ. For example, cable section 27 occupies the third place when Model 1 is utilised and the forth place when Model 2 is utilised. It can also be seen that Models 1 and 2 produce different indices. The indices of cable section 29 are 13.9 (k$/year) when Model 1 is used and 4.3 (k$/year) when Model 2 is used. This

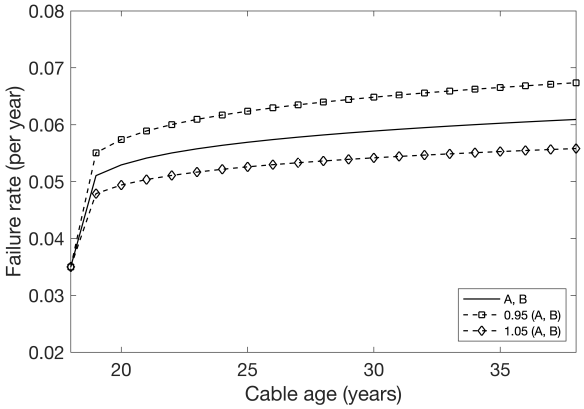


FIGURE 4.9: Failure rate calculated using Model 2 and varying the Arrhenius relationship parameters ($A$, $B$) [81]

difference is because the failure rate of Model 1 is higher than the failure rate of Model 2, as shown in Figure 4.7, producing higher expected system interruption costs.

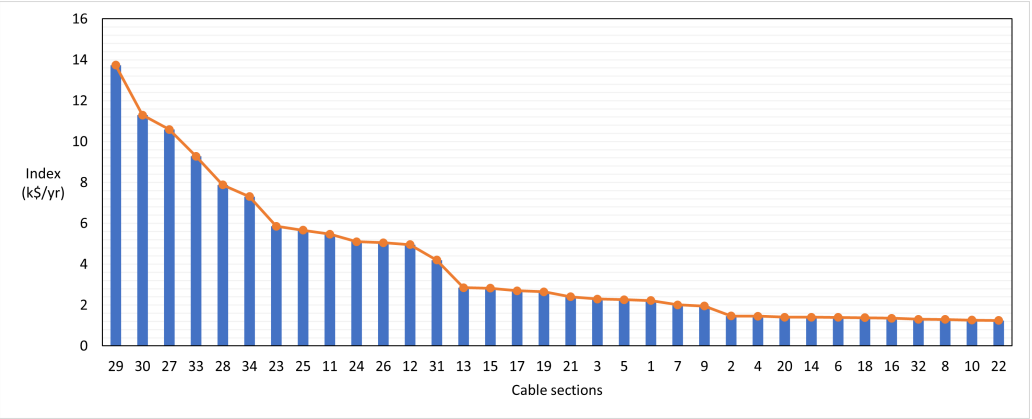


(a)

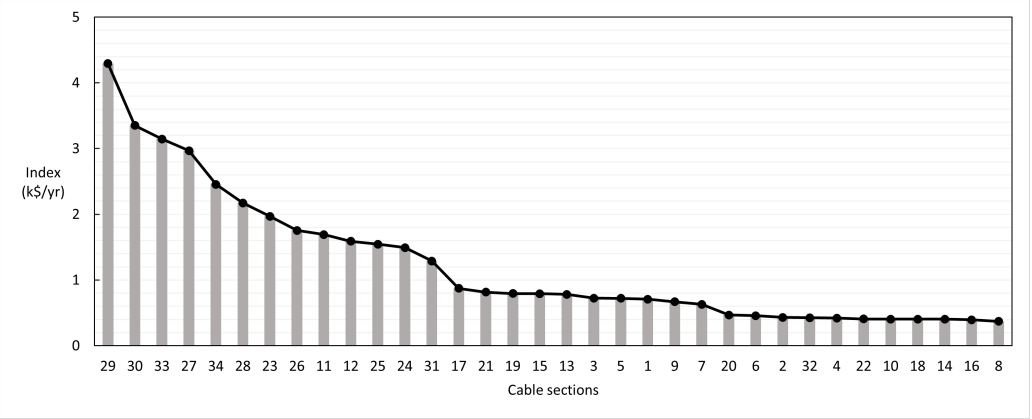


(b)

FIGURE 4.10: Maintenance potential index-based rankings for the 11-kV cable sections of the test system depicted in Figure 4.3 [81]. The index is calculated using (a) Model 1 and (b) Model 2.

## 4.9 Summary

This chapter presented an approach for prioritising the maintenance of ageing underground power distribution system cables. The approach is used to create cable rankings so that

maintenance activities can be targeted at critical cables. Cables are ranked by calculating their maintenance potential index, which considers the occurrence of both random and age-related repairable failures, their impact on the expected system interruption cost, and the reduction of the failure rate of cables if maintenance is performed.

The approach was applied to a radial power distribution system with 64 ageing cable sections and residential, commercial, and industrial customers. The results indicate that the contribution of age-related repairable failures to the maintenance potential index of each cable is greater than the contribution of random repairable failures. This emphasises the importance of modelling age-related repairable failures for the maintenance prioritisation of ageing cables.

This chapter also presented a detailed study of two age-related repairable failure models of underground cables. The study, which is the second contribution of the thesis, critically analyses their modelling assumptions, their methods for incorporating loading conditions, and their parameter estimation approaches, and evaluates the performance of both models through computer simulations. The simulation results show that the IEC-Arrhenius-Weibull model depends significantly on the shape parameter of the Weibull distribution, and that calculating the scale parameter through the Arrhenius relationship can reduce the failure rate of ageing cables.

# Chapter 5

# Estimating the Retirement of Power Transformers[1]

## 5.1 Introduction

A technical report published in 2015 by the International Electrotechnical Commission (IEC) indicated that power transmission systems in developed countries have a great number of assets that have exceeded their designed lifetime [15], and another report published in 2012 indicated that the average age of large power transformers installed in the U.S. is 40 years [98]. Having aged power transformers in operation increases the risk of power supply interruptions, and for that reason, asset managers must carefully plan their retirement. Planning the retirement of aged power transformers is a challenging task; it involves quantifying risks in economic terms, i.e., it is necessary to calculate both the probability of ageing (end-of-life) failures of power transformers and the potential economic losses caused by those events.

[1]This chapter is based on publication [97].

Previous works ([4], [41], [46]) have proposed several risk-based strategies for retiring power transformers. The strategies employ ageing failure models, perform non-sequential Monte Carlo simulations and contingency analysis, and calculate risk indices. However, the existing approaches have two important problems. First, some electric utilities do not have enough end-of-life failure data of power transformers [6], [33] (needed for calculating ageing failure model parameters). Second, power transformer condition—a factor that plays a key role in retirement decisions—has not been properly included in the traditional ageing failure model, as explained in Chapter 2 (Section 2.4).

Considering these problems, this chapter presents an advanced approach for retiring power transformers. First, the scale parameter of the Weibull distribution is calculated by combining the Arrhenius relationship with the IEC thermal model and a method to calculate the annual equivalent load of power transformers. Second, the apparent (condition-based) age of power transformers is calculated by using probabilistic health indices and linear regression models, and then, its value is adjusted using the model of the unavailability due to ageing failure. Third, the approach ranks the aged transformers of a power system through an index that calculates the potential benefits of retiring aged transformers for the reliability of the power system. Finally, the approach uses the economic comparison method developed in [4] to calculate their year of retirement. *The entire approach was published in [97].*

## 5.2 Overview of the Risk-Based Approach for Retiring Power Transformers

Figure 5.1 shows the basic steps of the proposed approach for retiring power transformers. The approach comprises three parts: data collection, rankings of power transformers, and

retirement year calculation. An overview of them is given below.

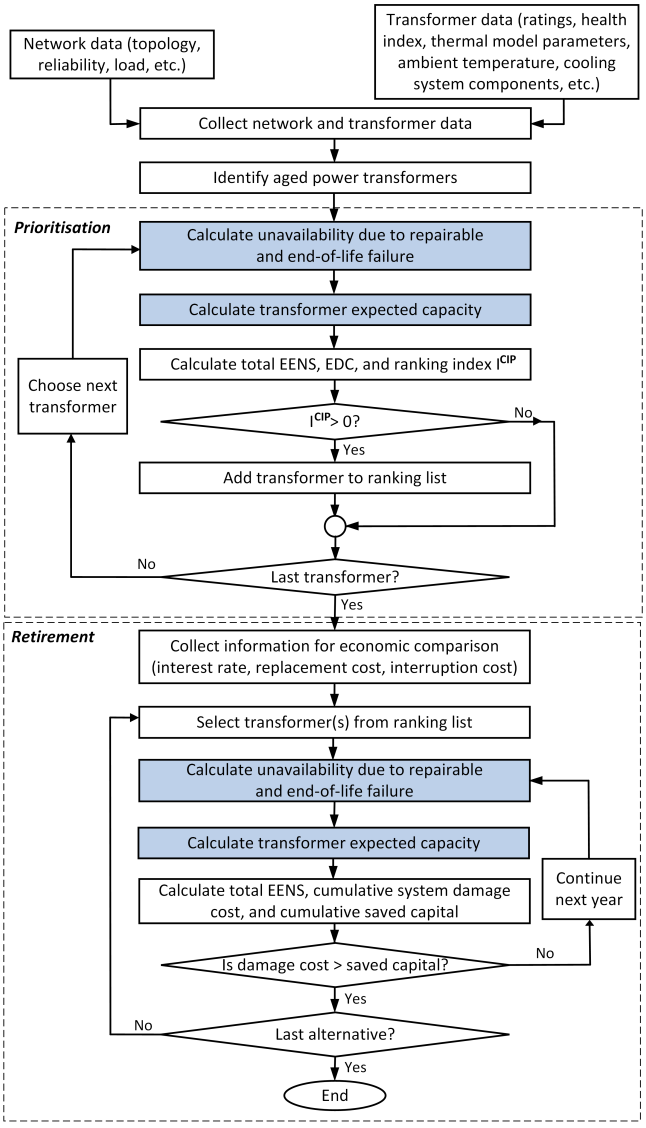


FIGURE 5.1: Basic steps of the proposed approach for retiring power transformers [97]

The first part involves collecting data of the power system that will be analysed (e.g., capacity of power generators, hourly load demand, annual demand growth, network topology, and average service interruption cost) as well as data of its power transformers (e.g., service age, average lifetime, failure and repair rates, health indices, and parameters

for winding-hottest spot temperature calculation). It is also necessary to collect ambient temperature data.

To proceed with the second part of the approach, it is necessary to identify which power transformers should be considered for retirement. This can be done by comparing the service age of each power transformer with its average lifetime, as suggested in [4]. If the service age of a transformer exceeds its average lifetime, the transformer is considered as aged. Another option is to employ health indices of power transformers (indices used for retirement planning). If the health index of a power transformer indicates that its condition is poor, the power transformer is considered as aged. Then, all aged transformers are ranked by calculating their credible improvement potential (CIP) index. This index quantifies how much the expected system damage cost (EDC) reduces if an aged transformer is replaced by a new one. The index also takes into account the unavailability due to repairable and ageing failures of each power transformer.

The final part of the approach involves calculating the year in which an aged power transformer should be retired. If an aged power transformer remains in operation, its expected damage cost (caused by ageing failures and capacity reduction) must be determined. Considering that the retirement of the aged power transformer is delayed, the capital investment needed for its replacement is not utilised (i.e., it is saved), but its value changes over time. The saved capital due to delaying the retirement of the transformer is compared with its expected damage cost for several years until the cumulative expected damage cost exceeds the cumulative saved capital [4].

## 5.3 Unavailability due to Ageing Failure Considering Apparent Age and Winding Temperature

This section details the procedure used to calculate the unavailability due to ageing failure of power transformers. The unavailability due to ageing failure is utilised in the second and third parts of retirement approach.

### 5.3.1 Arrhenius Relationship and IEC Thermal Model

The unavailability due to ageing failure of power transformers can be calculated using (3.14) and (3.21), as explained in Subsection 3.3.3. The probability of transition to ageing failure, given by (3.21), depends on the scale and shape parameters ($\alpha$, $\beta$) of the Weibull distribution. (The Weibull distribution is typically used to model the lifetime of a group of power system components, including transformers.) The scale parameter ($\alpha$) is the time at which 63% of all components under study experience end-of-life failures [99]. To model end-of-life failures of power transformers, the authors of [44] calculated the scale parameter using the Arrhenius relationship, which provides a life measure of the paper insulation for a constant winding hottest-spot temperature. This approximation was also used in this study, but other methods were incorporated to improve the scale parameter calculation. The Arrhenius relationship is given by [44]:

$$L(\theta_H) = c_1 \exp\left(\frac{c_2}{\theta_H}\right) \tag{5.1}$$

where $L(\theta_H)$ is a life measure of the paper insulation (in years), $\alpha = L(\theta_H)$, $\theta_H$ is the winding hottest-spot temperature (in $^\circ K$), and $c_1$ and $c_2$ are constants. An approach for calculating $c_1$ and $c_2$ will be presented in Section 5.3.2.

The winding hottest-spot temperature, $\theta_H$, changes over time depending on both loading conditions and ambient temperature, and can be calculated using the methods developed in IEEE Std. C57.91 [83] and IEC-60076-7 [100]. An annual equivalent load and an annual equivalent ambient temperature are employed in this study to calculate the winding hottest-spot temperature; this is done because the unavailability due to ageing failure is calculated annually (see (3.14)). The annual equivalent load of a power transformer, denoted as $L_E$, is calculated using the method explained in the previous chapter, see Subsection 4.2.1. The only difference is that the annual equivalent load of a power transformer is determined in real units (i.e., in MVA).

The annual equivalent ambient temperature is a constant, non-existent ambient temperature that produces the same ageing of the paper insulation as a time-varying temperature. To calculate the annual equivalent ambient temperature using the method given in [100], it is necessary to make two assumptions: the ambient temperature changes sinusoidally, and an increase of $6°K$ doubles the paper's ageing rate. The annual equivalent ambient temperature, $\theta_E$, is calculated as follows [100]:

$$\theta_E = \theta_{ya} + 0.01\big[2(\theta_{ma-max} - \theta_{ya})\big]^{1.85} \tag{5.2}$$

where $\theta_{ya}$ is the yearly average ambient temperature, and $\theta_{ma-max}$ is the monthly average temperature of the hottest month. $\theta_{ya}$ and $\theta_{ma-max}$ are calculated using historical ambient temperature data.

After the equivalent load of a power transformer and the equivalent ambient temperature are obtained, the winding hottest-spot temperature is calculated using the IEC thermal model [100]:

$$\theta_H = \theta_E + \Delta\theta_{o,r}\left(\frac{1 + RK^2}{1 + R}\right)^x + Hg_rK^y \tag{5.3}$$

where $\Delta\theta_{o,r}$ is the top-oil temperature rise in steady state at rated losses, $R$ is the ratio of load losses at rated current to no-load losses, $K$ is the load factor (which is calculated by dividing the annual equivalent load, $L_E$, by the power transformer capacity), $g_r$ is the average-winding-to-average-oil temperature gradient at rated current, $x$ and $y$ are oil and winding exponents, and $H$ is the hot-spot factor.

### 5.3.2 Arrhenius Relationship Parameters

The parameters of the Arrhenius relationship given in (5.1), $c_1$ and $c_2$, are usually calculated by performing multiple accelerated life tests. In an accelerated life test, a sample of insulating paper undergoes a constant temperature (higher than normal operating temperatures) until the sample reaches its end-of-life, and its lifetime is measured [101]. However, accelerated life test data cannot be directly used to calculate $c_1$ and $c_2$, because the Arrhenius relationship is used to model end-of-life failures of power transformers (not the end-of-life failures of paper insulation). Therefore, a different method is needed to estimate these parameters.

The method proposed in [44] was utilised to calculate the Arrhenius relationship parameters, and it was improved by incorporating the effects of moisture accumulation in paper insulation. The method determines the values of $c_1$ and $c_2$ by solving (5.1) twice. To solve the equations, it is necessary to know two ordered pairs: $(\theta_{H,1},\ L_1)$ and $(\theta_{H,2}, L_2)$. $L_1$ and $L_2$ represent two life measures (in years) whose values depend on two constant winding hottest-spot temperatures, $\theta_{H,1}$ and $\theta_{H,1}$.

The first ordered pair $(\theta_{H,1},\ L_1)$ is calculated through the DP (degree of polymerisation) reduction model. (The DP is usually used to indicate the condition of the paper insulation [47].) This model determines the time in which the degree of polymerisation

reduces from 1000, typical value for new transformers, to 200, value used as end-of-life criterion [102], when the paper insulation undergoes a constant temperature. The DP reduction model is shown below [102], [103]:

$$\frac{1}{DP_t} - \frac{1}{DP_0} = k \times t_{\theta_H} \tag{5.4}$$

where $DP_0$ and $DP_t$ are the initial and final DP, respectively, $t_{\theta_H}$ is the paper insulation lifetime, and $k$ is the ageing rate, which is calculated as follows [104]:

$$k = A \times \exp\left[\frac{-E_A}{R(\theta_H + 273)}\right] \tag{5.5}$$

where $E_A$ is the activation energy (128 kJ/mol), $R$ is the molar gas constant (8.314 kJ/mol/°K), and $A$ is a constant whose value depends on the paper moisture content.

$L_1$ is calculated using (5.4) and (5.5) for a winding hottest-spot temperature of $80°C$, i.e., $L_1 = t_{\theta_{H,1}}$. The pre-exponent factor $A$ is calculated considering that the paper moisture content increases by 0.5% each time the DP is halved [105], and that the relationship between the paper moisture content and the pre-exponent factor $A$ is given by [103]:

$$A = 9.37 \times 10^{13}x^2 + 1.03 \times 10^{13}x - 2.58 \times 10^{10} \quad (\text{hours})^{-1} \tag{5.6}$$

where $x$ is the paper moisture content. The values of $x$ used for calculating $A$ are 1% when the DP varies between 1000 and 500, 1.5% when the DP varies between 499 and 250, and 2% when the DP varies between 249 and 200. Hence, the value of $A$ changes in (5.5) as the DP reduces.

As mentioned above, a second ordered pair, ($\theta_{H,2}$, $L_2$), is required to calculate the

Arrhenius relationship parameters. At low operating temperatures, paper insulation degrades very slowly [83], and its lifetime is much greater than the average lifetime of power transformers. Hence, the DP reduction model cannot be used to calculate $L_2$. Because the average lifetime of power transformers is not significantly affected by low operating temperatures, it was assumed that the value of life measure $L_2$ is 100 years for a winding hottest-spot temperature of $36°C$. This assumption is similar to the one made in [44].

### 5.3.3 Apparent Age

The previous section detailed how the scale parameter of Weibull distribution is calculated. This is an important aspect of the unavailability due to ageing failure of power transformers. Another relevant aspect is their service age, as reflected in (3.14). The service age of a power transformer is the number of years that it has remained in operation, and so the service age does not provide information on the actual condition of a power transformer. Considering this problem, a methodology has been developed to calculate the age of power transformers using health index data. (Health indices are commonly used to determine the overall condition of power transformers [106].)

The proposed methodology consists of two parts. In the first part, the age of a power transformer is calculated by utilising the approach developed in [107] and [108], which models the relationships between the service age and the probability of a dominant condition state (a dominant condition state can be good, fair, poor, or faulty). Equations (5.7) and (5.8) give these relationships for two dominant condition states, good and fair. These equations were obtained using service age and health index data of 265 power transformers that operate in transmission systems with different voltage levels (110, 132,

275, and 330 kV) and linear regression methods [107]:

$$P_{HI,good} = -3.96 \times 10^{-3} T + 0.747 \tag{5.7}$$

$$P_{HI,fair} = 4.5 \times 10^{-3} T + 0.23 \tag{5.8}$$

where $P_{HI,good}$ and $P_{HI,fair}$ are the probabilities that the health index (HI) of a power transformer indicates that it is in good or fair condition, respectively, and $T$ is the service age. (Note that if different service age and health index information is used, equations (5.7) and (5.8) may vary.)

If the probabilistic health index of a power transformer is known, its condition-based age—also known as apparent age—can be easily calculated by solving (5.7) or (5.8) depending on whether the dominant condition state is good or fair. The resulting apparent age, $T$, may be greater or lower than the service age of the transformer.

In the second part of the methodology, the apparent age is adjusted to control the maximum variation of the unavailability due to ageing failure. This is important because the apparent age may vary significantly with respect to the service age, and this may affect the unavailability calculation. The proposed steps to adjust the apparent age are the following:

- The first step is to select a maximum allowed difference between the service age and the apparent age. For instance, if the service of age a power transformer is 45 years and the maximum allowed difference is 15 years, the apparent age of this transformer may vary between 30 and 60 years.

- The second step is to calculate the unavailability due to ageing failure using both the service age and the apparent age of the relevant transformer. This calculation is performed annually over a future period (e.g., eight years).

- The third step is to compare the unavailability calculated using the service age with the unavailability calculated using the apparent age. Because the unavailability due to ageing failure increases as components get older [31], the unavailability values of the last year are compared. If the unavailability calculated using the apparent age does not exceed a maximum variation (e.g., $\pm 50\%$) with respect to the unavailability calculated using the service age, the apparent age is accepted. On the other hand, if the unavailability exceeds the maximum variation, add or subtract accordingly one year to the apparent age.

- Steps 2 and 3 must be repeated until the maximum variation given in Step 3 is met.

It is worth mentioning that a different method to estimate the condition-based age of power transformers is proposed in [109]. The study was published after [97] was accepted. The authors of [109] also investigated how the condition-based age of power transformers influences their unavailability due to ageing failure and the EENS of a transmission system.

## 5.4 Expected Capacity of Aged Power Transformers

Transmission and distribution substations may have several power transformers connected in parallel to enhance power supply reliability [21]. If a power transformer fails, the remaining ones should be able to supply the entire load demand. However, as power transformers age, their capacity may reduce significantly, and this may lead to load curtailments. Hence, it is important to accurately calculate the expected capacity of aged

power transformers and to incorporate it into the retirement planning process. These topics will be covered in this section and Section 5.5.

Before presenting the method for calculating the expected capacity, it is necessary to explain important details about the ratings of power transformers. Liquid-immersed power transformers have several ratings listed in increasing order on their nameplates, along with cooling class designations. Cooling classes are designated using four-letter codes. The codes ONAN/ONAF, for example, indicate that a power transformer has a set of fans, and that its coolant circulates through natural convection; the codes ONAN/O-FAF indicate that a power transformer has fans and pumps to increase its power-carrying capacity during periods of high load [110]. Traditional risk assessment studies of composite (generation and transmission) systems use the maximum MVA rating of power transformers, ignoring that failures of fans and pumps can reduce the available capacity.

Special events, such as electrical and thermals faults as well as winding deformations, can also reduce the capacity of power transformers. When a special event occurs, power transformers may remain in service, but with reduced capacity [111]. Special events are caused by lightnings, maintenance errors, large load disconnections, external short-circuits, manufacturing and design errors, etc. [33]. Although the occurrence of special events is usually considered as random, some power transformers can experience special events more frequently. Transformer failure surveys have revealed that power transformers of distribution substations are more susceptible to winding deformations, because they are closer to distribution networks with overhead lines where short-circuits occur more frequently [112].

The expected capacity of aged power transformers was calculated using the method developed in [113], and it was improved in this study by incorporating the effects of both special events and winding hottest-spot temperature. The method treats the capacity of

aged power transformers as a discrete random variable whose states are the following: full capacity state, derated capacity states due to failures of transformer components, derated capacity states due to special events, and full failure state.

The full capacity state occurs when all components—bushings, tap changer, fans, pumps, paper insulation, etc.—are available (i.e., when all components are working correctly). The probability of the full capacity state, denoted as $P_{full}$, is calculated as follows [113]:

$$P_{full} = \prod_{i=1}^{M_c}(1 - U_i) \tag{5.9}$$

where $M_c$ is the total number of components, and $U_i$ is the total unavailability of component $i$.

To calculate the total unavailability of a component, it is important to consider that repairable and ageing failures can occur. The total unavailability of a component is given by [113]:

$$U_t = U_{r,c} + U_{a,c} - U_{r,c} \times U_{a,c} \tag{5.10}$$

where $U_{r,c}$ and $U_{a,c}$ are the unavailability due to repairable and ageing failures, respectively. The subscript $c$ indicates that the unavailability calculation is for transformer components. $U_{a,c}$ is calculated using the conventional ageing failure model, (3.14), whereas $U_{r,c}$ is calculated using (3.9).

Several derated capacity states due to failures of fans and pumps were considered. The probability of being at the $k$th derated capacity state, denoted as $P_{dk}$, is calculated as follows [113]:

$$P_{dk} = \sum_{j=1}^{M_k} \frac{\prod_{n=1}^{N_j} U_n}{\prod_{n=1}^{N_j}(1 - U_n)} P_{up} \tag{5.11}$$

where $M_k$ is the number of failure events that cause the $k$th derated state, $N_j$ is the number of failed components in the $j$th failure event, and $P_{up}$ is the probability that the relevant transformer is in the up state. $P_{up}$ is given by [113]:

$$P_{up} = 1 - (U_r + U_a - U_r \times U_a) \tag{5.12}$$

where $U_r$ and $U_a$ are the unavailability due to repairable and ageing failures of the relevant transformer, respectively. $U_a$ is calculated using the improved ageing failure model, described in Section 5.3; this allows us to incorporate the effect of the winding hottest-spot temperature into the expected capacity calculation. $U_r$ is calculated using (3.9).

As mentioned above, special events (winding deformations, and thermal and electrical faults) can also reduce the capacity of power transformers. Based on the classification of thermal and electrical faults given in [100] and information on winding deformations collected in transformer failure surveys [33], it was considered that special events can yield three derated capacity states. The first state is caused by partial discharges, thermal faults with a maximum temperature of 300°C, or winding deformations. The second state is caused by low energy discharges, thermal faults with temperatures between 300°C and 700°C, or winding deformations. The third state is caused by high energy discharges or thermal faults with temperatures greater than 700°C.

The probability of the $k$th derated state due to special events, denoted as $P_{dsk}$, is calculated as follows [97]:

$$P_{dsk} = \sum_{j=1}^{S_k} P_{se,j} \times P_{up} \tag{5.13}$$

where $S_k$ is the number of special events that cause the $k$th derated capacity state, and $P_{se,j}$ is the probability of the special event $j$, which can be calculated using failure data and maintenance records of power transformers.

Failures of critical components, such as paper insulation, windings, core, and tank, can lead to the full failure state, in which power transformers are removed from service. The probability of being at the full failure state, denoted as $P_{down}$, is given by [113], [97]:

$$P_{down} = 1 - P_{up} - \sum_{k=1}^{ND_f} P_{dk} - \sum_{k=1}^{ND_s} P_{dsk} \tag{5.14}$$

where $ND_f$ is the number of derated capacity states caused by failures of fans and pumps, and $ND_s$ is the number of derated capacity states caused by special events.

Once the probabilities $P_{full}$, $P_{dk}$, $P_{dsk}$, and $P_{down}$ have been calculated, the expected capacity of a power transformer can be easily determined by multiplying its full capacity and its derated capacity states (in MVA) by their relevant probabilities. The values of derated capacity states due to failures of fans and pumps can be calculated using the ratings and cooling classes provided on the nameplate of the transformer. However, determining the values of the derated capacity states due to the special events is more difficult. The authors of [114] mention that winding deformations can affect the performance of power transformers, but they do not specify capacity reductions. Considering this, it was assumed that special events can lead to 10%, 25%, and 50% capacity reductions [97]. For instance, partial discharges reduce the capacity of a power transformer to 90%, whereas high energy discharges reduce the capacity of a power transformer to 50%.

## 5.5 Ranking of Aged Power Transformers

Some power systems have several aged power transformers whose retirement must be carefully planned. As explained in Subsection 4.3.2, the credible improvement potential index can be used to identify the best candidates for the retirement planning process. The credible improvement potential index calculates how much the reliability of a power

system improves if an aged power transformer is replaced by a new one [41]. This index was enhanced by using the expected damage cost as the power system reliability indicator and the total unavailability of power transformers as their unreliability indicator, and by incorporating the effects of transformer capacity reduction [97].

The credible improvement potential (CIP) index, denoted as $I_i^{CIP}$, is calculated as follows [97]:

$$I_i^{CIP} = I_i^B \times (U_i^t - U_i^{(n)}) \quad (£/\text{year}) \tag{5.15}$$

where $I_i^B$ is the Birnbaum's measure of transformer $i$, $U_i^t$ is the total unavailability of transformer $i$ (which is calculated using (5.10)), and $U_i^{(n)}$ is the unavailability of the new transformer.

The Birnbaum's measure calculates the reduction of the expected damage cost ($EDC$) when the unavailability of transformer $i$ reduces from $U_i^t$ to $U_i^{(n)}$, and is given by [97]:

$$I_i^B = \frac{\partial EDC}{\partial U_i} \quad (£/\text{year}). \tag{5.16}$$

Instead of using (5.16), the Birnbaum's measure of transformer $i$ is calculated as follows [97]:

- Calculate the EENS caused by repairable and ageing failures of transformer $i$, by performing non-sequential Monte Carlo simulations and contingency analysis for a one-year period. To sample the state of transformer $i$, it is necessary to generate two random numbers. The first number is compared with the unavailability due to repairable failure, while the second number is compared with the unavailability due to ageing failure. To sample the states of other components, generate a random number and compare it with the unavailability due to repairable failure. Then,

the contingency analysis is performed, as explained in Section 3.5, and the EENS caused by failures of transformer $i$, which is denoted as $EENS_{dir}$, is calculated using (3.29). The subscript *dir* indicates that the EENS is directly caused by transformer $i$'s failures.

- If transformer $i$ is in a substation that has other transformers, calculate the EENS caused by the capacity reduction of transformer $i$. For instance, if a substation has an aged transformer (T1) and a non-aged transformer (T2), the expected capacity of T1 is calculated using the methodology presented in Section 5.4. The reduced capacity of T1 and the repairable failures of T2 may cause load curtailments, which are included in $EENS_{ind}$. The subscript *ind* indicates that the EENS is indirectly caused by transformer $i$.

- Assume that transformer $i$ is replaced with a new transformer whose unavailability due to repairable failures is $U_i^{(n)}$. Then, calculate the EENS caused by failures of the new transformer, denoted as $EENS_{new}$.

- Calculate the expected damage costs by multiplying $EENS_{dir}$, $EENS_{ind}$, and $EENS_{new}$ (in MWh/year) by the average unit interruption cost (in £/MWh). This simplified method for determining the expected damage costs is used because customer damage functions cannot be applied when ageing failures are modelled [17].

- Finally, calculate the Birnbaum's measure of transformer $i$ using (5.17).

$$I_i^B = EDC_{dir} + EDC_{ind} - EDC_{new} \quad (£/\text{year}) \tag{5.17}$$

## 5.6 Retirement Year

The credible improvement potential index, described in the previous section, allows us to rank aged power transformers whose retirement year needs to be determined. To calculate the year in which a power transformer should be retired, it is necessary to compare the cumulative expected damage cost—also known as expected risk cost—caused by both ageing failures and capacity reduction with the cumulative saved capital due to delaying its retirement.

This economic comparison is performed for a number of years until the cumulative expected damage cost exceeds the cumulative saved capital. In mathematical terms, the economic comparison is expressed as follows [4]:

$$\sum_{i=1}^{n_y} E_i > \sum_{i=1}^{n_y} (1+r)^{n_y-1} r \times V \tag{5.18}$$

where $E_i$ is the expected damage cost, $r$ is the interest rate, and $n_y$ is the year of retirement. The saved capital due to delaying the retirement of a transformer is calculated by multiplying the compound interest rate by the cost of installing a new transformer ($V$).

It is important to mention that the expected damage cost caused by ageing failures can be calculated using two cases [4]. In the first case, the states of all components are sampled using their unavailability due to repairable failure. In the second case, the unavailability due to ageing failure of the relevant transformer is also considered. The improved ageing failure model is utilised in the latter case, and this enables us to incorporate transformer condition and temperature information into the retirement year calculation. The expected damage cost caused by ageing failures is calculated by subtracting the expected damage cost obtained in the first case from the expected damage cost obtained in the second case.

## 5.7 Case Study

### 5.7.1 Test System

The 138-kV network of the 24-bus IEEE Reliability Test System (RTS), shown in Figure A.2, was modified by adding overhead lines and step-down power transformers at buses 1-7. Figure 5.3 shows the changes made to bus 1. As it can be seen, the new substations have single and parallel power transformers with different ratings (20, 33, and 75 MVA). Buses 2-7 suffered similar changes. The IEEE RTS was extended to investigate the retirement of transformers that supply the load demand of a 46-kV subtransmission system and a 23-kV distribution system. The ratings and maximum load demand of the step-down transformers were taken from a technical report of an Ecuadorian electric utility [115]. The maximum load demand at buses 1-7 is the same as the one specified for the IEEE RTS. Typical impedance values, taken from [116], were used for the step-down transformers.

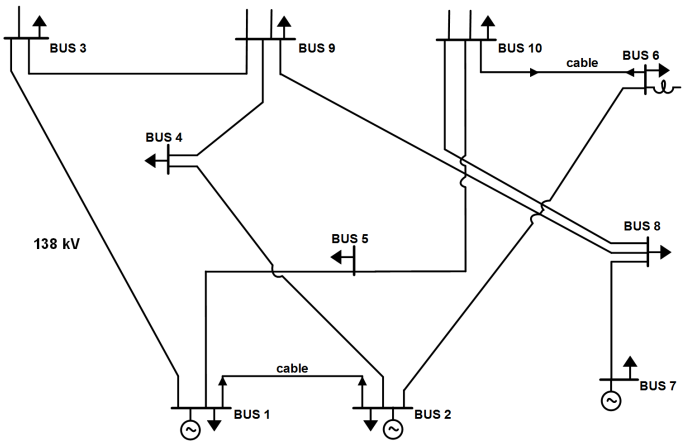


FIGURE 5.2: 138-kV network of the 24-bus IEEE RTS [16]

For the first part of the proposed retirement approach, service age and health index data of the test system's power transformers must be collected. However, this information

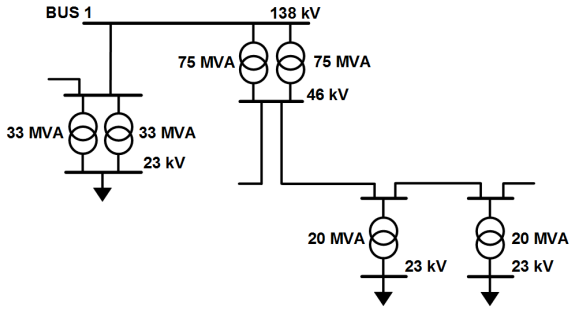


FIGURE 5.3: Changes made to bus 1 of the 24-bus IEEE RTS [97]. Several overhead lines and step-down power transformers were included in the test system.

is not available in [115], so it was assumed that there are 11 aged step-down power transformers, whose service age, probabilistic health index, and overall condition are given in Table 5.1. This information was taken from [107], and will be used to calculate the apparent age of the power transformers. The first column of the table indicates the substation and transformer number. For instance, S1-TR2 means substation 1 and transformer 2. All substations listed in the table have two transformers except substations 4 and 12.

TABLE 5.1: Service age and probabilistic health index of the power transformers used for the analysis [97], [107]. The first column indicates the substation and transformer number.

| Transformer | Service age (years) | Probabilistic health index | Overall condition |
|---|---|---|---|
| S1-TR2 | 39 | 0.51 | fair |
| S4-TR | 48 | 0.60 | good |
| S11-TR2 | 47 | 0.54 | fair |
| S12-TR | 40 | 0.55 | good |
| S14-TR1 | 44 | 0.56 | fair |
| S15-TR2 | 54 | 0.54 | fair |
| S16-TR1 | 58 | 0.50 | fair |
| S19-TR1 | 53 | 0.55 | fair |
| S20-TR1 | 45 | 0.52 | good |
| S23-TR1 | 37 | 0.50 | fair |
| S23-TR2 | 41 | 0.56 | fair |

### 5.7.2 Unavailability due to Ageing Failure

The unavailability due to ageing failure of the power transformers listed in Table 5.1 was calculated considering the following four cases:

- Case 1: The service age of power transformers and their Weibull distribution are utilised in (3.14). (This is the traditional way of calculating the unavailability due to ageing failure.)
- Case 2: The apparent age of power transformers, calculated using the methodology described in Subsection 5.3.3, and their Weibull distribution are utilised in (3.14).
- Case 3: The service age of power transformers and their Weibull distribution with the winding hottest-spot temperature, calculated using (5.1), are used in (3.14).
- Case 4: The apparent age of power transformers and their Weibull distribution with the winding hottest-spot temperature are used in (3.14). (This case considers, at the same time, the improvements for the unavailability calculation described in Section 5.3.)

The parameters of the Weibull distribution calculated in [44] were used to model the lifetime of the test system's power transformers for Cases 1 and 2. The parameters, $\alpha = 70.79$ (years) and $\beta = 5$, were calculated using mainly service age data of power transformers of the UK transmission system, in which few end-of-life failures of power transformers have occurred. The parameter $\beta = 5$ is also used for Cases 3 and 4, whereas the parameter $\alpha$ was calculated through the Arrhenius relationship, whose constants $c_1$ and $c_2$ have a value of 0.01 and 2803.5, respectively. They were calculated by following the procedure given in Subsection 5.3.2.

The apparent age and winding hottest-spot temperature, used in Cases 2-4, were determined as follows. The apparent age of each power transformer was calculated using the probabilistic health index given in Table 5.1 and the methodology explained in Subsection 5.3.3, which uses the linear regressions models (5.7) and (5.8). Although these models were created using data of power transformers that operate at 110, 132, 275, and 330 kV [107], it was assumed that the models can be used for the test system's power transformers, which operate at 69 and 138 kV. The models may vary for transformers of different power systems, but their calculation is excluded from this study. The hourly load demand profiles, the hourly ambient temperature, and the IEC thermal model parameters needed for the winding hottest-spot temperature calculation were taken from [16], [117], and [45] respectively. Furthermore, an annual load demand growth of 0.6% was utilised [118].

Figure 5.4 shows the unavailability due to ageing failure of transformer S14-TR1 for Cases 1-4; the unavailability was calculated over five years (2021-2025), and its values will be used to analyse the retirement of S14-TR1 in Section 5.7.4. When the apparent age is utilised, the unavailability values increase. For example, in 2021, the unavailability calculated using the apparent age is 1.6 times the unavailability calculated using the service age (see Cases 1 and 2). It can also be seen that the unavailability of S14-TR1 increases more quickly when the Weibull distribution with winding hottest-spot temperature is used. The unavailability increment over the five-year period for Case 2 (Weibull distribution) is 0.0032, whereas the unavailability increment for Case 4 (Weibull distribution with winding hottest-spot temperature) is 0.0076. The unavailability of S14-TR1 for Case 4 is further analysed below.

Figure 5.5 shows how increments of age and winding hottest-spot temperature influence the unavailability of S14-TR1. The results indicate that age increments play a more

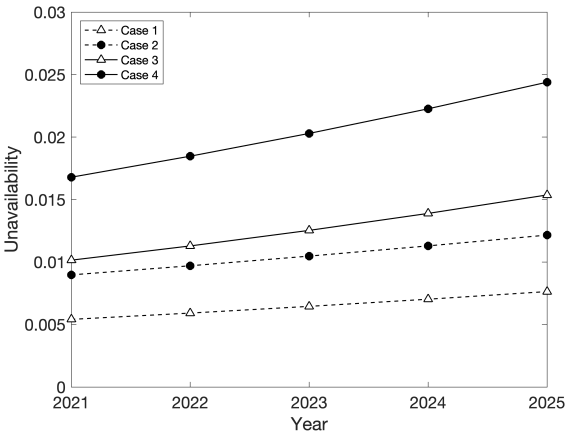


FIGURE 5.4: Unavailability due to ageing failure of transformer S14-TR1 using service age and Weibull distribution (Case 1), apparent age and Weibull distribution (Case 2), service age and Weibull distribution with winding temperature (Case 3), and apparent age and Weibull distribution with winding temperature (Case 4)

significant role in the unavailability. For instance, when the transformer age increases from 54 to 58 years and the winding hottest-spot temperature is 49.4°C, the unavailability increases from 0.023 to 0.030, whereas when the winding hottest-spot temperature increases from 49.4 to 50°C and the transformer age is 54 years, the unavailability only increases from 0.023 to 0.024. Furthermore, the red dots in Figure 5.5 indicate the combined effect of age and winding hottest-spot temperature increments; these unavailability values are the same as the ones shown in Figure 5.4 (Case 4).

The unavailability due to ageing failure of other power transformers is further analysed. Their unavailability values are shown in Tables 5.2 and 5.3 for Cases 3 and 4, respectively. Unlike the unavailability of S14-TR1, the unavailability of S4-TR reduces when its apparent age is employed (e.g., the unavailability reduced from 0.0147 to 0.0063 in 2025). This is because its apparent age, 38, is lower than its service age, 48. This result shows the importance of taking into account the condition of power transformers for their unavailability calculation when planning their retirement.

Another interesting result is given in Table 5.2. Although transformers S15-TR2 and

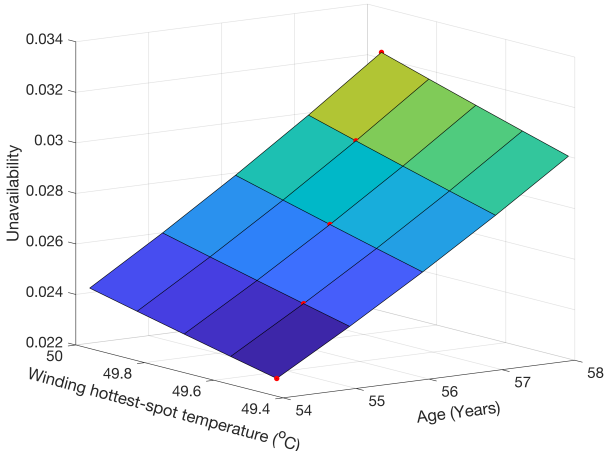


FIGURE 5.5: Unavailability due to ageing failure of transformer S14-TR1 using apparent age and Weibull distribution with winding temperature (Case 4) [97]

TABLE 5.2: Unavailability due to ageing failure of the test system's power transformers using service age and Weibull distribution with winding temperature (Case 3) [97]

| Year | S1-TR2 | S4-TR | S15-TR2 | S19-TR1 |
|---|---|---|---|---|
| 2021 | 0.0067 | 0.0101 | 0.0126 | 0.0099 |
| 2022 | 0.0075 | 0.0111 | 0.0138 | 0.0108 |
| 2023 | 0.0085 | 0.0122 | 0.0150 | 0.0117 |
| 2024 | 0.0095 | 0.0134 | 0.0163 | 0.0127 |
| 2025 | 0.0106 | 0.0147 | 0.0176 | 0.0138 |

TABLE 5.3: Unavailability due to ageing failure of the test system's power transformers using apparent age and Weibull distribution with winding temperature (Case 4) [97]

| Year | S1-TR2 | S4-TR | S15-TR2 | S19-TR1 |
|---|---|---|---|---|
| 2021 | 0.0108 | 0.0040 | 0.0204 | 0.0161 |
| 2022 | 0.0120 | 0.0045 | 0.0220 | 0.0174 |
| 2023 | 0.0133 | 0.0051 | 0.0238 | 0.0188 |
| 2024 | 0.0148 | 0.0057 | 0.0256 | 0.0202 |
| 2025 | 0.0164 | 0.0063 | 0.0276 | 0.0217 |

S19-TR1 have almost the same service age (54 and 53 years, respectively), their unavailability values are not similar. This is because the first transformer has higher load factors than the second transformer, and this yields higher winding hottest-spot temperatures and higher unavailability values for S15-TR2. (The same ambient temperature data was used for all transformers, so ambient temperature does not influence the results.) For instance, in 2021, the load factor of S15-TR2 is 0.388 p.u., whereas the load factor of

S19-TR1 is 0.356 p.u. This result shows the other benefit of the enhanced ageing failure model: it incorporates the influence of the winding hottest-spot temperature into the unavailability of each transformer. The traditional ageing failure model does not do this.

However, the proposed method to incorporate the effects of loading conditions—that is, the method that combines the Arrhenius relationship, the IEC thermal model, and (4.4)—has a disadvantage: Overloading periods, which can last a few hours, accelerate the ageing of transformers' paper insulation (as discussed in [83]), but the impact of these intermittent events is not considered by the proposed method, since it converts hourly loading conditions into a constant annual equivalent load for the calculation of the winding hottest-spot temperature.

### 5.7.3 Expected Capacity of Test System's Power Transformers

The data needed to calculate the expected capacity of the test system's power transformers —failure and repair rates as well as lifetime probability distributions —were selected based on the information found in [15], [33], [45]. For instance, normal probability distributions were used to model the lifetime of fans and pumps; the values of the mean lifetime and standard deviation are (20, 5) years for fans and (25, 5) years for pumps. Furthermore, it was assumed that fans and pumps are replaced after they reach their mean lifetimes. Table 5.4 shows the capacity levels of S16-TR1 and the possible states of its cooling system components. The nameplate ratings of S16-TR1 are 20/27/33 MVA (ONAN/ONAF/OFAF).

Figure 5.6 shows the capacity probability distributions of S16-TR1, which were calculated for five years (2021-2025). The probability of being at the full capacity state (33 MVA) reduces each year, whereas the probabilities of the derated capacity states (20, 23.5,

TABLE 5.4: States of cooling system components and capacity levels of transformer S16-TR1 [97]. Its nameplate ratings are 20/27/33 MVA (ONAN/ONAF/OFAF).

| Oil pump | Fan 1 | Fan 2 | Capacity, MVA |
|---|---|---|---|
| 0 | 0 | 0 | 20.0 |
| 0 | 0 | 1 | 23.5 |
| 0 | 1 | 0 | 23.5 |
| 0 | 1 | 1 | 27.0 |
| 1 | 0 | 0 | 20.0 |
| 1 | 0 | 1 | 30.0 |
| 1 | 1 | 0 | 30.0 |
| 1 | 1 | 1 | 33.0 |

27, and 30 MVA) caused by failures of the cooling system components increase each year. All these results indicate that the capacity of S16-TR1 fluctuates, i.e., it is not constant as considered in traditional power system reliability assessment studies. This finding will be further explored below.

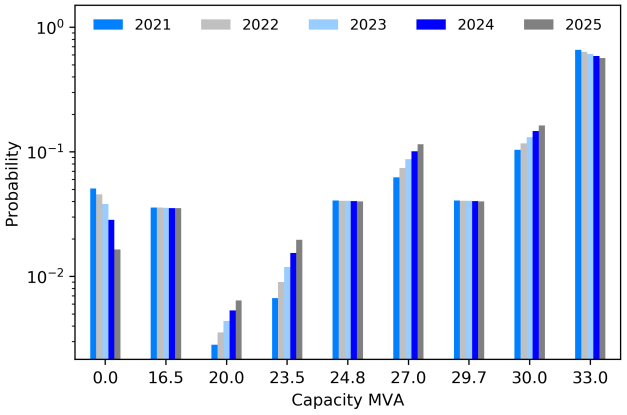


FIGURE 5.6: Capacity probability distributions of transformer S16-TR1 calculated using service age and Weibull distribution with winding temperature (Case 3) [97]

Table 5.5 shows the expected capacity of S16-TR1 calculated over 2021-2025 for Cases 1 and 4. The expected capacity changes each year, and all its values are lower than the transformer's maximum rating, 33 MVA. The expected capacity calculated using the apparent age and Weibull distribution with winding temperature (Case 4) is slightly lower than the expected capacity calculated using the service age and Weibull distribution

TABLE 5.5: Expected capacity of transformer S16-TR1 using service age and Weibull distribution (Case 1), and apparent age and Weibull distribution with winding temperature (Case 4) [97]

| Year | Case 1, MVA | Case 4, MVA |
|---|---|---|
| 2021 | 29.606 | 29.480 |
| 2022 | 29.668 | 29.515 |
| 2023 | 29.792 | 29.605 |
| 2024 | 29.980 | 29.754 |
| 2025 | 30.237 | 29.963 |

(Case 1). This is because as seen in Subsection 5.7.2, the probability of having S16-TR1 in operation decreases more rapidly if the improved ageing failure model is used. Note that the results of Table 5.5 may vary if a different replacement policy of the cooling system components is employed. For example, if asset managers allow cooling system components to operate beyond their average lifetime, their unavailability due to ageing failure may affect the expected capacity significantly.

### 5.7.4 Ranking and Year of Retirement of Power Transformers

The power transformers listed in Table 5.1 were ranked by calculating their credible improvement potential index, $I_i^{CIP}$, for two scenarios: using the full and expected capacity of power transformers. A six-step load model was created using the k-means algorithm described in Section 3.5 and, was used for calculating the EENS. Furthermore, two interruption costs were used to calculate the expected damage cost: 858.8 (£/MWh) for loads located at substations with single transformers and 1226.4 (£/MWh) for loads located at substations with parallel transformers [119]. All calculations were performed using the software MATLAB.

Table 5.6 shows the ranking of the power transformers for Cases 1-4 using their full capacity. The ranking list has eight transformers; the remaining transformers (S11-TR2, S19-TR1, and S20-TR1) are not part of the ranking because their credible improvement

potential indices are equal to zero. Transformer S16-TR1 occupies the first place in the ranking for Cases 1-4, and this indicates that its retirement should be prioritised. Transformers S12-TR and S4-TR occupy the second and third places for Case 1, respectively. However, if the apparent age and Weibull distribution with winding hottest-pot temperature (Case 4) are utilised for S4-TR, this transformer drops to the last place of the ranking; therefore, planning its retirement would not be a priority.

TABLE 5.6: Ranking of the test system's power transformers for Cases 1-4 using their full capacity (results follow the format (index in £/year, ranking)) [97]

| Case | S1-TR2 | S4-TR | S12-TR | S14-TR1 | S15-TR2 | S16-TR1 | S23-TR1 | S23-TR2 |
|---|---|---|---|---|---|---|---|---|
| 1 | (7.1, 7) | (36.5, 3) | (58.9, 2) | (7.4, 6) | (13.9, 4) | (138.6, 1) | (3.1, 8) | (9.2, 5) |
| 2 | (25.1, 3) | (10.7, 7) | (76.4, 2) | (13.4, 6) | (17.3, 5) | (158.2, 1) | (9.6, 8) | (24.0, 4) |
| 3 | (29.8, 7) | (68.0, 4) | (90.9, 2) | (47.3, 5) | (31.4, 6) | (681.8, 1) | (29.3, 8) | (74.2, 3) |
| 4 | (51.6, 7) | (43.9, 8) | (98.2, 3) | (86.7, 4) | (60.5, 6) | (701.9, 1) | (81.7, 5) | (115.4, 2) |

Table 5.7 shows the ranking of the power transformers for Cases 1-4 using their expected capacity. The new ranking list has ten power transformers, whose indices are slightly different except for S12-TR and S4-TR. When the expected capacity is employed, transformer S23-TR1 occupies the third place in the ranking (Case 4), instead of the fifth place given in Table 5.6. This result indicates that neglecting capacity reductions of power transformers may affect the retirement planning process.

TABLE 5.7: Ranking of test system's power transformers for Cases 1-4 using their expected capacity (results follow the format (index in £/year, ranking)) [97]

| Case | S1-TR2 | S4-TR | S12-TR | S14-TR1 | S15-TR2 | S16-TR1 | S23-TR1 | S23-TR2 | S11-TR2 | S19-TR1 |
|---|---|---|---|---|---|---|---|---|---|---|
| 1 | (7.7, 7) | (36.5, 3) | (58.9, 2) | (8.9, 6) | (14.5, 4) | (145.1, 1) | (5.1, 8) | (14.4, 5) | (1.9, 10) | (2.8, 9) |
| 2 | (26.1, 4) | (10.7, 8) | (76.4, 2) | (15.2, 7) | (18.0, 6) | (162.4, 1) | (18.9, 5) | (36.7, 3) | (1.7, 10) | (2.6, 9) |
| 3 | (30.7, 8) | (68.0, 4) | (90.9, 2) | (49.2, 5) | (32.0, 7) | (685.4, 1) | (42.2, 6) | (89.0, 3) | (1.5, 10) | (3.3, 9) |
| 4 | (52.2, 7) | (43.9, 8) | (98.2, 4) | (88.5, 5) | (61.1, 6) | (706.2, 1) | (104.5, 3) | (130.7, 2) | (1.6, 10) | (3.1, 9) |

Because transformer S16-TR1 occupies the first place in the rankings, its year of retirement was calculated by comparing the cumulative expected system damage cost (calculated using an interruption cost of 1226.4 (£/MWh)) with the cumulative saved

capital due to delaying its retirement (calculated using a replacement cost of £0.8 million and an interest rate of 5.0%). Table 5.8 shows their values for Cases 1 and 4 considering the transformer's full and expected capacity. If the improved ageing failure model (Case 4) and the full capacity are used, S16-TR1 should be retired in 2025 (year in which the cumulative expected system damage cost is greater than the cumulative saved capital), and if the expected capacity is incorporated, S16-TR1 should be retired in 2024. Both results seem reasonable since this transformer has a service age of 58 years.

TABLE 5.8: Cumulative expected system risk cost and cumulative saved capital for transformer S16-TR1 [97]

| Year | System risk cost, k£ | | | Saved capital, k£ |
|---|---|---|---|---|
| | Case 1 with full capacity | Case 4 with full capacity | Case 4 with exp. capacity | |
| 2021 | 7.9 | 29.2 | 31.5 | 40.0 |
| 2022 | 18.5 | 65.8 | 71.1 | 82.0 |
| 2023 | 31.6 | 110.1 | 118.9 | 126.0 |
| 2024 | 47.5 | 161.4 | 174.4 | 172.4 |
| 2025 | 66.8 | 228.1 | | 221.0 |

Table 5.8 also shows that if the conventional ageing failure model (Case 1) and the full capacity are utilised, the year of retirement of S16-TR1 cannot be determined, as the cumulative expected system damage cost does not exceed the cumulative saved capital.

A key aspect that can affect the application of the proposed retirement approach is that some power systems have substations with multiple power transformers connected in parallel, and when an aged power transformer fails, the amount of curtailed load is zero or minimal. In other words, failures of an aged power transformer do not cause any damage (or cause minimal damage) to the reliability of power systems, so its year of retirement cannot be calculated using the proposed approach. This situation occurred for one of the tests system's power transformers, S20-TR1. Failures of S20-TR1 did not cause load curtailments, and for that reason, this transformer is not part of the rankings given in

Tables 5.6 and 5.7. In such cases, asset managers should plan the retirement of power transformers by calculating appropriate health indices, as investigated in [106], [12].

## 5.8 Summary

This chapter presented a risk-based approach to plan the retirement of aged power transformers. The approach includes several methods that enhance the conventional ageing failure, by calculating the apparent age of power transformers and the scale parameter of the Weibull distribution. The strategy first ranks power transformers by using their credible improvement potential index, and then calculates their year of retirement by comparing the cumulative expected system risk cost (caused by ageing failures and capacity reduction) with the cumulative saved capital due to delaying the retirement of the relevant transformer.

The 138-kV network of the IEEE RTS was extended to evaluate the performance of the transformer retirement approach. The results suggest that incorporating the apparent age and the effects of both winding hottest-spot temperature and capacity reduction can enhance the retirement planning process of power transformers significantly when there is limited availability of end-of-life failure data.

The proposed approach provides a set of models and methodologies that exploit different types of data. For instance, health indices of power transformers are employed to estimate their apparent age, and load and weather data are utilised to determine their thermal stress. These models and methodologies improve the conventional ageing failure model, allowing asset managers to quantify risks posed by aged transformers more accurately and thus to make better capital investments.

# Chapter 6

# Transmission System Reinforcement Considering Seismic Events and Aged Equipment

## 6.1 Introduction

Earthquakes around the world have caused both significant damages to power system infrastructure and long, widespread power supply interruptions [14], [120]. To mitigate the impact of earthquakes on power systems, there are several strategies that have been investigated, and some of them already implemented, including the use of distributed generation and microgrids for power supply [121], replacement of old power equipment that was not seismically designed [70], and reinforcement of power transmission systems [67], [68]. This chapter focuses on the last strategy, i.e., determining the optimal number and location of new components (lines and transformers) that should be built in a transmission system with seismic risk.

The transmission reinforcement planning (TRP) problem (considering seismic events) has been studied in [67] and [68]. The authors of those studies applied stochastic optimisation and optimisation via simulation to determine reinforcement plans. In both studies, the availability of components is determined by calculating their peak ground acceleration and by using fragility curves to obtain the probability of damage of each component. However, existing fragility curves [71], [72], developed by U.S. government institutions and research centres, may not accurately predict seismic damages on power system infrastructure [122], because factors such as soil conditions, equipment ageing, voltage levels, and seismic design criteria vary in different countries, affecting the damage predictions given by fragility curves. Another drawback of [67] and [68] is that the capacities (or ratings) of power system components remain constant over the planning period, i.e., component ageing is neglected.

Considering these problems, a two-stage adaptive robust optimisation problem to determine optimal reinforcement decisions is presented in this chapter. The availability of components is modelled in a different (deterministic) way: Components are grouped based on their location with respect to an earthquake's epicentre, their ageing status, and their risk of being affected by a tsunami, and then a polyhedral uncertainty set is used for each group. (It is assumed that the test system is in close proximity to a coastal area where earthquakes or aftershocks are in mid sea to make tsunamis.) A method for calculating the uncertainty budgets of the polyhedral uncertainty sets is developed. The method models the uncertainty budget as a function of the peak ground acceleration, allowing us to create a link between seismic events and component availability. Furthermore, the main steps to calculate the expected capacity of aged components and its incorporation into the optimisation problem are described in detail.

## 6.2 Deterministic TRP Problem

This section describes the formulation of the deterministic TRP problem, in which the maximum future load demand is constant, and components are always available. This optimisation problem has been previously investigated in [66], and it determines the number and location of transmission lines and/or power transformers that should be built at the beginning of the planning period to supply the maximum future load demand, $P_d^{Dmax}$. The deterministic TRP problem's objective function and constraints are given below [66]:

$$\min_{\Delta} \quad \sum_{c \in \Omega^{C+}} I_c^C x_c^C + \sigma \left[ \sum_g C_g^E p_g^E + \sum_d C_d^{LS} p_d^{LS} \right] \tag{6.1}$$

subject to

$$\sum_{c \in \Omega^{C+}} I_c^C x_c^C \leq I^{C,max} \tag{6.2}$$

$$x_c^C = \{0,\ 1\} \quad \forall c \in \Omega^{C+} \tag{6.3}$$

$$\sum_{g \in \Omega_n^E} p_g^E - \sum_{c|s(c)=n} p_c^C + \sum_{c|r(c)=n} p_c^C = \sum_{d \in \Omega_n^D} \left( P_d^{Dmax} - p_d^{LS} \right) \quad \forall n \tag{6.4}$$

$$p_c^C = B_c \left( \theta_{s(c)} - \theta_{r(c)} \right) \quad \forall c \setminus c \in \Omega^{C+} \tag{6.5}$$

$$p_c^C = x_c^C B_c \left( \theta_{s(c)} - \theta_{r(c)} \right) \quad \forall c \in \Omega^{C+} \tag{6.6}$$

$$-F_c^{max} \leq p_c^C \leq F_c^{max} \quad \forall c \tag{6.7}$$

$$0 \leq p_g^E \leq P_g^{Emax} \quad \forall g \tag{6.8}$$

$$0 \leq p_d^{LS} \leq P_d^{Dmax} \quad \forall d \tag{6.9}$$

$$-\pi \leq \theta_n \leq \pi \quad \forall n \tag{6.10}$$

$$\theta_n = 0 \quad n\text{: ref.} \tag{6.11}$$

where the set $\Delta$ contains the decision variables, i.e., $\Delta = \{x_c^C,\ p_g^E,\ p_d^{LS},\ p_c^C,\ \theta_n\}$. $x_c^C$ is a binary variable that indicates whether or not a prospective component $c$ should be built. $p_g^E$ is the power produced by generating unit $g$, and $p_d^{LS}$ is the curtailed load by demand $d$. $p_c^C$ represents the power flow through component $c$, and $\theta_n$ is the voltage angle at node $n$. (The nomenclature of this chapter is given at the beginning of this dissertation.)

The objective function, (6.1), minimises the total costs, i.e., the costs of building new transmission lines and/or power transformers and the power generation and load shedding costs. However, the objective function does not employ the total cost of building a component $c$. It uses the annualised investment cost, $I_c^C$, which is a cost that occurs equally in every year of component $c$'s lifetime [123]. Because of this, power production and load-shedding costs are multiplied by a time factor $\sigma$ whose value is 8,760 hours [66].

Equation (6.2) controls that the investment costs do not exceed the maximum investment budget, $I^{C,max}$. Equation (6.3) sets the values for $x_c^C$. Equation (6.4) controls the power balance at each bus. The power transferred through existing and prospective components is calculated by (6.5) and (6.6). Power transfer and generation limits are given by (6.7) and (6.8), respectively. Load-shedding limits are modelled through (6.9). Finally, constraint (6.10) sets the limits for all voltage angles except the slack bus' voltage angle, whose value is set by (6.11).

## 6.3 TRP Problem Using Robust Optimisation

Optimisation problems can have uncertain parameters [124]. Stochastic optimisation solves these types of problems by modelling uncertain parameters through probability distributions [125]. However, in some cases, data needed to calculate probability distribution parameters are not available, or in other cases, uncertain parameters cannot be

modelled using probability distributions. Robust optimisation is a different approach for solving optimisation problems with uncertainty. It models uncertain parameters using deterministic approaches, also known as uncertainty sets [124]. There are different types of uncertainty sets, including quadratic, polyhedral, and cardinality-constrained uncertainty sets, whose size is controlled by a parameter known as uncertainty budget.

Robust optimisation was chosen in this study to solve the problem of reinforcing transmission systems with seismic risk, because probability distributions (i.e., fragility curves) sometimes provide inaccurate predictions about the availability of generating units, lines, and transformers, as reported in [122]. Before presenting the formulation of the robust TRP problem, it is necessary to first explain how its uncertain parameters are modelled.

### 6.3.1 Modelling Approach for Uncertain Parameters

Three uncertain parameters were considered for the TRP problem: the availability of generating units, $P_g^{Emax}$, the availability of transmission lines and power transformers, $F_c^{max}$, and the maximum future load demand, $P_d^{Dmax}$. These parameters are modelled by mainly using polyhedral uncertainty sets.

The polyhedral uncertainty set used to model the maximum future load demand is given by [66]:

$$P_d^{Dmax} \in \left[\underline{P}_d^{Dmax},\ \overline{P}_d^{Dmax}\right] \quad \forall d \tag{6.12}$$

$$\frac{\sum_d \left(P_d^{Dmax} - \underline{P}_d^{Dmax}\right)}{\sum_d \left(\overline{P}_d^{Dmax} - \underline{P}_d^{Dmax}\right)} \leq \Gamma_d \tag{6.13}$$

where $\underline{P}_d^{Dmax}$ and $\overline{P}_d^{Dmax}$ are the lower and upper bounds of the maximum future load demand, respectively. It can be seen in (6.12) that the uncertain parameter $P_d^{Dmax}$ is modelled as an independent, bounded random variable whose probability distribution

is unknown. $\Gamma_d$ represents the uncertainty budget, which controls the variation of the uncertain parameters. $\Gamma_d$ can take any values between 0 and 1. If $\Gamma_d$ equals 0, then $P_d^{Dmax} = \underline{P}_d^{Dmax}$, i.e., there is no uncertainty, whereas if $\Gamma_d$ equals 1, then $P_d^{Dmax}$ can take any value in the interval $\left[\underline{P}_d^{Dmax},\ \overline{P}_d^{Dmax}\right]$, i.e., there is maximum uncertainty [66]. In summary, the polyhedral uncertainty set given by (6.12) and (6.13) contains a set of values for the maximum future load demands that will be used to solve the TRP problem.

To model the availability of generating units, lines, and transformers, in addition to using polyhedral uncertainty sets, it is necessary to consider several factors. The first factor is the location of power system components with respect to an earthquake's epicentre. Components located near the epicentre are more likely to experience failures or damages than components located farther away from the epicentre [126]. The second factor is that some components—especially components located near coastal regions—can be affected by tsunamis. For example, several thermal and nuclear power generators, substations, and transmission lines were affected by the 2011 Japan earthquake's tsunami [127]. The last factor is the influence of both ageing and corrosion on the availability of components. Some components, in particular transmission lines and power transformers, have exceeded their design lifetimes and have been affected by corrosion, making them more vulnerable if a high magnitude earthquake occurs [128], [129].

Considering these factors, components were classified into several groups to model the remaining two uncertain parameters, $P_g^{Emax}$ and $F_c^{max}$. To do this, it was considered that components are located in high, moderate, and low seismic hazard zones. A high seismic hazard zone is located near a region where earthquakes tend to occur more frequently, whereas a low seismic hazard zone is located farther away from that region [126]. Generating units were classified into four groups: $\Omega_g = \{\Omega_g^{HH}, \Omega_g^{HHT}, \Omega_g^{MH}, \Omega_g^{LH}\}$; the group $\Omega_g^{HHT}$, for example, contains only generating units located in the high seismic

hazard zone and with risk of being damaged by a tsunami. Lines and transformers were classified into six groups: $\Omega_c = \{\Omega_c^{HH}, \Omega_c^{HHA}, \Omega_c^{MH}, \Omega_c^{MHA}, \Omega_c^{LH}, \Omega_c^{LHA}\}$; the group $\Omega_c^{LHA}$, for example, contains only aged lines and transformers located in the low seismic hazard zone. (Section 6.5 explains the criterion for identifying aged components.)

The proposed approach to model the availability of generating units, $P_g^{Emax}$, and the availability of lines and transformers, $F_c^{max}$, consists in utilising a polyhedral uncertainty set for each group in $\Omega_g$ and $\Omega_c$; hence, 10 polyhedral uncertainty sets are employed for the robust TRP problem. For instance, the polyhedral uncertainty set for components in the group $\Omega_c^{LHA}$ is given by:

$$F_c^{max} \in \left[0,\ \overline{F}_c^{max}\right] \quad \forall c \in \Omega_c^{LHA} \tag{6.14}$$

$$\frac{\sum_{c\in\Omega_c^{LHA}} \left(\overline{F}_c^{max} - F_c^{max}\right)}{\sum_{c\in\Omega_c^{LHA}} \overline{F}_c^{max}} \leq \Gamma_c^{LHA} \tag{6.15}$$

where $\overline{F}_c^{max}$ is the upper bound of component $c$'s capacity, and $\Gamma_c^{LHA}$ is the uncertainty budget of this polyhedral uncertainty set. Note in (6.14) that the lower bound of component $c$'s capacity is 0. This means that a line or transformer may be unavailable (i.e., in full failure state) if its parameter $F_c^{max}$ is equal to 0.

The uncertainty budgets used to control the variability of $P_g^{Emax}$ and $F_c^{max}$ also take values between 0 and 1. A method for calculating their values was developed and is described in Section 6.4.

### 6.3.2 Two-Stage Adaptive Robust TRP Problem Formulation

The two-stage adaptive robust optimisation problem that will be used to determine reinforcement decisions of transmission systems with seismic risk and aged components is based on the problem formulated in [66]. The optimisation problem takes into account

two stages (also known as sequence of decisions). In the first stage, reinforcement decisions are made at the beginning of the planning period. That is, a set of lines and/or transformers is chosen from all possible alternatives. Then, the values of the uncertain parameters (maximum future load demand and availability of generating units, lines, and transformers) are determined. In the second stage, remedial (adaptive) actions are performed. Remedial actions include power generation rescheduling and (in the worst case only) load curtailment, and they are aimed at reducing transmission system operation costs considering the realisations of the uncertain parameters.

The modified version of the two-stage adaptive robust TRP problem is given below:

$$\min_{x_c^C} \quad \max_{\Delta^{2ND}} \quad \min_{\Delta^{3RD}} \quad \sum_{c\in\Omega^{C+}} I_c^C x_c^C \quad +\sigma\left[\sum_g C_g^E p_g^E + \sum_d C_d^{LS} p_d^{LS}\right] \tag{6.16}$$

subject to

$$\sum_{g\in\Omega_n^E} p_g^E - \sum_{c|s(c)=n} p_c^C + \sum_{c|r(c)=n} p_c^C = \sum_{d\in\Omega_n^D} \left(P_d^{Dmax} - p_d^{LS}\right) \quad \forall n \tag{6.17}$$

$$p_c^C = B_c(\theta_{s(c)} - \theta_{r(c)}) \quad \forall c \setminus c \in \Omega^{C+} \tag{6.18}$$

$$p_c^C = x_c^C B_c(\theta_{s(c)} - \theta_{r(c)}) \quad \forall c \in \Omega^{C+} \tag{6.19}$$

$$-F_c^{max} \leq p_c^C \leq F_c^{max} \quad \forall c \tag{6.20}$$

$$0 \leq p_g^E \leq P_g^{Emax} \quad \forall g \tag{6.21}$$

$$0 \leq p_d^{LS} \leq P_d^{Dmax} \quad \forall d \tag{6.22}$$

$$-\pi \leq \theta_n \leq \pi \quad \forall n \tag{6.23}$$

$$\theta_n = 0 \quad n\text{: ref.} \tag{6.24}$$

subject to

$$P_g^{Emax} \in \left[0,\ \overline{P}_g^{Emax}\right] \quad \forall g \in \Omega_g \tag{6.25}$$

$$\frac{\sum_{g\in\Omega_g}\left(\overline{P}_g^{Emax}-P_g^{Emax}\right)}{\sum_{g\in\Omega_g}\overline{P}_g^{Emax}}\leq\Gamma_g \tag{6.26}$$

$$F_c^{max}\in\left[0,\ \overline{F}_c^{max}\right]\quad\forall c\in\Omega_c \tag{6.27}$$

$$\frac{\sum_{c\in\Omega_c}\left(\overline{F}_c^{max}-F_c^{max}\right)}{\sum_{c\in\Omega_c}\overline{F}_c^{max}}\leq\Gamma_c \tag{6.28}$$

$$P_d^{Dmax}\in\left[\underline{P}_d^{Dmax},\ \overline{P}_d^{Dmax}\right]\quad\forall d \tag{6.29}$$

$$\frac{\sum_d\left(P_d^{Dmax}-\underline{P}_d^{Dmax}\right)}{\sum_d\left(\overline{P}_d^{Dmax}-\underline{P}_d^{Dmax}\right)}\leq\Gamma_d \tag{6.30}$$

subject to

$$\sum_{c\in\Omega^{C+}}I_c^C x_c^C\leq I^{C,max} \tag{6.31}$$

$$x_c^C=\{0,\ 1\}\quad\forall c\in\Omega^{C+}. \tag{6.32}$$

The optimisation problem (6.16)-(6.32) has a three level structure with the following decision variables: $x_c^C$ represents the reinforcement decisions, the set $\Delta^{2ND}$ contains the realisations of the uncertain parameters (i.e., $\Delta^{2ND}=\{P_g^{Emax},\ F_c^{max},\ P_d^{Dmax}\}$), and the set $\Delta^{3RD}$ contains the system operation variables (i.e., $\Delta^{3RD}=\{p_g^E,\ p_d^{LS},\ p_c^C,\ \theta_n\}$).

Constraints (6.17)-(6.24), which were described in Section 6.2, form the feasible region for the system operation variables [66]. Constraints (6.25)-(6.28) are the polyhedral uncertainty sets used to model the availability of components, and must be applied for each group in $\Omega_g$ and $\Omega_c$. Constraints (6.29)-(6.30) form the polyhedral uncertainty set for the maximum future load demand.

Note that a power transmission system may be affected by earthquakes with different epicentres. In those cases, the groups of components in $\Omega_g$ and $\Omega_c$ may vary, and this must be considered when solving the two-stage adaptive robust TRP problem. This situation, earthquakes with different epicentres, will be analysed in Section 6.7.

## 6.4 Uncertainty Budget Calculation

As mentioned in Subsection 6.3.1, the availability of generating units, lines, and transformers depends on the uncertainty budgets $\Gamma_g$ and $\Gamma_c$. Each group in $\Omega_g$ and $\Omega_c$ has components with specific characteristics (different seismic hazard zone, ageing status, or risk of being damaged by a tsunami), so each group must have a different uncertainty budget. For example, generating units located in a high seismic hazard zone are more likely to experience failures or damages than generating units located further away from the epicentre, so their uncertainty budget $\Gamma_g^{HH}$ must be higher. A method for calculating the uncertainty budget of each polyhedral uncertainty set was developed, and is described below.

Considering that components are classified based on seismic hazard zones, the proposed method models the uncertainty budget as a function of the peak ground acceleration, which measures the maximum ground acceleration at a specific location [130]. Fragility curves of power system components show that their probability of damage increases as the peak ground acceleration increases [71]. Considering this, an exponential function is used to describe the relationship between the uncertainty budget and the peak ground acceleration, and is given by:

$$\Gamma = a \times \exp(b \times PGA) \tag{6.33}$$

where, $a$ and $b$ are constants, and $PGA$ is the peak ground acceleration.

The uncertainty budgets for the TRP problem are calculated as follows:

- Step 1: Calculate the peak ground acceleration of all components (generating units, lines, and transformers) using adequate attenuation models. Attenuation models

depend on several factors, including type of earthquake, type of shaking, type of soil, etc. [128].

- Step 2: Determine the highest peak ground acceleration for each group of components. This step is important because components located in a same seismic hazard zone may experience different peak ground accelerations, depending on their location and soil conditions. Choosing the highest values allows us to consider reinforcement decisions for the worst conditions.
- Step 3: Use the highest peak ground acceleration values and (6.33) to calculate the uncertainty budget for each polyhedral uncertainty set.

Steps 1-3 must be performed for each earthquake scenario. Earthquake scenarios must give both the location of the fault and the earthquake magnitude, which are critical factors for the calculation of the peak ground acceleration.

The constants $a$ and $b$ were determined by solving (6.33) twice. This method is also used in Chapter 5 (Subsection 5.3.2) to estimate the Arrhenius relationship parameters. Two ordered pairs, $(PGA_1,\ \Gamma_1)$ and $(PGA_2,\ \Gamma_2)$, must be provided to solve the equations. The values of $(PGA_1,\ \Gamma_1)$ and $(PGA_2,\ \Gamma_2)$ may be estimated using historical component damage data, the transmission system planner's criteria, and analytical approaches, like the ones used in [72].

## 6.5 Incorporation of Expected Capacity of Aged Components

As it can be seen in (6.25) and (6.27), the solution of the two-stage adaptive robust TRP problem depends on the upper bounds of the polyhedral uncertainty sets, $\overline{P}_g^{Emax}$ and $\overline{F}_c^{max}$.

The maximum production capacity of generating units and the maximum thermal ratings of lines and transformers—which are specified by their manufacturers—are employed as $\overline{P}_g^{Emax}$ and $\overline{F}_c^{max}$, respectively [66]. However, as components of generating units, lines, and transformers age, their ratings tend to reduce, as shown in Chapter 5 (Subsection 5.7.3).

Incorporating the expected capacity of aged components into the two-stage adaptive robust TRP problem is likely to help system planners make more accurate reinforcement decisions. Figure 6.1 shows the basic steps of the proposed methodology for incorporating the expected capacity. The steps are described below:

1. Classify generating units, lines, and transformers as aged or non-aged equipment by comparing, each year of the planning period, their service age with their average lifetime. If the service age of a component is greater than its average lifetime, the component is considered as aged. This classification method is used in [4].

2. Identify critical components of generating units, lines, and transformers whose failures or faults may affect the power generation and transfer capacity. Surveys on power equipment failures [33], [131] and technical reports [132], [133], [134] were employed in this study to identify critical components of hydro generators (insulation system, windings, and turbine), transmission lines (conductors, towers, and insulators), and power transformers (bushings, windings, insulation system, core, tank, and cooling system components). Then, collect data of repairable and ageing failures of critical components, e.g., failure rates, repair rates, and lifetime probability distributions.

3. Calculate the expected capacity of all generating units, lines, and transformers classified as aged equipment using the method explained in Chapter 5, Section 5.4. The

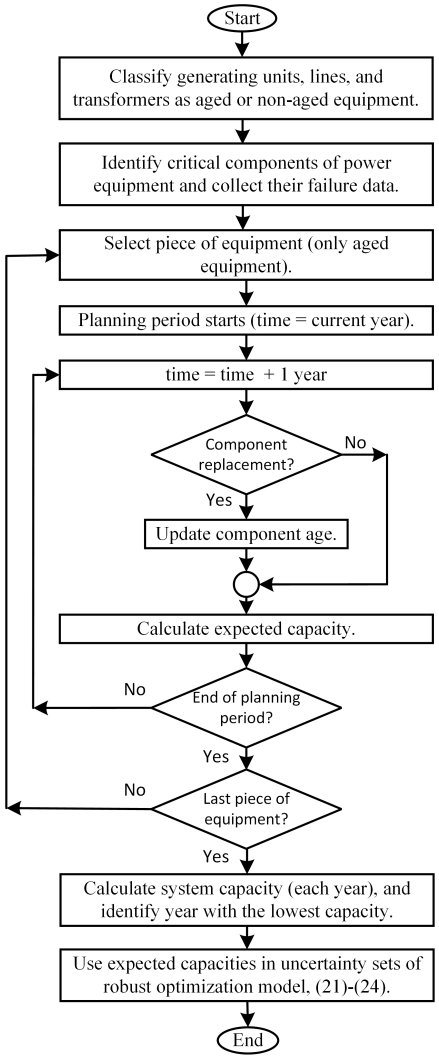


FIGURE 6.1: Basic steps for incorporating equipment ageing effects into the two-stage adaptive TRP problem

expected capacity must be calculated each year of planning period as follows [113], [97]:

$$EC = S_f P_f + \sum_{k}^{ND_f} S_{dk} P_{dk} + \sum_{k}^{ND_s} S_{dsk} P_{dsk} + S_d P_d \tag{6.34}$$

where $EC$ is the expected capacity. $S_f$ is the full capacity state (MW), whose probability is $P_f$. $S_{dk}$ is the $k$th derated capacity level due to component failures (MW), and its probability is $P_{dk}$. $S_{dsk}$ is the $k$th derated capacity level due to special events (MW), and its probability is $P_{dsk}$. $S_d$ is the full failure state, whose

probability is $P_d$. $ND_f$ and $ND_s$ are the number of derated capacity states due to component failures and due to special events, respectively.

When calculating the expected capacity, it is important to consider two factors. First, if equipment components (such as, the fans of a power transformer) are replaced, their service age must be updated accordingly. Second, if an aged generating unit, line, or transformer is replaced within the planning period, its expected capacity must be determined until the replacement year.

4. Calculate, each year of the planning period, the power generation and transfer capacity of the system under consideration.

5. Determine the year in which the system has its lowest total capacity, and use the corresponding expected capacity of aged generating units, lines, and transformers as the upper bounds of their polyhedral uncertainty sets. This step is performed because earthquakes can occur randomly during the planning period, and reinforcement decisions should be made considering the worst condition of the system in terms of power generation and transfer capacity.

## 6.6 Solution of Robust TRP Problem

The two-stage adaptive robust TRP problem has a nonlinear constraint, (6.19), in which the binary variable $x_c^C$ is multiplied by the continuous variable $\theta_n$. In other words, the optimisation problem is a mixed integer nonlinear programming (MINLP) problem. To facilitate its solution, it is necessary to substitute constraint (6.19) for the following linear inequalities [66]:

$$-x_c^C F_c^{max} \leq p_c^C \leq x_c^C F_c^{max} \quad \forall c \tag{6.35}$$

$$-\big(1-x_c^C\big)M \le p_c^C - B_c\big(\theta_{s(c)} - \theta_{r(c)}\big) \le \big(1-x_c^C\big)M \quad \forall c \tag{6.36}$$

where $M$ is a positive constant [135], [136].

The linear version of the two-stage adaptive robust TRP problem was decomposed into a master problem and a subproblem. They are solved by applying the Benders decomposition algorithm [66], [137], which is an iterative process that makes the master problem and subproblem exchange information: The master problem provides the reinforcement decisions ($x_c^C$), whereas the subproblem provides the realisations of the uncertain parameters ($P_g^{Emax}, F_c^{max}, P_d^{Dmax}$).

### 6.6.1 Master Problem

The master problem is shown below:

$$\min_{x_c^C,\ p_{g,v'}^E,\ p_{d,v'}^{LS},\ p_{c,v'}^C,\ \theta_{n,v'}} \quad \sum_{c\in\Omega^{C+}} I_c^C x_c^C + \eta \tag{6.37}$$

subject to

$$\sum_{c\in\Omega^{C+}} I_c^C x_c^C \le I^{C,max} \tag{6.38}$$

$$x_c^C = \{0,\ 1\} \quad \forall c \in \Omega^{C+} \tag{6.39}$$

$$\sum_{g\in\Omega_n^E} p_{g,v'}^E - \sum_{c|s(c)=n} p_{c,v'}^C + \sum_{c|r(c)=n} p_{c,v'}^C = \sum_{d\in\Omega_n^D} \big({P_{d,v'}^D}^{max,*} - p_{d,v'}^{LS}\big) \quad \forall n,\ \forall v' \le v \tag{6.40}$$

$$p_{c,v'}^C = B_c(\theta_{s(c),v'} - \theta_{r(c),v'}) \quad \forall c \setminus c \in \Omega^{C+}, \forall v' \le v \tag{6.41}$$

$$p_{c,v'}^C = x_c^C B_c(\theta_{s(c),v'} - \theta_{r(c),v'}) \quad \forall c \in \Omega^{C+}, \forall v' \le v \tag{6.42}$$

$$-F_{c,v'}^{max,*} \le p_{c,v'}^C \le F_{c,v'}^{max,*} \quad \forall c, \forall v' \le v \tag{6.43}$$

$$0 \le p_{g,v'}^E \le {P_{g,v'}^E}^{max,*} \quad \forall g,\ \forall v' \le v \tag{6.44}$$

$$0 \leq p^{LS}_{d,v'} \leq P^{Dmax,*}_{d,v'} \quad \forall d,\ \forall v' \leq v \tag{6.45}$$

$$-\pi \leq \theta_{n,v'} \leq \pi \quad \forall n,\ \forall v' \leq v \tag{6.46}$$

$$\theta_{n,v'} = 0 \quad n\text{:ref.},\ \forall v' \leq v \tag{6.47}$$

$$\eta \geq \sigma \Bigg[ \sum_{g} C^{E}_{g} p^{E}_{g,v'} + \sum_{d} C^{LS}_{d} p^{LS}_{d,v'} \Bigg] \quad \forall v' \leq v \tag{6.48}$$

where $v$ is the iteration counter, and $\eta$ is a continuous auxiliary variable used to reconstruct the problem's objective function. $P^{Emax,*}_{g,v'}$, $F^{max,*}_{c,v'}$, and $P^{D}_{d,v'}{}^{max,*}$ are the subproblem's optimal solution, and their values can change after each iteration. As it can be seen in (6.40)-(6.48), the size of the master problem increases after each iteration.

### 6.6.2 Subproblem

The subproblem's objective function and constraints are the following:

$$\max_{\Delta^{SUB}} \quad \sigma \Bigg[ \sum_{g} C^{E}_{g} p^{E}_{g} + \sum_{d} C^{LS}_{d} p^{LS}_{d} \Bigg] \tag{6.49}$$

subject to

$$\sigma C^{E}_{g} - \lambda_{n(g)} + \phi^{E,max}_{g} - \phi^{E,min}_{g} = 0 \quad \forall g \tag{6.50}$$

$$\sigma C^{LS}_{d} - \lambda_{n(d)} + \phi^{D,max}_{d} - \phi^{D,min}_{d} = 0 \quad \forall d \tag{6.51}$$

$$\lambda_{s(c)} - \lambda_{r(c)} - \phi^{C}_{c} + \phi^{C,max}_{c} - \phi^{C,min}_{c} = 0 \quad \forall c \setminus c \in \Omega^{C+} \tag{6.52}$$

$$\lambda_{s(c)} - \lambda_{r(c)} - \phi^{C+}_{c} + \phi^{C,max}_{c} - \phi^{C,min}_{c} = 0 \quad \forall c \in \Omega^{C+} \tag{6.53}$$

$$\begin{aligned} &\sum_{c \setminus c \in \Omega^{C+} | s(c)=n} B_c \phi^{C}_{c} + \sum_{c \in \Omega^{C+} | s(c)=n} x^{C,*}_{c} B_c \phi^{C+}_{c} - \sum_{c \setminus c \in \Omega^{C+} | r(c)=n} B_c \phi^{C}_{c} \\ &- \sum_{c \in \Omega^{C+} | r(c)=n} x^{C,*}_{c} B_c \phi^{C+}_{c} + \phi^{N,max}_{n} - \phi^{N,min}_{n} = 0 \quad \forall n \setminus n : \text{ref.} \end{aligned} \tag{6.54}$$

$$\sum_{c\setminus c\in\Omega^{C+}|s(c)=n} B_c\phi_c^C + \sum_{c\in\Omega^{C+}|s(c)=n} x_c^{C,*}B_c\phi_c^{C+} - \sum_{c\setminus c\in\Omega^{C+}|r(c)=n} B_c\phi_c^C - \sum_{c\in\Omega^{C+}|r(c)=n} x_c^{C,*}B_c\phi_c^{C+} + \phi_n^{N,max} - \phi_n^{N,min} - \chi^{ref} = 0 \quad \forall n \setminus n : \text{ref.} \tag{6.55}$$

$$0 \leq \phi_c^{C,max} \perp F_c^{max} - p_c^C \geq 0 \quad \forall c \setminus c \in \Omega^{C+} \tag{6.56}$$

$$0 \leq \phi_c^{C,min} \perp p_c^C + F_c^{max} \geq 0 \quad \forall c \setminus c \in \Omega^{C+} \tag{6.57}$$

$$0 \leq \phi_c^{C,max} \perp F_c^{max} - p_c^C \geq 0 \quad \forall c \in \Omega^{C+} \tag{6.58}$$

$$0 \leq \phi_c^{C,min} \perp p_c^C + F_c^{max} \geq 0 \quad \forall c \in \Omega^{C+} \tag{6.59}$$

$$0 \leq \phi_g^{E,max} \perp P_g^{Emax} - p_g^E \geq 0 \quad \forall g \tag{6.60}$$

$$0 \leq \phi_g^{E,min} \perp p_g^E \geq 0 \quad \forall g \tag{6.61}$$

$$0 \leq \phi_d^{D,max} \perp P_d^{Dmax} - p_d^{LS} \geq 0 \quad \forall d \tag{6.62}$$

$$0 \leq \phi_d^{D,min} \perp p_d^{LS} \geq 0 \quad \forall d \tag{6.63}$$

$$0 \leq \phi_n^{N,max} \perp \pi - \theta_n \geq 0 \quad \forall n \tag{6.64}$$

$$0 \leq \phi_n^{N,min} \perp \theta_n + \pi \geq 0 \quad \forall n \tag{6.65}$$

where $\Delta^{SUB}$ contains the realisations of the uncertain parameters ($P_g^{Emax},\ F_c^{max},\ P_d^{Dmax}$), the system operation variables ($p_g^E,\ p_d^{LS},\ p_c^C,\ \theta_n,$), and the dual variables ($\lambda_n,\ \phi_g^{E,max},\ \phi_g^{E,min},\ \phi_d^{D,max},\ \phi_d^{D,min},\ \phi_c^C,\ \phi_c^{C+},\ \phi_c^{C,max},\ \phi_c^{C,min},\ \phi_n^{N,max},\ \phi_n^{N,min}, \chi^{ref}$). The subproblem constraints were obtained by applying the Karush–Kuhn–Tucker conditions, as explained in [66], [137]. Constraints (6.17)-(6.30) are also part of the subproblem.

## 6.7 Case Study

### 6.7.1 Test System

The 24-bus IEEE Reliability Test System (RTS) [16] was utilised to evaluate the performance of the two-stage adaptive robust TRP model. Several prospective transmission lines (l39-l43, l45, l47) and power transformers (t44, t46) were added in the test system, see Figure 6.2. The length of prospective lines varies between 15 and 30 miles. Cables l1 and l10 were replaced with overhead lines, and the power generation capacity increased from 3,405 to 3,895 MW. Furthermore, an annual load demand growth of 0.8% was considered. More information on the test system is given in the appendix, Section A.2.

The annualised investment cost of prospective component $c$, $I_c^C$, was calculated as follows [123]:

$$I_c^C = \text{NPV} \times \frac{r(1+r)^n}{(1+r)^n - 1} \tag{6.66}$$

where NPV is the net present value. $r$ is the interest rate, and $n$ is the lifetime of a prospective component. The costs of building single circuit overhead transmission lines were taken from [138], e.g., \$1.5M/mile for 138-kV lines, and \$1.7M/mile for 230-kV lines.

### 6.7.2 Aged Equipment and Test System's Capacity

Before solving the optimisation model, it is necessary to identify aged components and calculate their expected capacity over the planning period. The service age of the test system's components was randomly selected, as this information is not available in [16]. For example, generating unit g1, line l1, and transformer t7 have been in service for 23, 30, and 30 years, respectively. Furthermore, typical average lifetimes of generating units, lines, and transformers (taken from [15]) were used for their classification.

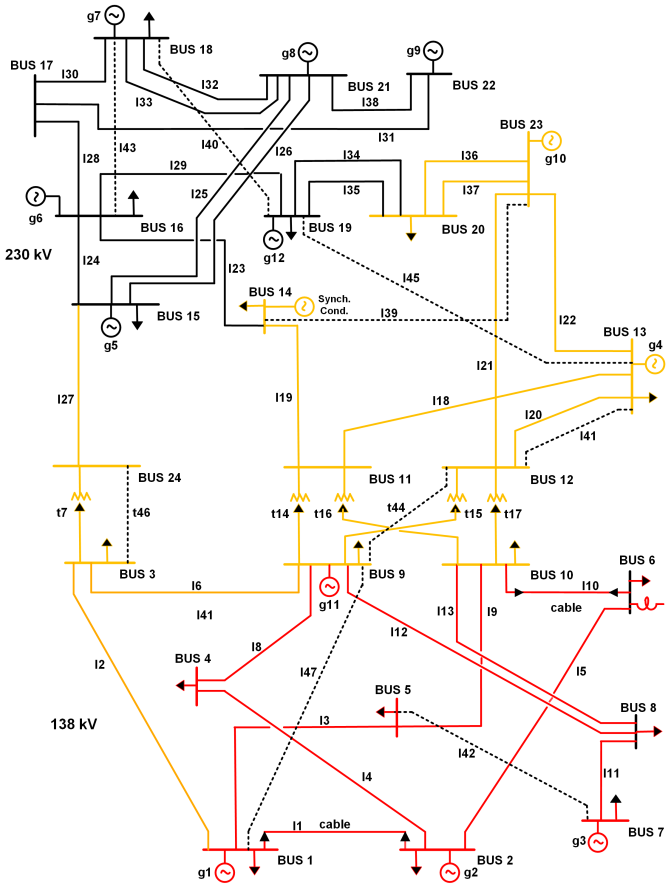


FIGURE 6.2: Modified version of the 24-bus IEEE Reliability Test System. Prospective lines (l39-l43, l45, l47) and transformers (t44, t46) were included in the original system. Its power generation capacity was also increased.

Figure 6.3 shows both the expected capacity and the nameplate capacity of generating unit g1, line l1, and transformer t7, from 2022 to 2041. It can be seen that the expected capacity of these components reduces as they get older. For example, in 2041, the capacity of g1, l1, and t7 would reduce by 53%, 19%, and 46%, respectively. These possible capacity reductions are significant, and should not be neglected by transmission systems planners. However, the method for calculating the expected capacity does not consider other factors that may influence its behaviour over the planning period, such as preventive maintenance, and loading and weather conditions. It is also important to mention that the availability of accurate equipment component failure data is essential for capturing and incorporating

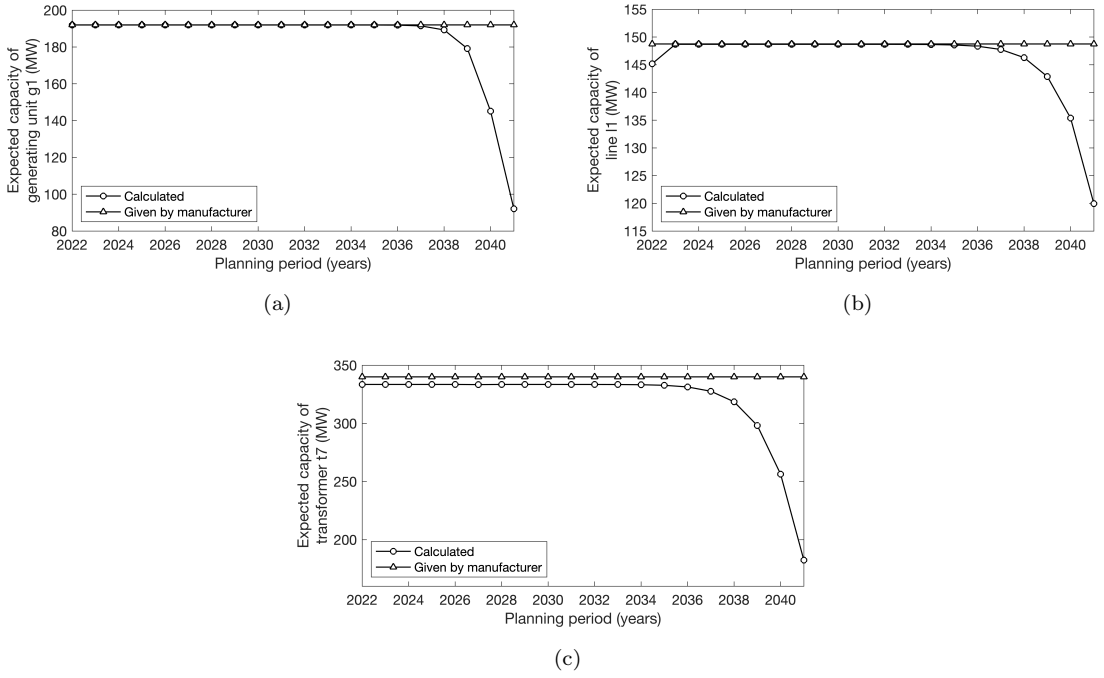


FIGURE 6.3: Expected and nameplate capacity of (a) generating unit g1, (b) transmission line l1, and (c) power transformer t7 over the planning period

the effects of equipment ageing into reinforcement decisions.

Figure 6.4 shows the total capacity (power generation and transfer capacity) of the test system for two cases: the first considers equipment ageing, whereas the second excludes equipment ageing. It can be seen that the capacity of the test system changes over the planning period (first case). An old power transformer is replaced by a new one in 2030, and this increases the total capacity. However, equipment ageing makes the total capacity reduce to 13.8 GW in 2041, which represents a 13% reduction.

2041 is the year in which the test system has its lowest capacity, so the expected capacity of aged components for this year is used in the polyhedral uncertainty sets.

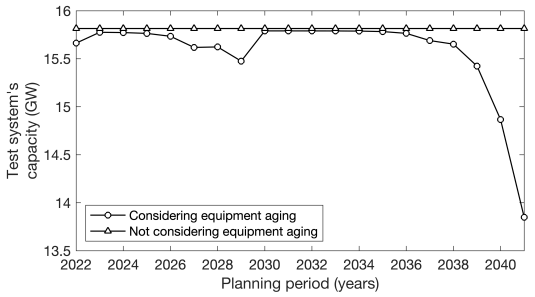


FIGURE 6.4: Comparison of test system's total capacity

### 6.7.3 Calculated Uncertainty Budget

Figure 6.5a shows the relationship between the uncertainty budget and the peak ground acceleration used to model the availability of generating units. The values of the uncertainty budget are higher for generating units that are exposed to both ground shaking and risk of being damaged by a tsunami. The uncertainty budget increases as the peak ground acceleration increases, and this indicates that higher peak ground accelerations would produce more damages to generating units. Figure 6.5b shows the relationship between the uncertainty budget and the peak ground acceleration used to model the availability of lines and transformers. The values of the uncertainty budget are higher for aged lines and transformers. That is, aged components would experience more damages than non-aged components for a given peak ground acceleration.

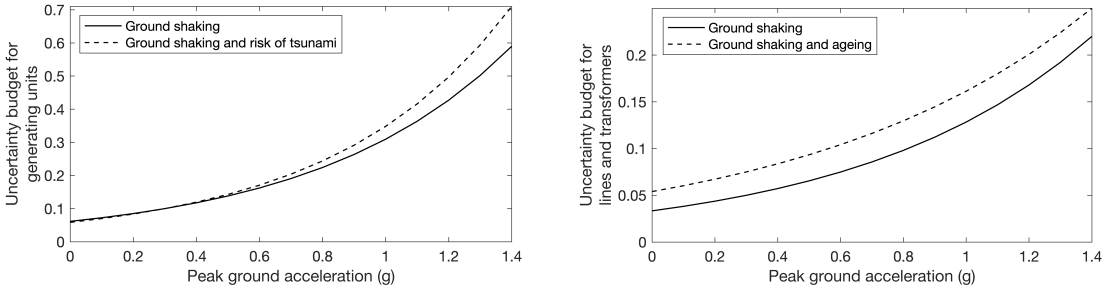


FIGURE 6.5: Uncertainty budgets for polyhedral uncertainty sets used to model (a) the availability of generating units and (b) the availability of lines and transformers

### 6.7.4 Test System Reinforcement Decisions

A program was created using the software GAMS to determine which lines or transformers should be built in the test system, considering two earthquake scenarios with epicentres located near buses 17 and 7. Figure 6.2 shows the test system for the second scenario; components in red, orange, and black colours are located in high, moderate, and low seismic hazard zones, respectively. (For the first scenario, the components in the seismic hazard zones are different). The peak ground acceleration of each component was not calculated, since information on the distance among components and soil conditions is not available for the IEEE RTS. So, the following peak ground accelerations for the high, moderate, and low seismic hazard zones were employed: 1.3, 0.8, and 0.3 (g) for the first scenario, and 1.2, 0.6, and 0.2 (g) for the second scenario. These values were chosen considering that a maximum peak ground acceleration of 1.407 (g) was registered during a 7.8 earthquake [139]. Then, the uncertainty budgets of each group of components were determined using the peak ground accelerations and the results shown in Figure 6.5.

The values of other parameters need to be determined before solving the optimisation problem. The uncertainty budgets for the maximum load demand are 0.20, 0.30, and 0.40 (higher values of $\Gamma^D$ indicate more uncertainty). The lower and upper limits of the maximum load demand ($\underline{P}_d^{Dmax}$, $\overline{P}_d^{Dmax}$) were calculated using the $\pm 10\%$ of the maximum load demand. Finally, an annualised investment budget of \$16,000,000 was utilised for both scenarios.

Table 6.1 shows the reinforcement decisions for Scenarios 1 and 2. The results indicate that as the uncertainty of the maximum load demand increases, more components should be built in the test system. When the uncertainty budget $\Gamma_d$ is 0.20, only line l39 should be built (Scenario 1), whereas when the uncertainty budget $\Gamma_d$ increases to 0.40, lines l39, l41, and l42 should be built.

TABLE 6.1: Lines and transformers that should be built in the test system

| $\Gamma_d$ | Scenario 1 | Scenario 2 |
|---|---|---|
| 0.20 | l39 | l43, l47 |
| 0.30 | l39 | l43, l47 |
| 0.40 | l39, l41, l42 | l40, t44, l47 |

The results of Table 6.1 also tell us that more components should be built when Scenario 2 is considered. This is an interesting result because the peak ground accelerations used in Scenario 2 (1.2, 0.6, and 0.2 (g)) are lower than the ones used in Scenario 1 (1.3, 0.8, and 0.3 (g)), that is, the test system's components are exposed to lower seismic motions in Scenario 2. However, more reinforcements are needed because the 138-kV network, located near the epicentre, has less power generation capacity. Most generating units are located in the 230-kV network, which is the part of the system that is less affected by the earthquake used in Scenario 2.

To investigate the influence of equipment ageing on reinforcement decisions, it was considered that more components in the test system exceed their average lifetime during the planning period. The results are depicted in Table 6.2. It can be seen that new components should be built: t44 and l47 in Scenario 1, and t46 and l39 in Scenario 2 (see Tables 6.1 and 6.2)

TABLE 6.2: Lines and transformers that should be built in the test system (considering more aged components).

| $\Gamma_d$ | Scenario 1 | Scenario 2 |
|---|---|---|
| 0.20 | l39, t44, l47 | l40, t46, l47 |
| 0.30 | l39, t44, l47 | l39, l40, l47 |
| 0.40 | l39, t44, l47 | l39, l40, l47 |

On the other hand, if equipment ageing is neglected (i.e., the nameplate capacity of generating units, lines, and transformers is utilised in the optimisation model, and

$\Omega_c$ has groups with only non-aged components), reinforcements are not required except for Scenario 2 and when the uncertainty budget $\Gamma_d$ is 0.40. Only in this case, line l47 should be built. Therefore, neglecting equipment ageing in the two-stage adaptive robust optimisation model yields completely different reinforcement plans.

The main benefit of using robust optimisation to solve the TRP problem is that component availability is modelled in a deterministic way, through polyhedral uncertainty sets (instead of fragility curves). This facilitates the modelling process that transmission system planners must do. However, the two-stage adaptive robust TRP problem does not include important factors such as the impact of distributed intermittent renewable power generation [140] and the load restoration process after an earthquake occurs, which can be influenced by the power stored in electric vehicles [141] or by the increased electric vehicle charging demand [142]. Incorporating these factors into the optimisation model would be the next research step.

### 6.7.5 Variation of Peak Ground Accelerations

The reinforcement decisions previously discussed consider three uncertain parameters ($P_g^{Emax}, F_c^{max}, P_d^{Dmax}$). However, other parameters, such as the peak ground acceleration ($PGA$, used in (6.33)), can also be a source of uncertainty. To analyse how variations of the peak ground acceleration may affect reinforcement plans, some of the peak ground accelerations used in Scenarios 1 and 2 were slightly increased.

Table 6.3 provides the new reinforcement decisions, which are compared with the results of Table 6.2. All components remain the same except for l41 in Scenario 1 and t44 and l45 in Scenario 2. These results tell us that small variations of the peak ground acceleration might affect the test system's reinforcement plans. Hence, the peak ground

acceleration of each component should be carefully calculated using appropriate attenuation models.

TABLE 6.3: Lines and transformers that should be built in the test system considering increments of peak ground accelerations

| $\Gamma_d$ | Scenario 1 | Scenario 2 |
|---|---|---|
| 0.20 | l39, l41, l47 | l40, t44, l47 |
| 0.30 | l39, l41, l47 | l39, l40, l45, l47 |
| 0.40 | l39, l41, l47 | l39, l40, l45, l47 |

As shown in Tables 6.1-6.3, reinforcement decisions vary for each earthquake scenario. A definitive reinforcement plan should be created, as this would benefit the use of the optimisation model. This topic will also be included in the final version of the work presented in this chapter.

## 6.8 Summary

This chapter presents a two-stage adaptive robust optimisation model to determine the best reinforcement decisions for power transmission systems that are subject to seismic events and have aged equipment. The model has three uncertain parameters (the availability of generating units, the availability of lines and transformers, and the future maximum load demand), which are modelled by using polyhedral uncertainty sets and by taking into account components' seismic hazard zones, ageing status, and risk of being damaged by a tsunami. An approach for calculating the expected capacity of aged components and incorporating it into the optimisation model is also developed.

The performance of the optimisation model was evaluated using a modified version of the 24-bus IEEE RTS; changes include two earthquake scenarios, aged equipment, load

demand growth, and prospective lines and transformers. The results indicate that the expected capacity of aged equipment (generating units, lines, and transformers) and the test system capacity tend to decrease, in a non-linear way, over the planning period. The results also show that the amount of aged equipment can influence the number of lines and transformers that should be built, and that neglecting equipment ageing may yield less accurate reinforcement plans.

Considering that fragility curves are not always reliable and that power systems in some parts of the world have a significant amount of aged equipment, the two-stage adaptive robust optimisation model can help transmission system planners incorporate hidden features into their expansion planning models. In that context, the proposed approach would make a solid foundation to fulfil critical planning objectives in a vulnerable power transmission system.

# Chapter 7

# Conclusions and Future Work

## 7.1 Conclusions

Power distribution systems, particularly those located in large cities, have a great number of medium voltage underground cables whose service age is close to or has exceeded their design lifetime. Ageing cables may fail more frequently, so asset managers must carefully plan their maintenance to maintain or improve the reliability of power distribution systems. Chapter 4 presented an approach to prioritise the maintenance of ageing cables.

The approach includes an age-related repairable failure model that considers the effects of cables' loading conditions. The approach also includes an index known as the maintenance potential index, which is used to create rankings of cables and thus to prioritise their maintenance. This index considers, for the first time, the impacts of random and age-related repairable failures as well as the effects of loading conditions. A radial distribution system with sixty four ageing cable sections was used to analyse the performance of the proposed approach. The results showed that the rankings of cable sections

significantly depend on their age-related repairable failures. For instance, age-related repairable failures contributed to the maintenance potential index of cable section 35 (the most important cable in the 33-kV network) by 63%, whereas random repairable failures contributed only by 37%. This result means that modelling age-related repairable failures of cables plays a critical role in the maintenance prioritisation process. Previous studies have not investigated the effects of cable ageing; they simply assume that cables have constant failure rates. However, in this study, failure rates increase as cables get older, and also vary depending on the loading level of each cable. Therefore, by incorporating the effects of ageing and loading conditions, the proposed approach can help asset managers significantly improve the maintenance prioritisation process of underground cables.

The second major finding was that if only random repairable failures are modelled (i.e., cable ageing is neglected in the test system), the rankings of cable sections may change in comparison to the case mentioned above (in which cable ageing is considered). This finding means that traditional approaches might target maintenance activities at the non-critical cable sections of a power distribution system. To avoid this problem, the proposed approach considers the influence of both random repairable failures and age-related repairable failures, identifying the most important cables and prioritising their maintenance in a more effective way.

Chapter 4 also presented a comprehensive comparison between the proposed age-related repairable failure model and the IEC-Arrhenius-Weibull model developed in [27]. Their modelling assumptions, methods for incorporating loading conditions, and parameter estimation approaches were compared and critically analysed. Furthermore, the test system with sixty four cable sections and computer simulations were employed to analyse the performance of both models. The simulation results indicated that using the Arrhenius relationship to incorporate the effects of loading conditions reduces the failure rate of

ageing cables and affects the rankings used to prioritise their maintenance. This finding means that the Arrhenius relationship might not be an appropriate method to develop age-related repairable failure models of cables, especially because it does not provide any information on the occurrence of repairable failures. The case study results also indicated that the failure rate function of the IEC-Arrhenius-Weibull model mainly depends on the shape parameter of the Weibull distribution. This dependence was not mentioned by the authors of the IEC-Arrhenius-Weibull model in [27], and could be considered as an important modelling drawback.

Modelling age-related repairable failures is a key aspect of maintenance planning, whereas modelling ageing (end-of-life) failures is a key aspect of retirement planning. Chapter 5 presented an approach for planning the retirement of power transformers. To improve the calculation of the unavailability due to ageing failure, the approach combines several methods to calculate the apparent age of power transformers and to incorporate their winding hottest-spot temperature. The proposed approach ranks the aged transformers of a power system using a modified version of the index known as credible improvement potential index, which considers the effects of capacity reduction—something that has not been previously done.

The retirement approach was carefully examined using a test system with single and parallel power transformers. Computer simulation results showed that the unavailability due to ageing failure calculated with the improved model increases faster than the one calculated with the conventional model (whose parameters were estimated using few transformer end-of-life failure data). This result indicates the potential benefits of incorporating the winding hottest-spot temperature. More accurate predictions of the unavailability due to ageing failure are important because they improve both the ranking of aged transformers and the calculation of their retirement year. Although the conventional

model was designed to predict the unavailability due to ageing failure using only end-of-life failure data, calculating the apparent age and incorporating the winding hottest-spot temperature can help to overcome the problem of limited transformer end-of-life failure data.

In the case study, the expected capacity of aged power transformers was calculated over a five-year period. For instance, the expected capacity of transformer S16-TR1 (whose maximum capacity is 33 MVA) is 29.480 MVA in 2021 and 29.963 MVA in 2025 (Case 4). These results indicate that the expected capacity of aged power transformers is lower than their maximum capacity. Traditional power system reliability assessment studies assume that the capacity of a power transformer is always equal to its maximum value, neglecting the ageing of its components. However, if the expected capacity is calculated and incorporated into the proposed approach, transformer retirement decisions can be further improved, as shown in the case study.

Chapter 6 presented a two-stage adaptive robust optimisation problem to determine reinforcement plans of power transmission systems that are subject to seismic events and have aged components. Robust optimisation was chosen because component availability modelling does not require probability distributions (i.e., fragility curves are not needed). To model the availability of generating units, lines, and transformers, the proposed approach creates several groups of components based on three factors—seismic hazard zone, ageing status, and risk of being damaged by a tsunami—, and then a polyhedral uncertainty set is used for each group. Furthermore, a procedure to incorporate the expected capacity of aged generating units, lines, and transformers into the optimisation problem was developed.

The performance of the optimisation problem was analysed through a case study, which used a modified version of the 24-bus IEEE RTS. The results suggested that if the

number of aged components (generating units, lines, and transformers) in the test system increases, more transmission lines and power transformers should be built. This result indicates that power systems with aged equipment might require more capital investment to mitigate the impacts of earthquakes. On the other hand, if equipment ageing is neglected in the test system, the results indicated that reinforcement plans could be completely different and could not improve the resilience of the transmission system. Although the availability of components significantly depends on the earthquake magnitude and their distance from the epicentre, incorporating other factors, such as ageing status and risk of being damage by a tsunami, can help system planners determine more realistic reinforcement decisions. These factors have not been considered by previous approaches for transmission system reinforcement planning, which rely on fragility curves to model the availability of components. Considering that some system planners may not have access to reliable fragility curves, the two-stage adaptive robust optimisation model presented in Chapter 6 is a better alternative that also incorporates the effects of equipment ageing.

## 7.2 Future Work

The following research topics are suggested based on the work presented in this thesis, and they are described with the aim of keeping developing the areas of power system asset management and expansion planning.

- *Impact of distributed power generation and transportation electrification on cable maintenance prioritisation and power transformer retirement.* The loading level of underground cables and power transformers can change considerably due to the incorporation of electric vehicles and distributed generation, and this might affect the occurrence of age-related repairable and non-repairable failures. Future research

studies could investigate how the maintenance prioritisation of ageing cables and the retirement of aged power transformers are affected by changes in loading conditions. This would require using long-term power generation and load forecasting methods, taking into account electric vehicle charging patterns, public electric vehicle charging stations, prosumers, etc.

- *Limiting the loading of aged power transformers for retirement planning studies.* If a substation has aged power transformers connected in parallel and sharing the total load demand, it may be difficult to determine the economic losses caused by ageing failures for retirement planning studies. Future research works could investigate the possibility of limiting the amount of load that an aged transformer can supply. For instance, if a substation has two aged transformers and one of them undergoes an ageing (non-repairable) failure, it could be assumed that the remaining transformer can use only 50% of its expected capacity to supply the load demand. This assumption would allow asset managers to extend the lifetime of the second transformer, by reducing its thermal stress, and to capture the impacts of the first transformer's ageing failure.

- *Retirement planning of underground power distribution system cables.* The approach for planning the retirement of aged power transformers (presented in Chapter 5) could also be applied to underground cables. A new method to calculate the apparent age of cables should be developed, as their service age might not give an indication of their actual condition. The method should use relevant cable condition monitoring data, e.g., partial discharge measurements. Moreover, a new method to calculate the EENS caused by cable ageing failures should be proposed. Unlike composite (generation and transmission) systems, distribution systems have switching devices that restore the power supply when components fail, and this should be considered in the EENS calculation.

- *System operation costs after a seismic event.* In the two-stage adaptive robust optimisation problem described in Chapter 6, system operation costs (i.e., power generation and load-shedding costs) are calculated considering a one-year period. The load restoration process, performed after a seismic event occurs, should be modelled and included in the optimisation problem to enhance the calculation of system operation costs. The modelling approach should consider that some components experience repairable failures, and others experience non-repairable failures, and that repair and replacement times may vary during earthquakes. Another interesting aspect that could be included in the load restoration process is the modelling of electric vehicle charging demand and intermittent renewable power generation. If an earthquake causes severe damages to buildings, hospitals, houses, etc., a great amount of people would attempt to travel to the affected areas to provide help, and this might increase the load demand of electric vehicles at different points of a transmission system. A possible solution to include the load restoration process would be to combine robust optimisation with optimisation via simulation. This would allow system planners to simulate component failures, repairs, and replacements, as well as load demand change and intermittent power generation.

# Appendix A

# Test Systems

## A.1 Radial Test System

The test system shown in Figure A.1 is used in Chapter 4 for analysing cable maintenance prioritisation. The test system's configuration, voltage levels, and location of components and load points were taken from [19]. The test system's load data (in MW) and the number of customers are given in Tables A.1 and A.2, respectively. Moreover, as mentioned in Subsection 4.5.1, the 24-bus IEEE Reliability Test System's hourly load profile (in p.u.) is used for the case study in Chapter 4. This information will be given in Section A.2.

## A.2 24-Bus IEEE Reliability Test System

Figure A.2 shows the 24-bus IEEE Reliability Test System and the changes made to it to analyse transmission system reinforcement in Chapter 6. Table A.3 shows the load data (in MW) of all load buses, and Tables A.4, A.5, and A.6 contain all the information to create

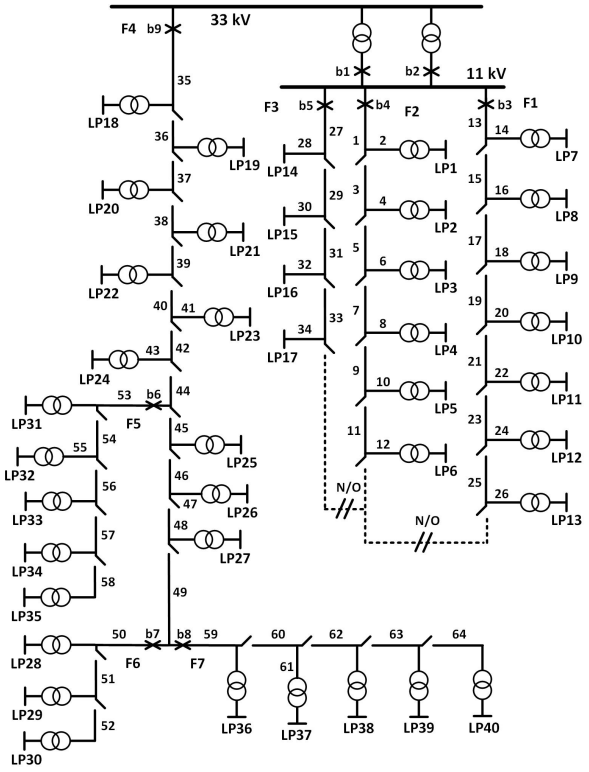


FIGURE A.1: Test system used in Chapter 4

TABLE A.1: Load data of the test system shown in Figure A.1

| Load point | Load, MW | Load point | Load, MW | Load point | Load, MW |
|---|---|---|---|---|---|
| 1 | 0.8869 | 16 | 0.8137 | 31 | 0.8869 |
| 2 | 0.8869 | 17 | 1.6300 | 32 | 0.8869 |
| 3 | 0.8869 | 18 | 0.8869 | 33 | 0.8869 |
| 4 | 0.8137 | 19 | 0.8869 | 34 | 0.8869 |
| 5 | 0.8137 | 20 | 0.8869 | 35 | 0.8137 |
| 6 | 0.6714 | 21 | 0.8869 | 36 | 0.8137 |
| 7 | 0.8869 | 22 | 0.8137 | 37 | 0.6714 |
| 8 | 0.8869 | 23 | 0.8137 | 38 | 0.6714 |
| 9 | 0.8869 | 24 | 0.6714 | 39 | 0.8869 |
| 10 | 0.8869 | 25 | 0.6714 | 40 | 0.8869 |
| 11 | 0.8137 | 26 | 0.8137 | | |
| 12 | 0.6714 | 27 | 0.8137 | | |
| 13 | 0.6714 | 28 | 0.8869 | | |
| 14 | 1.6300 | 29 | 0.8869 | | |
| 15 | 2.4450 | 30 | 0.8869 | | |

the hourly load profile of the 24-bus IEEE Reliability Test System. Furthermore, Table A.7 shows the impedance and ratings of existing and prospective lines and transformers.

TABLE A.2: Number of customers at load points

| Load point | No. of customers | Load point | No. of customers | Load point | No. of customers |
|---|---|---|---|---|---|
| 1 | 220 | 16 | 200 | 31 | 220 |
| 2 | 220 | 17 | 1 | 32 | 220 |
| 3 | 220 | 18 | 220 | 33 | 220 |
| 4 | 200 | 19 | 220 | 34 | 220 |
| 5 | 200 | 20 | 220 | 35 | 200 |
| 6 | 10 | 21 | 220 | 36 | 200 |
| 7 | 220 | 22 | 200 | 37 | 10 |
| 8 | 220 | 23 | 200 | 38 | 10 |
| 9 | 220 | 24 | 10 | 39 | 220 |
| 10 | 220 | 25 | 10 | 40 | 220 |
| 11 | 200 | 26 | 200 | | |
| 12 | 10 | 27 | 200 | | |
| 13 | 10 | 28 | 220 | | |
| 14 | 1 | 29 | 220 | | |
| 15 | 1 | 30 | 220 | | |

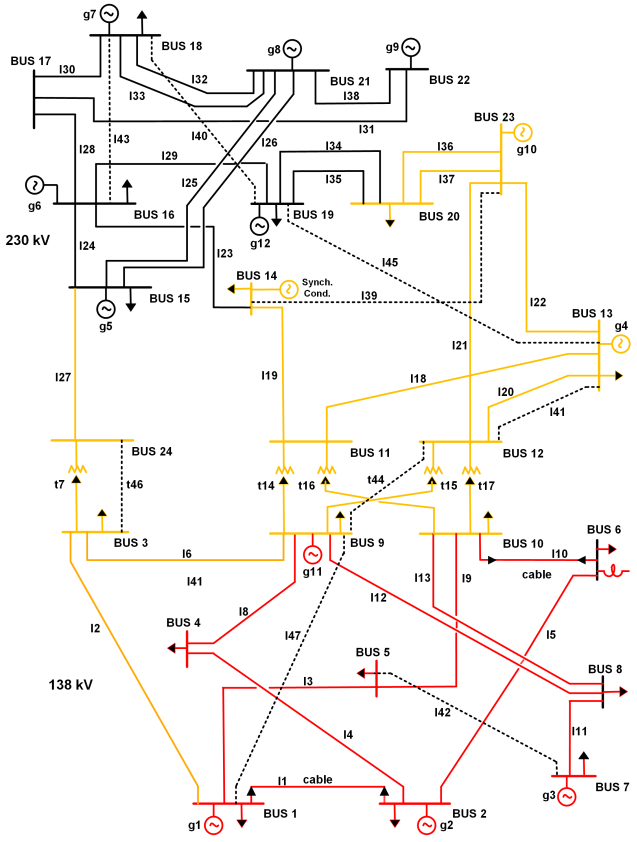


FIGURE A.2: Test system used in Chapter 6

TABLE A.3: Load data of test system shown in Figure A.2

| Bus | Load, MW | Bus | Load, MW |
|---|---|---|---|
| 1 | 126 | 10 | 228 |
| 2 | 113 | 13 | 310 |
| 3 | 211 | 14 | 227 |
| 4 | 86 | 15 | 371 |
| 5 | 83 | 16 | 117 |
| 6 | 159 | 18 | 390 |
| 7 | 146 | 19 | 212 |
| 8 | 200 | 20 | 150 |
| 9 | 205 | | |

TABLE A.4: Weekly peak load in percent of annual peak [16]

| Week | Peak load | Week | Peak load |
|---|---|---|---|
| 1 | 86.2 | 27 | 75.5 |
| 2 | 90.0 | 28 | 81.6 |
| 3 | 87.8 | 29 | 80.1 |
| 4 | 83.4 | 30 | 88.0 |
| 5 | 88.0 | 31 | 72.2 |
| 6 | 84.1 | 32 | 77.6 |
| 7 | 83.2 | 33 | 80.0 |
| 8 | 80.6 | 34 | 72.9 |
| 9 | 74.0 | 35 | 72.6 |
| 10 | 73.7 | 36 | 70.5 |
| 11 | 71.5 | 37 | 78.0 |
| 12 | 72.7 | 38 | 69.5 |
| 13 | 70.4 | 39 | 72.4 |
| 14 | 75.0 | 40 | 72.4 |
| 15 | 72.1 | 41 | 74.3 |
| 16 | 80.0 | 42 | 74.4 |
| 17 | 75.4 | 43 | 80.0 |
| 18 | 83.7 | 44 | 88.1 |
| 19 | 87.0 | 45 | 88.5 |
| 20 | 88.0 | 46 | 90.9 |
| 21 | 85.6 | 47 | 94.0 |
| 22 | 81.1 | 48 | 89.0 |
| 23 | 90.0 | 49 | 94.2 |
| 24 | 88.7 | 50 | 97.0 |
| 25 | 89.6 | 51 | 100.0 |
| 26 | 86.1 | 52 | 95.2 |

TABLE A.5: Daily peak load in percent of weekly peak [16]

| Day | Peak load |
|---|---|
| Monday | 93 |
| Tuesday | 100 |
| Wednesday | 98 |
| Thursday | 96 |
| Friday | 94 |
| Saturday | 77 |
| Sunday | 75 |

TABLE A.6: Hourly peak load in percent of daily peak [16]

| | Winter weeks 1-8 & 44-52 | | Summer weeks 18-30 | | Spring/fall weeks 9-17 & 31-43 | |
|---|---|---|---|---|---|---|
| Hour | Wkdy | Wknd | Wkdy | Wknd | Wkdy | Wknd |
| 12-1am | 67 | 78 | 64 | 73 | 63 | 75 |
| 1-2 | 63 | 72 | 60 | 70 | 62 | 73 |
| 2-3 | 60 | 68 | 58 | 66 | 60 | 69 |
| 3-4 | 59 | 66 | 56 | 65 | 58 | 66 |
| 4-5 | 59 | 64 | 56 | 64 | 59 | 65 |
| 5-6 | 60 | 65 | 58 | 62 | 65 | 65 |
| 6-7 | 74 | 66 | 64 | 62 | 72 | 68 |
| 7-8 | 86 | 70 | 76 | 66 | 85 | 74 |
| 8-9 | 95 | 80 | 87 | 81 | 95 | 83 |
| 9-10 | 96 | 88 | 95 | 86 | 99 | 89 |
| 10-11 | 96 | 90 | 99 | 91 | 100 | 92 |
| 11-Noon | 95 | 91 | 100 | 93 | 99 | 94 |
| Noon-1pm | 95 | 90 | 99 | 93 | 93 | 91 |
| 1-2 | 95 | 88 | 100 | 92 | 92 | 90 |
| 2-3 | 93 | 87 | 100 | 91 | 90 | 90 |
| 3-4 | 94 | 87 | 97 | 91 | 88 | 86 |
| 4-5 | 99 | 91 | 96 | 92 | 90 | 85 |
| 5-6 | 100 | 100 | 96 | 94 | 92 | 88 |
| 6-7 | 100 | 99 | 93 | 95 | 96 | 92 |
| 7-8 | 96 | 97 | 92 | 95 | 98 | 100 |
| 8-9 | 91 | 94 | 92 | 100 | 96 | 97 |
| 9-10 | 83 | 92 | 93 | 93 | 90 | 95 |
| 10-11 | 73 | 87 | 87 | 88 | 80 | 90 |
| 11-12 | 63 | 81 | 72 | 80 | 70 | 85 |

TABLE A.7: Impedance, ratings, and voltage levels of transmission lines and power transformers (most of the data was taken from [16])

| From bus | To bus | X, p.u. | Rating, MVA, | Voltage level, kV |
|---|---|---|---|---|
| 1 | 2 | .0139 | 175 | 138 |
| 1 | 3 | .2112 | 175 | 138 |
| 1 | 5 | .0845 | 175 | 138 |
| 2 | 4 | .1267 | 175 | 138 |
| 2 | 6 | .1920 | 175 | 138 |
| 3 | 9 | .1190 | 175 | 138 |
| 3 | 24 | .0839 | 400 | Transformer |
| 4 | 9 | .1037 | 175 | 138 |
| 5 | 10 | .0883 | 175 | 138 |
| 6 | 10 | .0605 | 175 | 138 |
| 7 | 8 | .0614 | 175 | 138 |
| 8 | 9 | .1651 | 175 | 138 |
| 8 | 10 | .1651 | 175 | 138 |
| 9 | 11 | .0839 | 400 | Transformer |
| 9 | 12 | .0839 | 400 | Transformer |
| 10 | 11 | .0839 | 400 | Transformer |
| 10 | 12 | .0839 | 400 | Transformer |
| 11 | 13 | .0476 | 500 | 230 |
| 11 | 14 | .0418 | 500 | 230 |
| 12 | 13 | .0476 | 500 | 230 |
| 12 | 23 | .0966 | 500 | 230 |
| 13 | 23 | .0865 | 500 | 230 |
| 14 | 16 | .0389 | 500 | 230 |
| 15 | 16 | .0173 | 500 | 230 |
| 15 | 21 | .0490 | 500 | 230 |
| 15 | 21 | .0490 | 500 | 230 |
| 15 | 24 | .0519 | 500 | 230 |
| 16 | 17 | .0259 | 500 | 230 |
| 16 | 19 | .0231 | 500 | 230 |
| 17 | 18 | .0144 | 500 | 230 |
| 17 | 22 | .1053 | 500 | 230 |
| 18 | 21 | .0259 | 500 | 230 |
| 18 | 21 | .0259 | 500 | 230 |
| 19 | 20 | .0396 | 500 | 230 |
| 19 | 20 | .0396 | 500 | 230 |
| 20 | 23 | .0216 | 500 | 230 |
| 20 | 23 | .0216 | 500 | 230 |
| 21 | 22 | .0678 | 500 | 230 |
| 14 | 23 | .0490 | 500 | 230 |
| 18 | 19 | .0259 | 500 | 230 |
| 12 | 13 | .0519 | 500 | 230 |
| 5 | 7 | .1037 | 175 | 138 |
| 16 | 18 | .0490 | 500 | 230 |
| 9 | 12 | .0678 | 400 | Transformer |
| 13 | 19 | .0519 | 500 | 230 |
| 3 | 24 | .0678 | 400 | Transformer |
| 1 | 9 | .1037 | 175 | 138 |

# Bibliography


[1] A. J. Wood, B. F. Wollenberg, and G. B. Sheblé, *Power Generation, Operation, and Control*. John Wiley & Sons, 2013.

[2] S. R. Khuntia, J. L. Rueda, S. Bouwman *et al.*, "A literature survey on asset management in electrical power [transmission and distribution] system," *International Transactions on Electrical Energy Systems*, vol. 26, no. 10, pp. 2123–2133, 2016.

[3] L. Bertling, *Infrastructure Asset Management with Power System Applications*. CRC Press, 2018.

[4] W. Li, J. Zhou, J. Lu, and W. Yan, "A probabilistic analysis approach to making decision on retirement of aged equipment in transmission systems," *IEEE Transactions on Power Delivery*, vol. 22, no. 3, pp. 1891–1896, 2007.

[5] P. Hilber and L. Bertling, "Component reliability importance indices for electrical networks," in *International Power Engineering Conference*. IEEE, 2007, pp. 257–263.

[6] P. Jarman, R. Hooton, L. Walker *et al.*, "Transformer life prediction using data from units removed from service and thermal modelling," in *Proc. CIGRE Session (A2 212)*, 2010.

[7] U.S. Department of Energy, "Quadrennial technology review 2015 (Chapter 3)," Tech. Rep., 2015.

[8] Department of Energy and Climate Change, "Delivering UK energy investment: Networks," Tech. Rep., 2015.

[9] A. Stephen, "Asset stewardship report," Tech. Rep., 2014.

[10] L. Aniti. Major utilities continue to increase spending on U.S. electric distribution systems. [Online]. Available: https://www.eia.gov/todayinenergy/detail.php?id=36675

[11] M. Wang, A. Vandermaar, and K. Srivastava, "Review of condition assessment of power transformers in service," *IEEE Electrical Insulation Magazine*, vol. 18, no. 6, pp. 12–25, 2002.

[12] CIGRE WG A2.49, "Condition assessment of power transformers," Tech. Rep., 2019.

[13] A. Mate, T. Hagan, E. Cotilla-Sanchez *et al.*, "Impacts of earthquakes on electrical grid resilience," in *IEEE/IAS 57th Industrial and Commercial Power Systems Technical Conference*. IEEE, 2021, pp. 1–5.

[14] M. Toyoma, "Power system damage, recovery and challenges from Great East Japan Earthquake," Tech. Rep., 2013.

[15] IEC, "Strategic asset management of power networks," Tech. Rep., 2015.

[16] Reliability Test System Task Force, "IEEE reliability test system," *IEEE Transactions on Power Apparatus and Systems*, vol. PAS-98, no. 6, pp. 2047–2054, 1979.

[17] W. Li, *Risk Assessment of Power Systems*. John Wiley, 2014.

[18] R. Billinton and R. Allan, *Reliability Evaluation of Engineering Systems*. Springer, 1994.

[19] R. Billinton and P. Wang, "Teaching distribution system reliability evaluation using monte carlo simulation," *IEEE Transactions on Power Systems*, vol. 14, no. 2, pp. 397–403, 1999.

[20] S. K. Awadalla, J. V. Milanovic, Z. Wang *et al.*, "Overview of power system reliability assessment considering age related failure of equipment," in *IEEE Power & Energy Society General Meeting*, 2015, pp. 1–6.

[21] H. L. Willis and R. R. Schrieber, *Aging Power Delivery Infrastructures*. CRC Press, 2017.

[22] K. Kapur and M. Pecht, *Reliability Engineering*. John Wiley & Sons, 2014.

[23] L. H. Crow, "Reliability analysis for complex, repairable systems," AMSAA, Tech. Rep., 1975.

[24] H. Kim and C. Singh, "Reliability modeling and simulation in power systems with aging characteristics," *IEEE Transactions on Power Systems*, vol. 25, no. 1, pp. 21–28, 2009.

[25] H. Rinne, *The Weibull Distribution: A Handbook*. CRC press, 2008.

[26] S. Sachan, C. Zhou, G. Bevan *et al.*, "Failure prediction of power cables using failure history and operational conditions," in *11th International Conference on the Properties and Applications of Dielectric Materials (ICPADM)*. IEEE, 2015, pp. 380–383.

[27] M. Buhari, V. Levi, and S. K. Awadallah, "Modelling of ageing distribution cable for replacement planning," *IEEE Transactions on Power Systems*, vol. 31, no. 5, pp. 3996–4004, 2015.

[28] K. Kopsidas and S. Liu, "Power network reliability framework for integrating cable design and ageing," *IEEE Transactions on Power Systems*, vol. 33, no. 2, pp. 1521–1532, 2017.

[29] C. Zhou, X. Jing, Z. Tang *et al.*, "Statistical approaches for analysis of failure data in power cables." CIGRE, 2012, pp. 1–9.

[30] J. F. Lawless, "Regression methods for poisson process data," *Journal of the American Statistical Association*, vol. 82, no. 399, pp. 808–815, 1987.

[31] W. Li, "Incorporating aging failures in power system reliability evaluation," *IEEE Transactions on Power Systems*, vol. 17, no. 3, pp. 918–923, 2002.

[32] K. Xie and W. Li, "Analytical model for unavailability due to aging failures in power systems," *International Journal of Electrical Power & Energy Systems*, vol. 31, no. 7-8, pp. 345–350, 2009.

[33] Working Group A2.37, "Transformer reliability survey," CIGRE, Tech. Rep., 2015.

[34] D. Martin, J. Marks, T. K. Saha *et al.*, "Investigation into modeling Australian power transformer failure and retirement statistics," *IEEE Transactions on Power Delivery*, vol. 33, no. 4, pp. 2011–2019, 2018.

[35] W. Li, "Evaluating mean life of power system equipment with limited end-of-life failure data," *IEEE Transactions on Power Systems*, vol. 19, no. 1, pp. 236–242, 2004.

[36] D. Zhou, Z. Wang, and C. Li, "Data requisites for transformer statistical lifetime modelling—Part I: Aging-related failures," *IEEE Transactions on Power Delivery*, vol. 28, no. 3, pp. 1750–1757, 2013.

[37] D. Zhou, Z. Wang, P. Jarman, and C. Li, "Data requisites for transformer statistical lifetime modelling—Part II: Combination of random and aging-related failures," *IEEE Transactions on Power Delivery*, vol. 29, no. 1, pp. 154–160, 2013.

[38] S. K. Awadallah, J. V. Milanović, and P. N. Jarman, "Quantification of uncertainty in end-of-life failure models of power transformers for transmission systems reliability studies," *IEEE Transactions on Power Systems*, vol. 31, no. 5, pp. 4047–4056, 2015.

[39] J. Teh, "Uncertainty analysis of transmission line end-of-life failure model for bulk electric system reliability studies," *IEEE Transactions on Reliability*, vol. 67, no. 3, pp. 1261–1268, 2018.

[40] W. Li, P. Choudhury, D. Gillespie, and J. Jue, "A risk evaluation based approach to replacement strategy of aged HVDC components and its application at BCTC," *IEEE Transactions on Power Delivery*, vol. 22, no. 3, pp. 1834–1840, 2007.

[41] S. K. Awadallah, J. V. Milanović, and P. N. Jarman, "Reliability based framework for cost-effective replacement of power transmission equipment," *IEEE Transactions on Power Systems*, vol. 29, no. 5, pp. 2549–2557, 2014.

[42] L. Cheim, "Machine learning tools in support of transformer diagnostics," in *CIGRE conference*, 2018, pp. 1–10.

[43] P. Lorin, L. Cheim, L. Pettersson *et al.*, "Transformer health index and probability of failure based on failure mode effects analysis (FMEA) of a reliability centered maintenance (RCM) program," in *CIGRE conference*, 2016, pp. 1–8.

[44] S. K. Awadallah, J. V. Milanović, and P. N. Jarman, "The influence of modeling transformer age related failures on system reliability," *IEEE Transactions on Power Systems*, vol. 30, no. 2, pp. 970–979, 2014.

[45] S. Awadallah, "Probabilistic methodology for prioritising replacement of ageing power transformers based on reliability assessment of transmission system," Ph.D. dissertation, The University of Manchester, 2014.

[46] D. Zhang, W. Li, and X. Xiong, "Replacement strategy for aged transformers based on condition monitoring and system risk," *Automation of Electric Power Systems*, vol. 37, no. 17, pp. 64–71, 2013.

[47] T. K. Saha and P. Purkait, *Transformer Ageing*. Wiley, 2017.

[48] J. Zhong, W. Li, R. Billinton, and J. Yu, "Incorporating a condition monitoring based aging failure model of a circuit breaker in substation reliability assessment," *IEEE Transactions on Power Systems*, vol. 30, no. 6, pp. 3407–3415, 2015.

[49] M. Buhari, V. Levi, and A. Kapetanaki, "Cable replacement considering optimal wind integration and network reconfiguration," *IEEE Transactions on Smart Grid*, vol. 9, no. 6, pp. 5752–5763, 2017.

[50] W. A. Vasquez and D. Jayaweera, "Methodology for overhead conductor replacement considering operational stress and aging characteristics," in *IEEE Power & Energy Society General Meeting*, 2018, pp. 1–5.

[51] M. Rausand and A. Høyland, *System Reliability Theory: Models, statistical methods, and applications*. John Wiley & Sons, 2004.

[52] J. Setréus, P. Hilber, S. Arnborg, and N. Taylor, "Identifying critical components for transmission system reliability," *IEEE Transactions on Power Systems*, vol. 27, no. 4, pp. 2106–2115, 2012.

[53] G. Hamoud, "Assessment of transmission system component criticality in the deregulated electricity market," in *International Conference on Probablistic Methods Applied to Power Systems*. IEEE, 2008, pp. 1–8.

[54] B. Lami and K. Bhattacharya, "Identification of critical components of composite power systems using minimal cut sets," in *Innovative Smart Grid Technologies Conference*. IEEE, 2015, pp. 1–5.

[55] P. Hilber and L. Bertling, "Monetary importance of component reliability in electrical networks for maintenance optimization," in *Conference on Probabilistic Methods Applied to Power Systems*. IEEE, 2004, pp. 150–155.

[56] G. Latorre, R. D. Cruz, J. M. Areiza, and A. Villegas, "Classification of publications and models on transmission expansion planning," *IEEE Transactions on Power Systems*, vol. 18, no. 2, pp. 938–946, 2003.

[57] R. Sioshansi and A. J. Conejo, *Optimization in Engineering*. Springer, 2017.

[58] L. L. Garver, "Transmission network estimation using linear programming," *IEEE Transactions on Power Apparatus and Systems*, no. 7, pp. 1688–1697, 1970.

[59] R. Villasana, L. Garver, and S. Salon, "Transmission network planning using linear programming," *IEEE Transactions on Power Apparatus and Systems*, vol. PAS-104, no. 2, pp. 349–356, 1985.

[60] H. Youssef and R. Hackam, "New transmission planning model," *IEEE Transactions on Power Systems*, vol. 4, no. 1, pp. 9–18, 1989.

[61] Y. Dusonchet and A. El-Abiad, "Transmission planning using discrete dynamic optimizing," *IEEE Transactions on Power Apparatus and Systems*, vol. PAS-92, no. 4, pp. 1358–1371, 1973.

[62] N. Alguacil, A. L. Motto, and A. J. Conejo, "Transmission expansion planning: A mixed-integer lp approach," *IEEE Transactions on Power Systems*, vol. 18, no. 3, pp. 1070–1077, 2003.

[63] S. De La Torre, A. J. Conejo, and J. Contreras, "Transmission expansion planning in electricity markets," *IEEE Transactions on Power Systems*, vol. 23, no. 1, pp. 238–248, 2008.

[64] L. Baringo and A. Baringo, "A stochastic adaptive robust optimization approach for the generation and transmission expansion planning," *IEEE Transactions on Power Systems*, vol. 33, no. 1, pp. 792–802, 2017.

[65] A. Bagheri, J. Wang, and C. Zhao, "Data-driven stochastic transmission expansion planning," *IEEE Transactions on Power Systems*, vol. 32, no. 5, pp. 3461–3470, 2016.

[66] A. J. Conejo, L. Baringo, S. J. Kazempour, and A. S. Siddiqui, "Investment in electricity generation and transmission," *Cham Zug, Switzerland: Springer International Publishing*, vol. 106, 2016.

[67] N. R. Romero, L. K. Nozick, I. D. Dobson *et al.*, "Transmission and generation expansion to mitigate seismic risk," *IEEE Transactions on Power Systems*, vol. 28, no. 4, pp. 3692–3701, 2013.

[68] T. Lagos, R. Moreno, A. N. Espinosa *et al.*, "Identifying optimal portfolios of resilient network investments against natural hazards, with applications to earthquakes," *IEEE Transactions on Power Systems*, vol. 35, no. 2, pp. 1411–1421, 2019.

[69] E. Nery *et al.*, *Resiliência de Sistemas Eletroenergéticos.* Interciencia, 2019.

[70] Y. Shumuta, "Practical seismic upgrade strategy for substation equipment based on performance indices," *Earthquake Engineering & Structural Dynamics*, vol. 36, no. 2, pp. 209–226, 2007.

[71] Department of Homeland Security, "Multi-hazard loss estimation methodology: Earthquake model," Tech. Rep., 2003.

[72] J.-R. Huo and H. H. Hwang, "Seismic fragility analysis of equipment and structures in a Memphis electric substation," Tech. Rep., 1995.

[73] D. Ostrom, "Database of seismic parameters of equipment in substations," Pacific Earthquake Engineering Research Center, Tech. Rep., 2004.

[74] M. Panteli, C. Pickering, S. Wilkinson *et al.*, "Power system resilience to extreme weather: fragility modeling, probabilistic impact assessment, and adaptation measures," *IEEE Transactions on Power Systems*, vol. 32, no. 5, pp. 3747–3757, 2016.

[75] S. Dunn, S. Wilkinson, D. Alderson *et al.*, "Fragility curves for assessing the resilience of electricity networks constructed from an extensive fault database," *Natural Hazards Review*, vol. 19, no. 1, p. 04017019, 2018.

[76] M. Farhoumandi, F. Aminifar, and M. Shahidehpour, "Generation expansion planning considering the rehabilitation of aging generating units," *IEEE Transactions on Smart Grid*, vol. 11, no. 4, pp. 3384–3393, 2020.

[77] CIGRE, "Transmission asset risk management," 2010.

[78] R. Billinton and W. Li, *Reliability Assessment of Electric Power Systems Using Monte Carlo Methods*. Springer Science & Business Media, 1994.

[79] M. T. Schilling, J. Praca, J. De Queiroz *et al.*, "Detection of ageing in the reliability analysis of thermal generators," *IEEE Transactions on Power Systems*, vol. 3, no. 2, pp. 490–499, 1988.

[80] W. A. Vasquez and D. Jayaweera, "Prioritization of aging underground power distribution cables for maintenance activities," in *International Conference on Probabilistic Methods Applied to Power Systems (PMAPS)*. IEEE, 2020, pp. 1–6.

[81] W. A. Vasquez and D. Jayaweera, "A study of repairable failure models of aging underground power distribution cables," in *IEEE PES Innovative Smart Grid Technologies Conference (Europe)*. IEEE, 2021, pp. 1–5.

[82] W. Li, E. Vaahedi, and P. Choudhury, "Power system equipment aging," *IEEE Power and Energy Magazine*, vol. 4, no. 3, pp. 52–58, 2006.

[83] "IEEE guide for loading mineral-oil-immersed transformers," *IEEE Std C57.91*, vol. 57, pp. 1–112, 1995.

[84] C. Zhou, M. Michel, D. M. Hepburn, and X. Song, "On-line partial discharge monitoring in medium voltage underground cables," *IET Science, Measurement & Technology*, vol. 3, no. 5, pp. 354–363, 2009.

[85] J. Z. Hansen, "Results from Danish failure statistics for medium voltage XLPE cables," in *22nd International Conference and Exhibition on Electricity Distribution (CIRED)*. IET, 2013, pp. 1–4.

[86] A. Avramidis, "Math3013: Simulation and queues." School of Mathematics, University of Southampton, 2012.

[87] W. R. Gilks, S. Richardson, and D. Spiegelhalter, *Markov Chain Monte Carlo in Practice*. Chapman and Hall/CRC, 1995.

[88] Z. W. Birnbaum, "On the importance of different components in a multicomponent system," University of Washington, Tech. Rep., 1968.

[89] R. N. Allan, R. Billinton, I. Sjarief *et al.*, "A reliability test system for educational purposes-basic distribution system data and results," *IEEE Transactions on Power systems*, vol. 6, no. 2, pp. 813–820, 1991.

[90] R. Zimmerman, C. Murillo, and R. Thomas, "MATPOWER: Steady-state operations, planning, and analysis tools for power systems research and education," *Transactions on Power Systems*, vol. 26, pp. 12–19, 2010.

[91] P. Denholm, M. O'Connell, G. Brinkman, and J. Jorgenson, "Overgeneration from solar energy in California," National Renewable Energy Lab. (NREL), Tech. Rep., 2015.

[92] J. G. Smart and S. D. Salisbury, "Plugged in: How Americans charge their electric vehicles," Idaho National Lab.(INL), Idaho Falls, ID (United States), Tech. Rep., 2015.

[93] Iberdrola. Which countries are most threatened by and vulnerable to climate change? [Online]. Available: https://www.iberdrola.com/environment/top-countries-most-affected-by-climate-change

[94] L. Souto and S. Santoso, "Overhead versus underground: Designing power lines for resilient, cost-effective distribution networks under windstorms," in *2020 Resilience Week (RWS)*, 2020, pp. 113–118.

[95] G. Wolf. Hardening the grid is manageable. [Online]. Available: https://www.tdworld.com/transmission-reliability/article/21173856/hardening-the-grid-is-manageable

[96] British Standards, "Electric cables—calculation of the current rating part 1-1: Current rating equations (100% load factor) and calculation of losses—general," IEC 60287-1-1, Tech. Rep., 2014.

[97] W. A. Vasquez and D. Jayaweera, "Risk-based approach for power transformer replacement considering temperature, apparent age, and expected capacity," *IET Generation, Transmission & Distribution*, vol. 14, no. 21, pp. 4898–4907, 2020.

[98] U.S. Department of Energy, "Large power transformers and the U.S. electricity grid," Tech. Rep., 2012.

[99] D. Galar and U. Kumar, *eMaintenance: Essential Electronic Tools for Efficiency*. Academic Press, 2017.

[100] British Standards, "Power transformers-part 7: Loading guide for oil-immersed power transformers," 2005.

[101] Q. Zhong, "Power transformer end-of-life modelling: Linking statistics with physical ageing," Ph.D. dissertation, The University of Manchester (United Kingdom), 2012.

[102] Task Force D1.01.10, "Ageing of cellulose in mineral-oil insulated transformers," CIGRE, Tech. Rep., 2007.

[103] D. Feng, "Life expectancy investigation of transmission power transformers," Ph.D. dissertation, The University of Manchester, 2013.

[104] T. W. Dakin, "Electrical insulation deterioration treated as a chemical rate phenomenon," *Transactions of the American Institute of Electrical Engineers*, vol. 67, no. 1, pp. 113–122, 1948.

[105] A. Emsley, X. Xiao, R. Heywood, and M. Ali, "Degradation of cellulosic insulation in power transformers. part 3: Effects of oxygen and water on ageing in oil," *IEE Proc.-Science, Measurement and Technology*, vol. 147, no. 3, pp. 115–119, 2000.

[106] A. Jahromi, R. Piercy, S. Cress, J. Service, and W. Fan, "An approach to power transformer asset management using health index," *IEEE Electrical Insulation Magazine*, vol. 25, no. 2, pp. 20–34, 2009.

[107] S. Li, H. Ma, T. Saha, and G. Wu, "Bayesian information fusion for probabilistic health index of power transformer," *IET Generation, Transmission & Distribution*, vol. 12, no. 2, pp. 279–287, 2017.

[108] S. Li and H. Dong, "Transformer apparent age estimation based on probabilistic health index," in *IEEE Innovative Smart Grid Technologies-Asia*, 2019, pp. 3936–3940.

[109] S. K. Awadallah, J. Milanovic, and P. Jarman, "Deriving transformer equivalent age for power system reliability assessment from asset condition score," in *International Conference on Probabilistic Methods Applied to Power Systems (PMAPS)*. IEEE, 2020, pp. 1–6.

[110] IEEE, "IEEE standard for general requirements for liquid-immersed distribution, power, and regulating transformers," pp. 1–74, May 2016.

[111] S. Tang, C. Hale, and H. Thaker, "Reliability modeling of power transformers with maintenance outage," *Systems Science & Control Engineering*, vol. 2, no. 1, pp. 316–324, 2014.

[112] D. Martin, J. Marks, and T. Saha, "Survey of Australian power transformer failures and retirements," *IEEE Electrical Insulation Magazine*, vol. 33, no. 5, pp. 16–22, 2017.

[113] W. Li, P. Choudhury, and J. Gurney, "Evaluating capacity probability distributions of aged power equipment: Method and example," in *IEEE Canada Electric Power Conference*, 2008, pp. 1–7.

[114] V. Sokolov and B. Vanin, "Experience with detection and identification of winding buckling in power transformers," in *Proc. 68th Annu. Int. Conf. Doble Clients*, 2001.

[115] Empresa Electrica Quito (EEQ), "Expansion plan 2016-2025 Quito Electricity Company (Plan de Expansión 2016-2025 de la Empresa Eléctrica Quito)," Tech. Rep., 2016.

[116] J. Grainger and W. Stevenson, *Power System Analysis*. McGraw-Hill Education, 1994.

[117] NOAA. National centers for environmental information. [Online]. Available: https://www.ncdc.noaa.gov

[118] US-EIA, "Annual energy outlook 2019 with projections to 2050," Tech. Rep., 2019.

[119] CONELEC, "Plan maestro de electrificacion 2013-2022," Tech. Rep., 2012.

[120] SENPLADES, "Evaluacion de los costos de reconstruccion sismo en Ecuador," Tech. Rep., 2016.

[121] C. Marnay, H. Aki, K. Hirose *et al.*, "Japan's pivot to resilience: How two microgrids fared after the 2011 earthquake," *IEEE Power and Energy Magazine*, vol. 13, no. 3, pp. 44–57, 2015.

[122] I. Kongar, T. Rossetto, and S. Giovinazzi, "The effectiveness of existing methodologies for predicting electrical substation damage due to earthquakes in New Zealand," in *Vulnerability, Uncertainty, and Risk: Quantification, Mitigation, and Management*, 2014, pp. 752–761.

[123] R. E. Brown, *Business Essentials for Utility Engineers*. CRC press, 2010.

[124] D. Bertsimas, D. B. Brown, and C. Caramanis, "Theory and applications of robust optimization," *SIAM review*, vol. 53, no. 3, pp. 464–501, 2011.

[125] B. L. Gorissen, İ. Yanıkoğlu, and D. den Hertog, "A practical guide to robust optimization," *Omega*, vol. 53, pp. 124–137, 2015.

[126] US-Geological-Survey. What is a seismic zone, or seismic hazard zone? [Online]. Available: https://www.usgs.gov

[127] N. Mimura, K. Yasuhara, S. Kawagoe *et al.*, "Damage from the Great East Japan earthquake and tsunami-A quick report," *Mitigation and Adaptation Strategies for Global Change*, vol. 16, no. 7, pp. 803–818, 2011.

[128] AmericanLifelinesAlliance, "Seismic fragility formulations for water systems Part 1 - Guideline," Tech. Rep., 2001.

[129] D. Brunsdon, "Critical infrastructure and earthquakes: Understanding the essential elements of disaster management (Paper No. 28)," pp. 1–8, 2003.

[130] R. L. Boroschek, V. Contreras, D. Y. Kwak, and J. P. Stewart, "Strong ground motion attributes of the 2010 mw 8.8 Maule, Chile, earthquake," *Earthquake Spectra*, vol. 28, pp. 19–38, 2012.

[131] CIGRE WG A1.10, "Survey of hydrogenerator failures," Tech. Rep., 2009.

[132] A. Merkhouf, S. Bernier, J. Cave *et al.*, "Operational limits of a large hydro generator with bypassed coils and circuits," in *IEEE Workshop on Electrical Machines Design, Control and Diagnosis*, vol. 1, 2019, pp. 177–180.

[133] D. Franklin, "Resolving problems of high vibration in hydroelectric machinery," *Hydro Review;(United States)*, vol. 12, no. 5, 1993.

[134] J. Wareing, "Failure modes in overhead lines," in *IEE Colloquium on Distribution Overhead Lines-Economics, Practice and Technology of Reliability Assessment.* IET, 1998, pp. 1–10.

[135] S. Binato, M. V. F. Pereira, and S. Granville, "A new Benders decomposition approach to solve power transmission network design problems," *IEEE Transactions on Power Systems*, vol. 16, no. 2, pp. 235–240, 2001.

[136] P. Tsamasphyrou, A. Renaud, and P. Carpentier, "Transmission network planning: An efficient Benders decomposition scheme," in *Proceedings of the 13th PSCC*, 1999, pp. 487–494.

[137] A. J. Conejo, E. Castillo, R. Minguez *et al.*, *Decomposition Techniques in Mathematical Programming: Engineering and Science Applications.* Springer Science & Business Media, 2006.

[138] MISO, "Transmission cost estimation guide MTEP19," Tech. Rep., 2019.

[139] F. Lanning, A. Haro, M. Liu *et al.*, "M7.8 Muisne, Ecuador earthquake on April 16, 2016," Tech. Rep., 2016.

[140] B. C. McLellan, Q. Zhang, N. A. Utama *et al.*, "Analysis of Japan's post-Fukushima energy strategy," *Energy Strategy Reviews*, vol. 2, no. 2, pp. 190–198, 2013.

[141] Z. Yang, P. Dehghanian, and M. Nazemi, "Seismic-resilient electric power distribution systems: Harnessing the mobility of power sources," *IEEE Transactions on Industry Applications*, vol. 56, no. 3, pp. 2304–2313, 2020.

[142] S. A. Adderly, D. Manukian, T. D. Sullivan, and M. Son, "Electric vehicles and natural disaster policy implications," *Energy Policy*, vol. 112, pp. 437–448, 2018.